Copyright Warning & Restrictions

The copyright law of the United States (Title 17, United States Code) governs the making of photocopies or other reproductions of copyrighted material.

Under certain conditions specified in the law, libraries and archives are authorized to furnish a photocopy or other reproduction. One of these specified conditions is that the photocopy or reproduction is not to be "used for any purpose other than private study, scholarship, or research." If a, user makes a request for, or later uses, a photocopy or reproduction for purposes in excess of "fair use" that user may be liable for copyright infringement,

This institution reserves the right to refuse to accept a copying order if, in its judgment, fulfillment of the order would involve violation of copyright law.

Please Note: The author retains the copyright while the New Jersey Institute of Technology reserves the right to distribute this thesis or dissertation

Printing note: If you do not wish to print this page, then select "Pages from: first page # to: last page #" on the print dialog screen

Order Number 9401726

Competition between two microbial populations in a sequencing fed-batch reactor and its implications for waste treatment applications

Dikshitulu, Sitaram, Ph.D.

New Jersey Institute of Technology, 1993

U·M·I
300 N. Zeeb Rd.
Ann Arbor, MI 48106

COMPETITION BETWEEN TWO MICROBIAL POPULATIONS IN A SEQUENCING FED-BATCH REACTOR AND ITS IMPLICATIONS FOR WASTE TREATMENT APPLICATIONS

by
Sitaram Dikshitulu

A Dissertation
Submitted to the Faculty of
New Jersey Institute of Technology
in Partial Fulfillment of the Requirements for the Degree of
Doctor of Philosophy

Department of Chemical Engineering,
Chemistry, and Environmental Science

May 1993

ABSTRACT

Competition Between Two Microbial Populations in a Sequencing Fed-Batch Reactor and its Implications for Waste Treatment Applications

by
Sitaram Dikshitulu

Pure and simple competition between two microbial populations in a sequencing fed-batch reactor (SFBR) was studied both at the theoretical and experimental level. Competition occurred for a single chemical pollutant which could serve as the sole carbon and energy source for both competitors. A mathematical model describing the process under inhibitory kinetics (as is usually the case with hazardous and toxic substances) was derived and theoretically analyzed. The model predicts that the dynamics of a SFBR, and the kinetics of biodegradation, result in a complex set of operating regimes in which neither species, only one species, or both species survive in a steady cycle. The model also predicts the existence of multiple outcomes, achievable from different start-up conditions, in some domains of the operating parameter space.

The experimental system involved phenol as the model pollutant, and two species capable of utilizing phenol as their sole carbon and energy source. These species were *Pseudomonas putida* (ATCC 17514) and *Pseudomonas resinovorans* (ATCC 14235). A methodology was developed to accurately determine the kinetics of phenol biodegradation by each individual species in pure culture batch experiments. It was found that both species biodegrade phenol following Andrews' kinetics. The experimentally determined kinetic parameters were then used with the model equations to predict the behavior of a SFBR employing both species together.

The model predictions were experimentally tested by inoculating a SFBR with both species and operating under conditions falling in different regimes of the operating

parameter space. In all cases there was excellent agreement between the predicted and measured concentrations of phenol, total biomass, and the biomass of each individual species. All different types of behavior of the system predicted by the analysis of the model were experimentally confirmed including the existence of multiple outcomes under the same operating, but different start-up conditions.

This study shows how serious discrepancies can arise in scale-up of biological treatment systems if population dynamics are not taken into account. This study also confirms experimentally the theory of microbial competition in periodically forced bioreactors.

APPROVAL PAGE

Competition Between Two Microbial Populations
in a Sequencing Fed-Batch Reactor and its Implications
for Waste Treatment Applications

Sitaram Dikshitulu

Dr. Basil C. Baltzis, Thesis Advisor — Date
Associate Professor of Chemical Engineering, NJIT

Dr. Gordon A. Lewandowski, Thesis Advisor — Date
Professor of Chemical Engineering and Chairperson of the Department
of Chemical Engineering, Chemistry and Environmental Science, NJIT

Dr. Piero M. Armenante, Committee Member — Date
Associate Professor of Chemical Engineering, NJIT

Dr. Dana E. Knox, Committee Member — Date
Associate Professor of Chemical Engineering, NJIT

Dr. David Kafkewitz, Committee Member — Date
Associate Professor of Microbiology
Department of Biological Sciences, Rutgers University (Newark)

BIOGRAPHICAL SKETCH

Author: Sitaram Dikshitulu

Degree: Doctor of Philosophy in Chemical Engineering

Date: May 1993

Undergraduate and Graduate Education:

- Master of Science in Chemical Engineering
  Indian Institute of Technology, Kanpur, India, 1984

- Master of Science in Chemistry
  Birla Institute of Technology and Science, Pilani, India, 1982

- Bachelor of Science in Chemical Engineering
  Birla Institute of Technology and Science, Pilani, India, 1982

Major: Chemical Engineering

Presentations and Publications:

" Competition between Two Microbial Populations in a Sequencing Fed-Batch Reactor: Theory, Experimental Verification, and Implications for Waste Treatment Applications." *Biotechnology and Bioengineering.* (In press)

" The Effect of Population and Substrate Interactions on SBR Design Optimization"- EPA Annual Symposium on Bioremediation of Hazardous Wastes: Research, Development and Field Evaluations, Dallas, TX (May 4-6, 1993)

" Aerobic Biodegradation of Phenolics in Optimally Designed Sequencing Batch Reactors." ACS 4th Chemical Congress of North America, New York, NY (August 25-30, 1991)

" Biodegradation of Single and Multiple Hazardous Substances in a Sequencing Batch Reactor: Theory and Experimental Results."- AIChE Annual Meeting, Chicago, IL (November 11-16, 1990)

ACKNOWLEDGMENT

The author wishes to express his sincere gratitude to his supervisors, Drs. Basil Baltzis and Gordon Lewandowski, for their guidance, encouragement and moral support throughout this research.

Special thanks to Dr. Stavros Pavlou (University of Patras, Greece) for his help in the numerical analysis part of this dissertation.

The author is grateful to Drs. Piero Armenante, Dana Knox, and David Kafkewitz for serving as members of the committee.

The author appreciates the timely help and suggestions from other members of the Biodegradation laboratory, including: Socrates Ioannides, Nirupam Pal, Zarook Shareefdeen, Kung-Wei Wang, and Jesse Zahn.

Ms. Gwen San Augustin, Mr. Clint Brockway and Mr. Bill Guzy provided timely and expert assistance with the experimental set-up and analytical instruments.

Finally, the author thanks his family members: Padma and Divya, Prasad and Sharmilla, for their patience, support, and constant encouragement without which this work could not have been accomplished.

TABLE OF CONTENTS

Chapter **Page**

LIST OF TABLES

LIST OF FIGURES

CHAPTER 1

INTRODUCTION

Hazardous compounds can be eliminated from aqueous environments by using biological methods. A significant advantage of biological treatment is that it can be very cost effective in comparison to other waste treatment processes such as incineration, adsorption, or catalytic destruction. Most commonly used systems for biological treatment of wastewaters involve fixed film systems and activated sludge systems. In fixed film systems organisms grow attached to a surface while in activated sludge systems organisms grow in suspension. In both cases mixed, rather than pure, cultures of microorganisms convert the contaminants to carbon dioxide, water, new cell mass and other end products. Wastewaters are usually treated in continuous flow systems (CSTRs) using activated sludge and a series of tanks; the contaminated water flows from one tank into the next on a continuous basis and virtually all tanks have a predetermined liquid volume.

An innovative, alternate wastewater technology is that of Sequencing Batch Reactors (SBRs). SBRs are time oriented systems, with flow, energy input and tank volume varying according to some predetermined, periodic, operating strategy. SBRs result in an unsteady state operation. These systems have a number of advantages such as a strong control over organism selection (43), cycling between anoxic and aerobic periods of operation, greater flexibility in meeting changes in feed conditions, better control in the settling characteristics of the sludge, effective control of the process and the quality of discharge, and the fact that they do not need a separate clarifier.

Even though SBRs are currently used quite successfully with activated sludge systems (35, 80), and have been studied by a number of researchers (20, 35, 41-44, 65), they have largely been approached empirically with regard to mixed microbial populations.

The current approach to bioremediation of contaminated wastewaters is to use a so called "activated sludge". This is a highly heterogeneous microbial culture consisting of species indigenous to a particular site. Although, it is reasonable to expect that indigenous microbial populations will be adapted to the pollutants, there is no reason to believe that optimal pollutant degrading strains will always be present. Finn (24) has argued that biological treatment could be significantly improved by using well defined and not necessarily complex cultures. Microbial cultures can be viewed as catalysts in the classical chemical engineering sense. Unless the microbial system is well characterized, it is almost impossible to duplicate results and derive rational design criteria. One of the main problems with non-characterized heterogeneous cultures is that the effects of species interactions are neglected. Such interactions are always present in mixed cultures and lead to changes in biomass composition depending on the conditions of operation. These composition changes imply a change in the catalyst, in the chemical engineering sense, and thus, in the rate of the process. One of the most common interactions among microbial populations inhabiting a common environment, is competition for nutrients and other resources. Knowledge of the dynamics of interactions arising among microbial populations inhabiting a bioreactor is important when a biomass of a specific species composition is required.

In the present study the effect of microbial competition on the dynamics of a sequencing batch reactor has been investigated. A special case of SBR was considered; namely, one in which reaction occurs during the fill phase and settling of solids is neglected. In such a case, a SBR can be called a Sequencing Fed-Batch Reactor (SFBR). Pure and simple competition by two species for a single substrate was considered. A theoretical model describing the process was developed, analyzed, and then experimentally validated. The model equations were numerically solved for different values of some key parameters of SFBR operation. The various possible outcomes of competition were examined for their stability and attainability during actual operation. Two species,

Pseudomonas putida (ATCC 17514) and *Pseudomonas resinovorans* (ATCC 14235) both capable of growing on phenol (which was selected as the model toxic compound for the study) as the sole carbon and energy source, were selected for the experimental validation of the model. The kinetics of phenol biodegradation by the aforementioned species were revealed from pure culture batch experiments. These kinetic parameters were used in the numerical studies with the model. Numerical simulations revealed the regions of various outcomes in the operating parameter space and guided the design of experiments for model validation. The experimental results from SFBR operation agreed very well with the model predictions.

CHAPTER 2

LITERATURE REVIEW

2.1 Kinetics of Phenol Biodegradation

Phenol which has been selected as the model compound for the present study, is a toxic substance and its microbial degradation can best be described by a mechanism of substrate inhibition. The Haldane (29) or Andrews' (3) equation has been predominantly used to describe the degradation of phenol by pure as well as mixed cultures (3, 16, 23, 62, 70). Allsop et al. (1) have concluded that the inhibition of phenol permeases or hydroxylases by high concentrations of phenol is the probable cause for the inhibitory degradation kinetics. Janke et al. (45) reported that the conversion of phenol to catechol by a strain of *Pseudomonas putida* having only the meta clevage pathway was inhibited by phenol levels exceeding 23.5 g m^{-3}, although the data did not allow for a distinction between permease and hydroxylase association inhibition. Wedding et al. (78) reported the in vitro complexing of phenol with cytochrome b_5 reductase (NADH) and (NAD^+) in porcine cell homogenates. Since these co-enzymes are necessary for phenol hydroxylase activity, the formation of complexes suggests a permease or hydroxylase based reaction interference by phenol (1). Studies on phenol uptake rate by Sokol (68, 69) and Sokol and Howell (70) also support a permease-or hydroxylase- based interference. Since the mechanism used in deriving the Haldane equation assumes a direct linkage between phenol concentration and phenol uptake, such an interference may be termed Haldane-like. Kinetics described by this behavior have also been reported as Andrews (3) kinetics.

The kinetics of phenol biodegradation have been investigated in continuous (13,15, 32, 47, 79), as well as batch experiments (27, 32, 50, 56, 62, 75-77). Kinetic parameters

Table 2.1 Andrews model parameters for microbial populations degrading phenol.

Reference	Culture	T	pH	μ^*	K_S	K_I	Y
		°C		h^{-1}	$g\ m^{-3}$	$g\ m^{-3}$	$g\ g^{-1}$
Chi and Howell (13)	*Pseudomonas sp.*	30	-	0.369	5.94	227	-
Colvin and Rozich (15)	UMC	22	7.2	0.19	7.9	139	0.9
Colvin and Rozich (15)	UMC	22	7.2	1.07	79	172	0.47
D'Adamo, Rozich, and Gaudy (16)	UMC	25	6.8-7.0	0.204-0.363	5-266	142-1199	-
Guptapal (27)	*P. resinovorans* (ATCC 14235)	28	7.2	0.947	13.06	151.88	0.596
Hill and Robinson (32)	*P. putida* (ATCC 17484)	30	6.5	0.534	<1	470	0.52
Hutchinson and Robinson (39)	*P. putida* (ATCC 17484)	30	6.7	0.388	1.06	903	0.70
Jones, Jansen, and McKay (47)	*P. putida* (NCIB 8250)	20	-	0.44	<1	110	-
Kotturi, Robinson, and Inniss (50)	*P. putida* (Q5)	10	7.0	0.119	5.27	377	0.55
Molin and Nilsson (59)	*P. putida* (ATCC 11172)	25	6.7	0.4	<3	500	-
Pawlowsky and Howell (62)	UMC	28	6.6	0.26	25.4	173.0	0.55
Pawlowsky and Howell (62)	UMC	28	6.6	0.223	5.86	934.5	0.62
Sokol and Howell (70)	UMC	30	-	0.44-1.61	0.16-5.2	7.5-19.4	-
Szetella and Winnicki (75)	UMC	20	6.8	0.326	19.2	229.3	-
Tang and Fan (76)	UMC	23	8.5	0.365	10.948	113	0.496
Wang (77)	*P. putida* (ATCC 17514)	21	7.2	1.55	27.9	12.4	0.537
Yang and Humphrey (79)	*P. putida* (ATCC 17514)	30	0.6	0.567	2.39	106.0	0.85

UMC: Unidentified mixed culture

obtained from these studies are shown in Table 2.1. The initial rate method is used in batch experiments whereas steady state measurements are required for continuous experiments. The large medium requirement is the major disadvantage of continuous culture experiments. Batch experiments require an accurate estimation of the initial rate of microbial growth; for this to be achieved, a large number of measurements is needed, and the experimenter must have the ability to distinguish between the various stages of growth. The batch method is based on the use of data from the exponential phase of growth. Unless the inoculum size is small enough, especially at low initial substrate concentrations and for fast growing organisms, one cannot get enough data for an accurate determination of the rate (51).

Determination of biodegradation kinetics by mixed cultures is problematic when the mixed culture is treated as a single functional population. This can be seen from the following studies with phenol. D'Adamo et al. (16) studied phenol biodegradation by using a heterogeneous seed population obtained from a municipal treatment plant. The degradation of a synthetic medium containing phenol (50-1000 g m^{-3}) was studied in batch experiments and the specific growth rates were fitted to the Andrews' (3) model. These authors reported values of μ^* from 0.131 to 0.363 h^{-1}, K_S from 5 to 266 g m^{-3}, and K_I from 142 to 1199 g m^{-3}, from experiments performed over a period of six months. The wide ranges of the biokinetic constants clearly suggest that the species composition of the mixed culture had been altered over the period the experiments were performed.

Pawlowsky and Howell (62) used a mixed culture derived from soil and activated sludge organisms to degrade a synthetic medium containing phenol. The mixed culture consisted of a diverse population ranging from spherical and rod shaped bacteria to filamentous forms, and of distinctive predators such as protozoa and a few rotifers. These mixed cultures were acclimated in a chemostat with a feed medium containing 100 g m^{-3} phenol. With a 6 hour residence time, spherical bacteria dominated with several predators present, whereas with a 4 hour residence time filamentous bacteria were dominant with

very few predators present. Two sets of batch experiments were performed using seeds from the two chemostat runs. The fitted biokinetic parameters - μ^*, K_S, K_I- for the two sets were 0.26 h^{-1}, 25.4 g m^{-3}, 173.0 g m^{-3} and 0.223 h^{-1}, 5.86 g m^{-3}, and 934.5 g m^{-3}, respectively. From these data it is clear that kinetic constants are meaningless when they do not refer to a specified species composition.

Szetela and Winnicki (75) obtained cultures from an aeration tank operated by a municipal sewage treatment plant. The microorganisms were adapted to biodegrade phenol using it as their sole carbon and energy source. The adaptation process was carried out with the organisms immobilized in an anion exchange resin bed. The cultures were subsequently isolated from the carrier by mixing at a high intensity. A set of batch experiments- with phenol in the range of 20-800 g m^{-3}- were performed. There was no scatter in the specific growth rate data, something that was observed in the work of Pawlowsky and Howell (62). The reason for this could be that the adaptation method used, caused the isolation of microorganisms with similar characteristics.

Colvin and Rozich (15) studied phenol degradation kinetics in a two stage continuous culture system. Mixed cultures from a wastewater treatment plant were used. The reactors -which were connected in series- were inoculated with phenol acclimated biomass. The dilution rate of the two reactors was different. The steady state biomass composition was different in the two reactors. Batch experiments were then performed, using biomass from each of the reactors, with phenol in the range of 50 - 800 g m^{-3}. A wide range of specific growth rates, for each of the phenol concentrations studied, was observed. This clearly indicates again that the kinetic constants have to be associated with a specific biomass composition. These results also suggest that the mode of operation (e.g., two reactors in series) can alter the biomass composition. Instead of the foregoing conclusions, the authors claim that the two-stage continuous flow method could not be used as a technique for determining the biokinetic constants for heterogeneous populations.

Most of the existing studies on phenol biodegradation (or biodegradation of any other compound) involve unidentified mixed cultures. This is due to the fact that the current practice in the waste treatment industry is to use activated sludge. This practice evolved from technologies that had been developed earlier for treatment of municipal wastes, and relies on rules-of-thumb and highly empirical approaches to reactor design. However, such a "black box" approach often fails when addressing problems in hazardous waste treatment as the activated sludge may not have the desired and/or constant biomass composition. Furthermore, a highly heterogeneous culture may lead to reduced biodegradation rates. For example, Jones et al. (47) studied the biodegradation of phenol in a two stage chemostat. An activated sludge containing numerous bacterial populations was used, but only two species of the *Acineobacter-Moraxella* group were found responsible for the biodegradation. The survival of the other species in the system could be attributed to predation on the phenol degrading species, thereby reducing the efficiency of the reaction system. These authors concluded that industrial wastewaters can be treated by bacterial ecosystems much simpler than those involved in municipal sewage treatment units.

2.2 Species Interactions

The wide range of kinetic parameters observed when mixed cultures are used, shows that bacterial interactions need to be considered while studying the dynamics of the system. Knowledge of the system dynamics is required in order to design effective and optimal treatment units. Furthermore, a control strategy may be necessary for the attainment and maintenance of steady state conditions as industrial processes are never free from fluctuations in input variables. To study the dynamic responses in a rational way, mathematical models must be constructed and analyzed. These models must be taking into

account the species interactions while for the kinetics they should involve those of the individual species present in the mixed culture.

The interactions among microbial populations in mixed cultures have been reviewed by Fredrickson (26) and Slater (66). Competition, alone or in combination with another interaction appears to be the most common microbial interaction. Microbial competition, is defined as the situation in which two populations use a resource and that resource has a dynamical effect on at least one of them. The pattern of microbial competition studied the most, is pure and simple competition. Microbial populations are engaged in pure and simple competition when they interact in no other way except competition for a single nutrient whose availability affects the growth rate of all populations involved in the interaction (26).

Pure and simple competition in a chemostat which operates under time invariant inputs has been the subject of several experimental (30, 31, 46, 58) and theoretical (4, 8, 9, 12, 36, 38, 63) studies. The conclusion from these studies is that if the chemostat is ideal and the resource competed for is not biologically renewable within the reactor, there is no steady state which may involve more than two populations. Even the coexistence of two species is only mathematically predicted and cannot be practically realized. It requires operation at discrete values of the chemostat dilution rate, which is not practically feasible owing to the random fluctuations in the flowrate (72). As pointed out by Powell (64), the system of ordinary differential equations at the discrete dilution rate values where coexistence is obtained, is structurally unstable. Baltzis and Fredrickson (8) observed that if the bioreactor is non-ideal in the sense that cells attach to the vessel walls, steady state coexistence of two species is possible over a wide range of operating parameter values provided that the population which grows slower under the given operating conditions is the one which exhibits wall attachment. Coexistence, not at a steady state but rather in a state of sustained oscillations (limit cycles), is possible in an ideal chemostat whose inputs are constant, provided that pure and simple competition occurs for a resource which is

biologically produced within a reactor by a third bacterial population which is not involved in the competitive pattern (9).

If the pattern of competition is not pure and simple, steady state coexistence of microbial competitors has been found to occur. For example, coexistence of two bacterial populations under substrate competition and product inhibition has been observed experimentally (18). Coexistence has been also observed in cases where competition occurs for multiple substrates. In such cases coexistence is even easier to attain when each population grows faster on a different substrate. Coexistence of two organisms competing for mixed nutrients has been observed by Lewis (55). Lester (53) has reported coexistence of six species. Competition for mixed substrates by microbial populations in a chemostat has been also studied by Yoon et al. (81). These researchers found that coexistence of several species at steady state was possible and concluded that diversity of nutrient sources in municipal wastes may be a key factor in supporting a heterogeneous population. Industrial wastes on the other hand may not have such a wide diversity of nutrients, thereby a simpler ecosystem should be expected in industrial waste bioremediation units.

Hutchinson (40) was the first to suggest that seasonal variations may be an explanation for the observed diversity of competing species in physical habitats. Using this idea for the case of pure and simple competition between two populations in a chemostat, a number of theoretical studies have shown that periodic variation of the chemostat dilution rate (12, 57, 71, 73), or of the limiting nutrient concentration in the feed (28, 37, 67), allows the two microbial populations to coexist in a stable state of sustained oscillations. These studies have assumed that the species growth rate adapts instantaneously to the changes occurring in the reactor. Under this assumption, a necessary condition for coexistence is that the specific growth rate curves of the two competitors cross each other and thus, under periodic operation of the chemostat, the competitive advantage alternates between the two populations so that they are able to

coexist. Pavlou et al. (63) have shown that a time delay in the adaptation of the growth rate may allow for coexistence of two species even in cases where the specific growth rate curves do not cross. The only experimental work reported in the literature that shows that pure and simple competitors persist in a reactor where conditions vary periodically is the one by Davison and Stephanopoulos (17). These investigators used pH as the varying parameter and operated the chemostat for part of the cycle under one pH and for the rest of the cycle under a different pH value.

The present study is the first to show that periodic variation of the inlet flowrate (as in a SFBR) can lead to coexistence of two pure and simple competitors.

2.3 Stability Analysis

The analysis of the dynamics of any chemically or biochemically reacting system from the stability view point is of paramount importance in assessing the performance of a reactor. Stability analysis of bioreactors where mixed cultures are employed is even more important and complex as the dynamics get complicated by the presence of species interactions. Biochemical reactors with mixed cultures often exhibit multiple types of behavior involving steady and/or oscillatory states. Most chemical and biochemical systems are described by nonlinear differential equations. Stability of steady states can be determined by studying the character of the eigenvalues of the Jacobian matrix (2). These results are local in character due to the required linearization. They provide useful information which can then be used in generalizing the results for the global behavior of the system usually by the use of numerical methods. The stability of the oscillatory states is more difficult to determine and is based on the Poincaré theory and the so called Floquet multipliers of the system. Review of these mathematical methods is out of the scope of this dissertation. It needs only to be stated that for the SFBR system considered here there are only oscillatory states, due to the external forcing of the flowrate, and that the stability of

these cycles was numerically determined using proper software originally developed by Doedel (21).

2.4 Periodic Operation of Reactors

Periodic operation of chemical reactors has experienced a revival in chemical engineering research in recent years. Periodic processes may have advantages over steady state processes in terms of productivity or selectivity (6, 7, 22, 34).

In biological treatment of wastes, an example of periodic reactor operation is that of Sequencing Batch Reactors (SBRs). In recent years SBRs have become more popular in waste treatment as a result of automated control, improved decanting mechanism, and aeration equipment that is resistant to plugging during start/stop operation. SBRs are currently used successfully with activated sludge systems (44, 75) as their operation is flexible and can be altered to accommodate a wide variety of waste waters. SBRs have been proposed as a means of negating filamentous bulking in activated sludge systems, as the ratio of fill to react periods affect the settleability of the sludge (20, 33). Earlier research (14, 20, 35, 41-44, 65) has shown that SBRs present a number of advantages over conventional activated sludge systems, including: cycling between anoxic and aerobic periods of operation, greater flexibility in meeting changes in feed conditions, better control in settling characteristics of the sludge, effective control of the process and the quality of discharge, and the fact that they do not require a separate clarifier. In classical SBRs, reaction occurs only during the "react" period. More recent work has demonstrated that if the reaction starts during the fill period, the presence of intermediates which are toxic and/or inhibitory for the biomass (such as nitrite in the denitrification process), can be substantially reduced during SBR operation (11, 54). Baltzis et al.(10), have also shown that in general, the volumetric efficiency of the SBRs is greater than that of the CSTRs; SBRs achieve the same level of treatment, at an equivalent throughput, in a

volume much smaller than the CSTRs, something which may result in significant savings in mixing and aeration costs.

A lack of widely accepted design standards is the major obstacle for bringing the SBR technology to a broader practical application (5). Most of the studies on SBRs are empirical and have not resulted in final conclusions. SBR technology can be substantially improved if a fundamental approach is used for analyzing the process involved. For waste treatment which involves mixed cultures, such a fundamental approach needs to consider species interactions. This dissertation studies microbial competition in a periodically operated reactor used for treating a hazardous waste and contributes to the basic understanding of SBR technology and to the further development of the theory of microbial competition.

CHAPTER 3

OBJECTIVE

The objective of this dissertation was to study the dynamics of two species which are involved in pure and simple competition for phenol in a Sequencing Fed-Batch Reactor (SFBR). The approach adopted was as follows:

1. Develop an experimental methodology in order to obtain accurate kinetic parameters for the pure cultures.
2. Mathematically model the SFBR system, and solve the equations numerically, using the previously determined kinetic parameters.
3. Explore the different types of behavior in the operating parameter space.
4. Experimentally verify all possible outcomes of competition predicted by the mathematical model.

CHAPTER 4

MATHEMATICAL DESCRIPTION OF THE SYSTEM

4.1 Model Derivation

A sequencing batch reactor operates in a cyclic mode. Each cycle is comprised of five distinct periods: fill, react, settle, draw, and idle. In most cases SBRs use activated sludge. The settle phase, in these cases, is required to separate the solids from the liquid. In the special case considered here there are no settle and idle phases and the biomass remains suspended in the reactor throughout the cycle. It is also assumed that reaction occurs throughout the cycle. This special case of SBR can be called Sequencing Fed-Batch Reactor (SFBR).

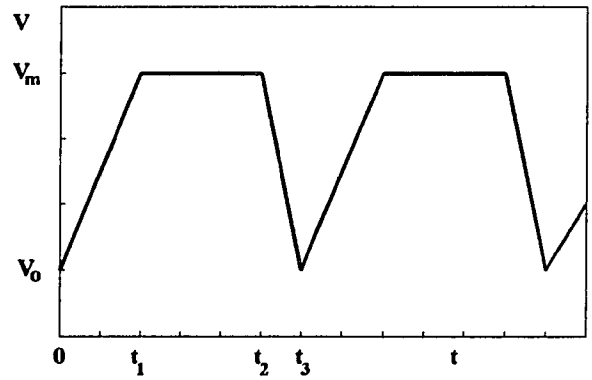

Figure 4.1 Schematic representation of the variation of the liquid volume during SFBR operation

The flowrate of inlet (untreated waste) during the fill phase is constant, and the same is true for the flowrate of the outlet (treated waste) during the draw-down phase. The values of the two flowrates are not necessarily equal. Constant flowrates imply linear changes in the volume of the reactor contents. The minimum volume of reactor contents (beginning of fill-phase, and end of draw-phase) cannot be zero in order for at least some biomass to remain

in the vessel. Biomass is not externally fed to the reactor. Figure 4.1 shows a schematic of the variations of the volume of the reactor contents during the cyclic operation.

If the beginning of a cycle is set as time zero, then t_1 indicates the end of the fill phase, t_2 denotes the end of the period during which the reactor operates without any input or output, and t_3 marks the end of the cycle which immediately starts repeating itself. The reactor is originally inoculated with two phenol degraders which will be called species 1 and 2. The specific growth rate of both species follows Andrews' inhibitory expression, i.e., $\mu_j = \mu_j^* S / (K_j + S + S^2/K_{Ij}), j = 1, 2$. Assuming that the bacterial cells do not exhibit any tendency for attachment to the reactor walls, that biomass maintenance requirements are negligible, and that the density of reactor contents is constant and equal to that of the untreated waste (inlet), the process can be described in general, by the following equations:

Overall mass balance:

$$\frac{dV}{dt} = Q_f - Q \qquad (1)$$

where,

V = Volume of the reactor contents, m^3

t = time, hours

Q_f = flowrate at which the untreated waste is fed into the reactor, $m^3\ h^{-1}$

Q = flow rate at which the treated waste is removed from the reactor, $m^3\ h^{-1}$

Mass balance on substrate:

$$\frac{d(VS)}{dt} = Q_f S_f - QS - \frac{\mu_1 b_1 V}{Y_1} - \frac{\mu_2 b_2 V}{Y_2} \qquad (2)$$

where,

S = concentration of the phenol in the reactor, $g\ m^{-3}$

S_f = concentration of the phenol in the untreated feed stream, $g\ m^{-3}$

μ_j = specific growth rate of species j on phenol, h^{-1}

b_j = biomass concentration of species j, $g\ m^{-3}$

Y_j = yield coefficient of species j on phenol, (grams- biomass / grams- substrate)

Substituting (1) in (2) we get,

$$\frac{dS}{dt} = \frac{Q_f}{V}(S_f - S) - \frac{b_1}{Y_1}\mu_1 - \frac{b_2}{Y_2}\mu_2 \tag{3}$$

Mass balance on individual species:

$$\frac{d(Vb_j)}{dt} = -Qb_j + \mu_j b_j V \tag{4}$$

Substituting (1) in (4) we get,

$$\frac{db_j}{dt} = (\mu_j - \frac{Q_f}{V})b_j,\ j = 1, 2 \tag{5}$$

Equations (1), (3), and (5) in dimensionless form are given as,

$$\frac{dV'}{d\theta} = Q'_f - Q' \tag{6}$$

$$\frac{du}{d\theta} = \frac{Q'_f}{V'}(u_f - u) - \beta[x_1 f_1(u) + \eta x_2 f_2(u)] \tag{7}$$

$$\frac{dx_j}{d\theta} = [\beta f_j(u) - \frac{Q'_f}{V'}]x_j,\ j = 1, 2 \tag{8}$$

where,

$$V' = \frac{V}{V_m},\quad \theta = \frac{tQ^*_f\sigma_1}{V_m},\quad Q'_f = \frac{Q_f}{Q^*_f\sigma_1},\quad Q' = \frac{Q}{Q^*_f\sigma_1},\quad u = \frac{S}{K_1},$$

$$u_f = \frac{S_f}{K_1},\quad \beta = \frac{\mu^*_1 V_m}{Q^*_f\sigma_1},\quad \eta = \frac{Y_1}{Y_2},\quad x_j = \frac{b_j}{Y_1K_1},\ j = 1, 2,$$

$$\sigma_1 = \frac{t_1}{t_3},\quad \sigma_2 = \frac{t_2 - t_1}{t_3},\quad \sigma_3 = \frac{t_3 - t_2}{t_3},\quad \omega = \frac{K_2}{K_1},\quad \phi = \frac{\mu^*_2}{\mu^*_1},$$

$$\delta = \frac{V_0}{V_m},\quad \gamma_j = \frac{K_1}{K_{Ij}},\ j = 1, 2.$$

where Q_f^* is a reference flowrate taken as the flowrate during the fill-phase, V_0 and V_m are the minimum and the maximum volume, respectively, of the reactor contents during the cycle.

Functions $f_1(u)$ and $f_2(u)$ represent -in dimensionless form- the specific growth rate of species 1 and 2, respectively, and are given as

$$f_1(u) = \frac{u}{1+u+\gamma_1 u^2} \quad \text{and} \quad f_2(u) = \frac{\phi u}{\omega + u + \gamma_2 u^2}$$

During the first phase of the cycle (fill-period), we have $Q' = 0$ and $Q_f' = 1/\sigma_1$. Subject to the initial condition $V' = \delta$ at $\theta = 0$, equation (6) when integrated, yields

$$V' = \delta + \frac{1}{\sigma_1}\theta \tag{9}$$

The first phase of the cycle ends at time θ_1 at which $V' = 1$. Thus, equation (9) implies that

$$\theta_1 = \sigma_1(1-\delta) \tag{10}$$

During the second phase of the cycle, $Q_f' = Q' = 0$ while during the third and final phase, $Q_f' = 0$ and $Q' \neq 0$. If a steady cyclic pattern of operation is to be reached, the volume of the material fed into the reactor during the first period of the cycle must be equal to the volume of the reactor contents emptied during the third phase of the cycle. Hence,

$$Q_f^* t_1 = Q(t_3 - t_2), \text{ or } Q' = \frac{1}{\sigma_3} \tag{11}$$

Considering equation (11) and that $Q_f' = 0$, the volume change during the third phase of the cycle is given by

$$V' = 1 - \frac{1}{\sigma_3}(\theta - \theta_2) \tag{12}$$

which is obtained by integrating equation (6) subject to the condition $V' = 1$ at $\theta = \theta_2$. At the end of the cycle ($\theta = \theta_3$), we have $V' = \delta$ and thus, equation (12) implies that

$$\theta_3 - \theta_2 = \sigma_3(1-\delta) \tag{13}$$

From the definition of σ_3 one can easily see that $\theta_3 - \theta_2 = \sigma_3\theta_3$, which combined with equation (13) results in

$$\theta_3 = 1-\delta \tag{14}$$

From the foregoing analysis it can be concluded that the system is described by the following sets of equations:

I. First phase of cycle, i.e., $0 \le \theta \le \sigma_1(1-\delta)$

$$\frac{du}{d\theta} = \frac{u_f - u}{\delta\sigma_1 + \theta} - \beta[x_1 f_1(u) + \eta x_2 f_2(u)] \tag{15}$$

$$\frac{dx_j}{d\theta} = [\beta f_j(u) - \frac{1}{\delta\sigma_1 + \theta}]x_j \,, j = 1, 2 \tag{16}$$

II. Second and third phase of the cycle, i.e., $\sigma_1(1-\delta) \le \theta \le 1-\delta$

$$\frac{du}{d\theta} = -\beta[x_1 f_1(u) + \eta x_2 f_2(u)] \tag{17}$$

$$\frac{dx_j}{d\theta} = \beta f_j(u) x_j \,, j = 1, 2 \tag{18}$$

The analysis of the model equations [(15)-(18)] is discussed in the next section. It should be mentioned that if one sets $x_2 = 0$ the equations given above reduce to a model describing biodegradation of a single pollutant in a SFBR by a pure culture.

4.2 Analysis of Model Equations

The system of model equations (15)-(18) possesses four classes of periodic solutions: (1) extinction of both species (washout state): $x_1(t) = 0$, $x_2(t) = 0$, $u(t) = u_f$; (2) extinction of species 2 only (1-state): $x_1(t) > 0$, $x_2(t) = 0$, $0 < u(t) < u_f$; (3) extinction of species 1 only (2-state): $x_1(t) = 0$, $x_2(t) > 0$, $0 < u(t) < u_f$; (4) coexistence of the two species (coexistence state): $x_1(t) > 0$, $x_2(t) > 0$, $0 < u(t) < u_f$. It is important to determine the stability characteristics of these solutions, since only stable solutions are actually attainable by the system. The stability of the periodic solutions is determined by their characteristic (or Floquet) multipliers. From equations (15)-(18) one can easily see that after transients decay and the system reaches an actual periodic orbit, the following stoichiometric relation holds: $u(t) - x_1(t) - \eta x_2(t) = u_f$. Computer simulations show that this relation is valid well before the final orbit is reached. Because of the stoichiometric relation, the system of three differential equations is asymptotically dynamically equivalent to a system of two differential equations. Thus, the stability of the periodic states of the system can be studied by considering two (rather than three) Floquet multipliers.

Depending on the nature and magnitude of the two Floquet multipliers, λ_1 and λ_2, a periodic solution falls into one of the following categories: (1) stable node, when λ_1 and λ_2 are real , and $|\lambda_1|$, $|\lambda_2| < 1$; (2) stable focus, when λ_1 and λ_2 are complex conjugate, and $|\lambda_1|$, $|\lambda_2| < 1$; (3) saddle, when λ_1 and λ_2 are real and $0 < |\lambda_1| < 1 < |\lambda_2|$; (4) unstable node, when λ_1 and λ_2 are real and $1 < |\lambda_1|$, $|\lambda_2|$; (5) unstable focus , when λ_1 and λ_2 are complex conjugate and $1 < |\lambda_1|$, $|\lambda_2|$. For a periodic solution to be stable, the magnitude of both its characteristic multipliers must be less than one, i.e., both of them must lie inside the unit circle in the complex plane.

The system considered here involves four operating parameters, namely β, u_f , δ, and σ_1. As these operating parameters are varied, the periodic states, as well as their characteristic multipliers, change. Thus, at certain values of the operating parameters, at

least one characteristic multiplier of a periodic solution crosses the unit circle in the complex plane, and the stability characteristics of the periodic state change. This is where a bifurcation of the periodic solution occurs. Two types of bifurcation are of relevance for the system considered in the present study. They both occur when one real multiplier (λ_1) crosses the unit circle at +1. The first is a *transcritical bifurcation*, when two periodic solutions exchange their stability characteristics. Depending on the location of the second multiplier, there may be an exchange between a saddle and a stable node when $|\lambda_2| < 1$, or a saddle and an unstable node when $|\lambda_2| > 1$. The second is a *saddle-node bifurcation*, when a saddle and a node collide and disappear. This is also called *turning point* or *limit point bifurcation.* Depending on the location of the second multiplier, this may be a saddle-stable node (saddle-sink) bifurcation when $|\lambda_2| < 1$, or a saddle-unstable node (saddle-source) bifurcation when $|\lambda_2| > 1$. Several other types of bifurcation are possible and have been observed in similar systems (53), but do not occur in the system studied in this dissertation

Among the operating parameters, β and u_f seem to be the most important ones since they may be undergoing variation during operation due to changes in inlet flowrate and strength of the waste (phenol concentration), respectively. Hence, one would like to know the dependence of the dynamic behavior of the system on the values of β and u_f, i.e., the range of values of these parameters over which each one of the periodic states of the system is stable. This is accomplished by constructing the operating diagram of the system, i.e., a diagram in the β - u_f plane where the regions of qualitatively different dynamic behavior of the system are marked. In order to construct the operating diagram, the boundaries of the various regions need to be determined, i.e., the curves in the β - u_f plane on which a qualitative change in the dynamic behavior of the system (a bifurcation) occurs. To do this, the periodic solutions (stable and unstable) of the system are computed, their characteristic multipliers calculated, and a pair of β and u_f values determined for which one of the characteristic multipliers becomes unity. A continuation algorithm (21) is used for

tracing the curve in the 2-parameter space (β - u_f) on which the characteristic multiplier remains at unity. A more detailed description of the numerical methods used in this study is given in the literature (48, 49, 60, 61). This analysis of the model equations is general and applies to any system of two species competing for a single substrate.

A characteristic operating diagram for the system considered here, is given on page 47 after the determination of the kinetic parameters from independent batch experiments.

CHAPTER 5

EXPERIMENTAL SYSTEM

5.1 Materials and Apparatus

5.1.1 Chemicals and Microorganisms

Phenol (crystals-CH-9470, Fluka Chemie AG., Switzerland) was used as the toxic substance whose biodegradation was studied in pure and mixed culture experiments. The bacterial strains used were *Pseudomonas putida* - ATCC 17514 and *Pseudomonas resinovorans* - ATCC 14235 (American Type Culture Collection, Rockville, MD). The chemicals used for the synthetic media preparation were: dihydrogen potassium phosphate, K_2HPO_4 (P288-3 Fisher Scientific, Fairlawn, NJ); potassium phosphate, monobasic KH_2PO_4 (P284-500 Fisher Scientific); ammonium sulfate $(NH_4)_2SO_4$ (A702-3, Fisher Scientific); magnesium sulfate, $MgSO_4$ (M63-500, Fisher Scientific); manganese sulfate $MnSO_4$ (2550-1, J. T Baker Chemical Co., Phillipsburg, NJ); and ferric chloride, $FeCl_3$ (Matheson Coleman and Bell, Norwood, Ohio).

5.1.2 Growth medium

The synthetic waste medium was prepared by adding phenol, as required, from a stock solution of 6 kg m^{-3} to a 50 mM phosphate buffer (K_2HPO_4 and KH_2PO_4) solution of pH 7.2. Other chemicals which were added (per liter of buffer) are 0.5g $(NH_4)_2SO_4$, 0.1g $MgSO_4$, 0.01 g $MnSO_4$, 0.0005g $FeCl_3$ and 100 ml of tap water. The synthetic growth medium was sterilized in an autoclave (121°C, 20 min). A nutrient broth (BBL-11479, Becton Dickinson and Co, Cockeysville, MD) solution was used for reviving the cultures from freeze-dried samples as well as for maintaining the cultures. Nutrient agar (001-01-8, Difco labs, Detroit, MI) was used for storing the cultures.

5.1.3 Experimental Set-up

A 4-liter jacketed lucite reactor with an internal diameter of 0.14m was used. The reactor was fitted with two air dispersion tubes (Pyrex brand-coarse, 211-138B), a dissolved oxygen probe (New Brunswick Scientific Co., series 900), a thermometer, feed and discharge lines and a sampling port. A magnetic stirrer was used for mixing the reactor contents. A schematic diagram of the experimental setup is shown in Figure 5.1. The cyclic operation of the reactor was automated by using a programmable sequence controller (Omron, model SCY-PO). Variable flow pumps (Sage Instruments-375A / Manville Corp.-C17125 LP) were used for feeding and discharging the reactor. Water was circulated in the reactor jacket using a circulating hot water bath (Endocal RTE-8), in order to maintain the reactor contents at 28.5°C. The reactor contents were aerated at a rate of 800 ml min^{-1} by using an air pump. When required, the air stream was enriched with oxygen (Industrial grade, Liquid Carbonic Ltd.) The same reactor was used in batch experiments for determination of the kinetic parameters. During batch experiments the controller was not activated

5.2 Analytical Procedures

5.2.1 Biomass Assay

The total biomass concentration in the reactor was determined by measuring the optical density of the samples. This method has been widely practiced as reported in the literature (79). The optical density was measured with a spectrophotometer (Varian-DMS 200) at a wavelength of 540 nm, with deionised water as the reference sample. A calibration plot was prepared between optical density and biomass concentration[1] as follows: *P. putida,* was grown in the synthetic growth medium, with phenol as the sole carbon and energy

[1]The units of concentration used in this study are g m^{-3}. In the literature on hazardous wastes it is more common to see the unit of parts per million (ppm). However, there is an ambiguity whether it is on a weight/weight, weight/volume, or volume/volume basis.

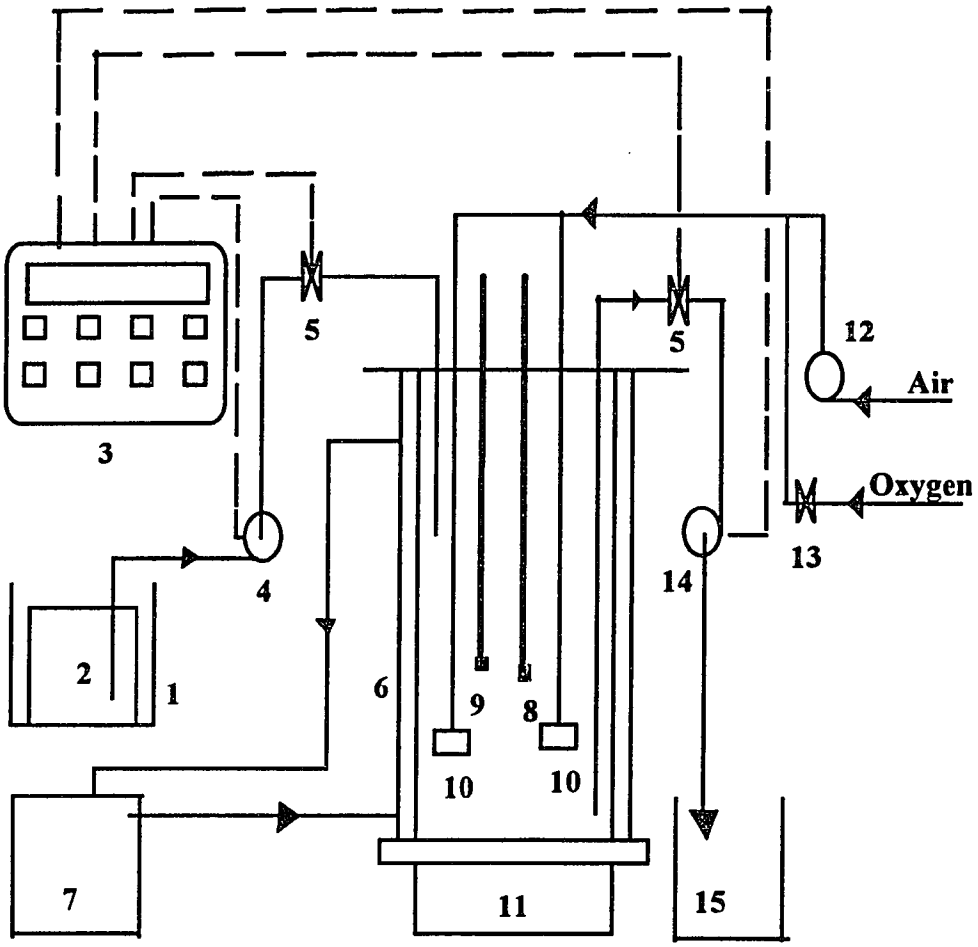

Figure 5.1 : Schematic of the experimental unit: (1) constant temperature water bath for feed tank; (2) feed tank, i.e., closed tank containing the untreated waste; (3) programmable sequence controller which is used for automating the SFBR cyclic mode of operation; (4) peristaltic feed pump; (5) solenoid valve; (6) jacketed reactor; (7) circulating water bath; (8) thermometer; (9) dissolved oxygen (D.O.) probe; (10) air diffusion tubes; (11) magnetic stirrer; (12) air pump; (13) oxygen regulating valve; (14) peristaltic discharge pump; (15) discharge tank.

source. The biomass was collected by filtration using a Nylaflo Membrane filter (No 66600, Gelman Sciences Inc., Ann Arbor, MI), and was resuspended in deionised water. This ensured that the salts present in the growth medium would not be present when the weight of the biomass was determined. The optical density of this biomass resuspension was measured and subsequently a 100 ml sample was dried, on aluminum pans, at 60°C in order to determine the weight of the biomass. The original biomass resuspension was diluted with different amounts of deionised water and the optical density of the resulting solutions was measured. The calibration data are given in Table 5.1 while the calibration curve is given in Figure 5.2. There is a linear relationship till an optical density of 0.6 with a slope of 273.3827 g m^{-3} per unit of optical density.

For the SFBR mode of operation, where both bacterial species were used, determination of the concentration of each individual species was required. Unfortunately, both species give rise to colonies of the same shape and size on nutrient agar. However, tests with oxi-ferm tubes (Roche Diagnostic Systems, Nutley, NJ) showed that *P. resinovorans* was citrate positive (in 24 hours) while *P. putida* was not.

On an agar medium with sodium citrate as the sole carbon source it was found that *P. resinovorans* colonies appeared after a 24h incubation at 30°C, while the appearance of *P. putida* colonies required an incubation period of at least 36h. This property led to the use of the following methodology. A 20 μl sample from the reactor was diluted with 5 ml of deionised water. A 20 μl sample of this solution was diluted again with 5ml of deionised water. If the biomass concentration was too high, 10 μl (rather than 20 μl) samples were used in the above procedure. Samples (10 μl) taken from the final solution, were spread plated on nutrient agar and sodium citrate containing agar, using L-shaped glass rods. The plates (petri dishes) were incubated for 24 h at 30°C and then, the colonies on the plates were counted using a colony counter (Gallenkamp Inc.). The ratio of the colony count (average from two plates) from sodium citrate agar plates to the colony

Table 5.1 Data of biomass concentration and corresponding optical density readings for calibration.

Sample.No	Optical Density U.O.D	Biomass Concentration g m^{-3}
1	0	0
2	0.087	21.2
3	0.167	42.4
4	0.244	63.6
5	0.320	84.8
6	0.399	106.0
7	0.473	127.2
8	0.544	148.4
9	0.604	169.6
10	0.667	190.8
11	0.733	212.0

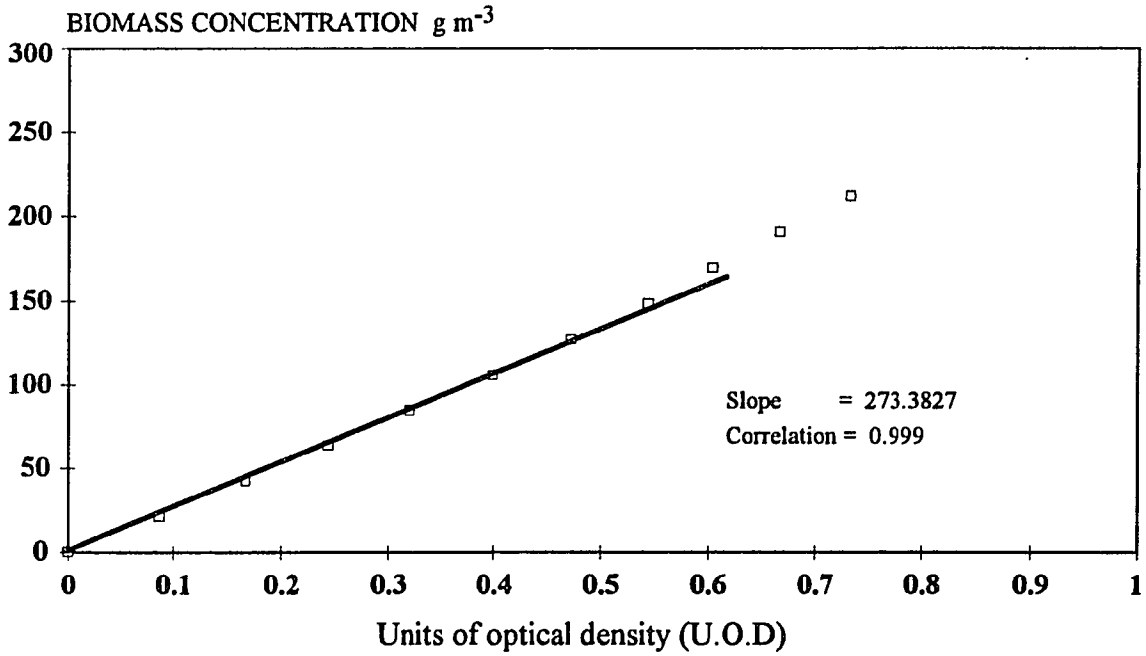

Figure 5.2: Calibration curve for determination of biomass concentration from optical density readings

Table 5.2 Data of phenol concentration and corresponding peak area from HPLC measurements

Phenol g m^{-3}	Area
5.02	70389
15.07	212362
25.12	345631
50.24	686040
75.36	1016599
100.48	1357182
150.72	1999270

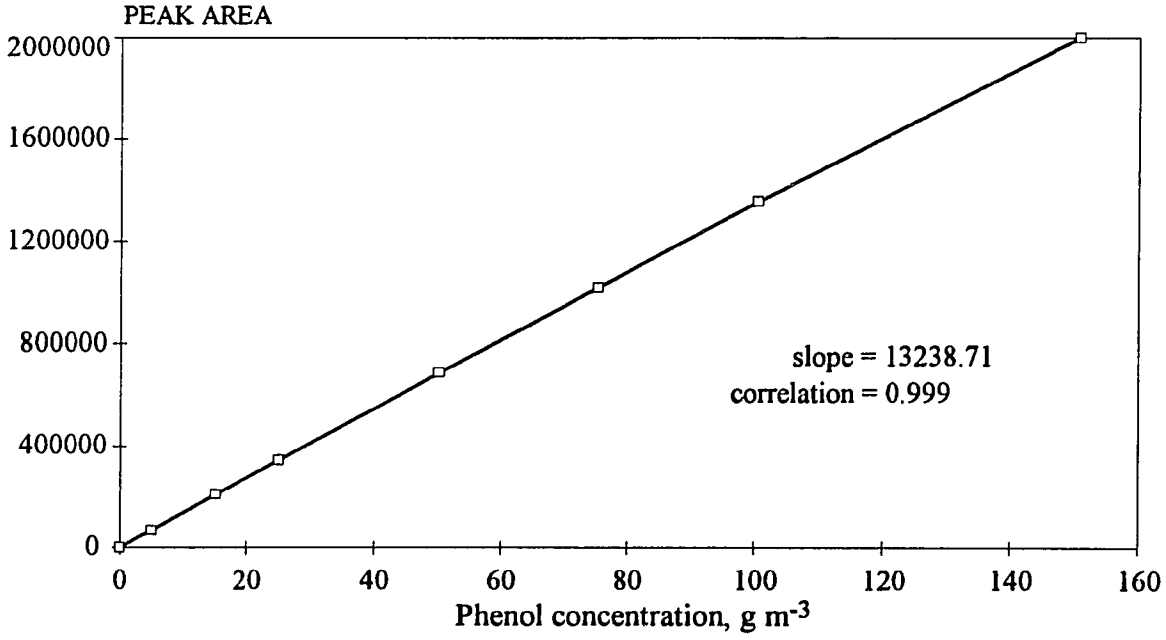

Figure 5.3 Calibration curve for determination of phenol concentration from HPLC peak area

count from the nutrient agar plates represented the fraction of the total biomass consisting of *P. resinovorans*, and was translated to biomass concentration by multiplying the total biomass (from optical density reading) with this fraction. The difference between the total biomass concentration and that of *P. resinovorans*, was the biomass concentration of *P. putida*. This approach minimized the error coming from the serial dilutions of the sample and did not require any knowledge of, or assumption regarding the size of the cells.

5.2.2 Phenol Assay

Phenol concentration was measured as follows. A sample (about 5 ml) was taken from the reactor, and a drop of 6N HCl solution was added to it to kill the microorganisms and to ensure that all phenol was in the molecular form. The sample was then filtered through a 0.2 μm filter paper (Gelman Sciences Inc., Ann Arbor, MI) and the filtrate was immediately processed on a HPLC (SP8800- Spectra Physics Analytical, Piscataway, NJ). The mobile phase was a 55:45(per volume) ratio of A:B, where A is methanol with 1% acetic acid, and B is deionized water with 1% acetic acid. The flow rate was 1 ml/min. The column used was a Lichrospher 50-RP-Select B (EM Separations, Gibbstown, NJ). The UV detector, a spectra 200 (Spectra Physics Analytical), was set at a wavelength of 280 nm. The data were processed on an IBM-compatible computer using a PE Nelson model 2600 chromatography software Rev 5.10. The data/computer interface was a PE Nelson 900 series interface (PE Nelson Systems Inc, Cuppertino, CA). A calibration curve was originally prepared and then frequently tested against standard phenol solutions to ensure the validity of the readings on actual samples. The calibration data are shown in Table 5.2

5.3 Experimental Procedure

5.3.1 Kinetics of Phenol Biodegradation

The kinetics of phenol biodegradation were studied in pure culture batch experiments with each one of the species employed. A number of batch experiments were performed, with

each one of the species, with initial phenol concentrations in the range of 20 to 180 g m^{-3}. In all experiments the initial biomass concentration was kept low (about 4 g m^{-3}). Small inocula lead to an extended exponential growth phase, thus allowing for enough data collection for determination of the kinetics. The pure cultures, grown in nutrient broth solution, were initially acclimatized to the synthetic medium containg phenol as the sole carbon and energy source at a concentration of 100 g m^{-3} as follows. A 2 ml sample from the culture which was cultivated in the nutrient broth, was transferred in 100 ml of the synthetic medium and placed in an incubator shaker (250 rpm) at 28°C until all phenol had been depleted. At that point, a 2 ml sample was transferred in 100 ml of fresh synthetic medium, to form the secondary culture, and the procedure was repeated once more to get the tertiary culture. When phenol had been depleted again, the culture was declared a stock culture and inocula were taken from it to run experiments at various phenol concentrations. The stock cultures were maintained by spiking them periodically with phenol and by occasionally transferring a loop to fresh medium, when it was felt that chemicals other than phenol needed replenishment.

The batch experiments were performed in the jacketed lucite reactor shown in Figure 5.1 with a working volume of 1.5 liters. Before each experiment the reactor was cleaned with a dilute solution of hydrogen peroxide to avoid any contamination and then thoroughly washed with water. The synthetic medium with the desired initial phenol concentration was loaded to the reactor at 28.5°C and inoculated with the acclimatized culture. The inoculum size was such that the initial biomass concentration was around 4 g m^{-3} (optical density = 0.015). The temperature of the reactor contents was maintained at 28.5°C, while the pH of the synthetic medium was 7.2. Samples of about 5ml were drawn at intervals of about 15 minutes to measure the biomass and phenol concentration. The pH, dissolved oxygen and temperature were also measured.

5.3.2 SFBR Experiments

The reactor was operated in the cyclic mode by activating the programmable timer. During the fill phase, the feed rate was constant and the volume of the reactor contents increased from the V_0 to V_m. In the second phase, the reactor operated in a batch mode. The contents of the reactor were drawn down to V_0 in the third phase. Immediately after the end of the third phase the cycle repeated itself. The synthetic waste with the desired phenol concentration was prepared in 20 liter feed tanks and sterilized in an autoclave. The tubing was also sterilized, and the reactor cleaned with a dilute solution of hydrogen peroxide and thoroughly washed with water, before each experiment. SFBR experiments were first performed with each of the two species (pure culture) in order to see if the model could describe these simpler systems before starting the more complex mixed culture experiments. For mixed culture SFBR experiments the feed concentration and the initial conditions in the reactor were chosen in ways that would allow verification of the different types of behavior of the system predicted by the preprepared operating diagram. The total biomass and phenol concentration were determined as in the case of a batch reactor. Individual biomass concentrations were also measured at appropriate intervals by spread plating the samples on nutrient agar and citrate based agar plates as explained earlier. The dissolved oxygen was carefully monitored. If the dissolved oxygen fell below 85% of its saturation value in water, pure oxygen was mixed with the airstream used for aeration. The experiments were allowed to run for a prolonged period of time in order for the system to reach its eventual steady cycle.

Wall growth was not observed. Furthermore, attachment of cells to the walls of the lucite reactor (to form invisible mono- or oligo- layers) did not seem to occur. This was confirmed as follows. At the end of some preliminary experiments, the reactor was completely drained, filled with tap water and drained again, and finally filled with the synthetic waste. The vessel was allowed to run (in batch mode) over a long period of time and was aerated as during the actual experiments. The measurements indicated that no

change occured in the phenol concentration which implied that cells of the two species did not attach to the lucite. However, attachment of biomass to the air dispersion tubes was observed during preliminary runs. In susequent experiments, the air dispersion tubes were changed frequently in order to avoid interference from this phenomenon.

CHAPTER 6

RESULTS AND DISCUSSION

6.1 Determination of Kinetic Parameters

The kinetics of phenol biodegradation were determined from batch experiments. The initial biomass concentration was kept low (about 4 g m^{-3}) in all experiments. If the initial biomass concentration b_0, is not significantly lower than the product of the yield coefficient and the initial phenol concentration (YS_0), the growth will not be in the exponential phase (25). A semilogarithmic plot of the biomass concentration versus time was prepared for each of the experimental runs. The initial data fell on a line but data towards the end of the run deviated from linearity. In order to understand this behavior and to decide how kinetics can be best determined, a theoretical analysis of the growth in a batch reactor was performed and is presented in the following subsections.

6.1.1 Effect of Initial Biomass Concentration: The kinetic parameters of a species exhibiting inhibitory behavior (Andrews model) were chosen as $\mu^* = 0.9259\ h^{-1}$, $K_s = 11.248\ g\ m^{-3}$, $K_I = 141.142\ g\ m^{-3}$, and $Y = 0.6045$. The mass balance equations on the substrate and biomass (equations 3 and 5 of Chapter 4 with $b_2 = Q_f = 0$) were integrated using a fourth order Runge-Kutta method with double precision. Two cases were considered. The initial biomass concentration was assumed to be 10 g m^{-3} in case A and 100 g m^{-3} in case B. The initial phenol concentration in both cases was assumed to be 100 g m^{-3}.

The growth of biomass was observed by preparing a semilogarithmic plot of biomass concentration versus time. These plots are shown in Figures 6.1 and 6.2. From these figures it is clear that the exponential growth phase lasts longer when the initial biomass concentration is low. This suggests that in order to get a good number of data in

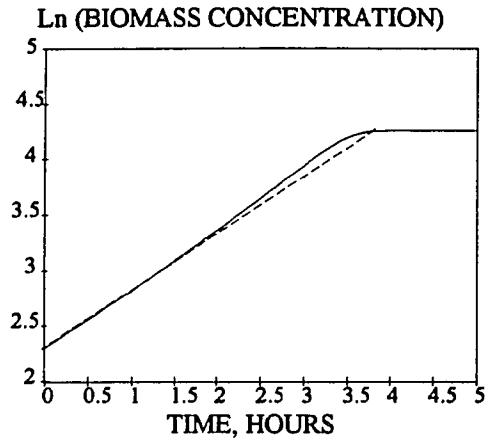

Fig 6.1: Predicted biomass concentration values versus time when b_0 = 10 g m^{-3}. Case A

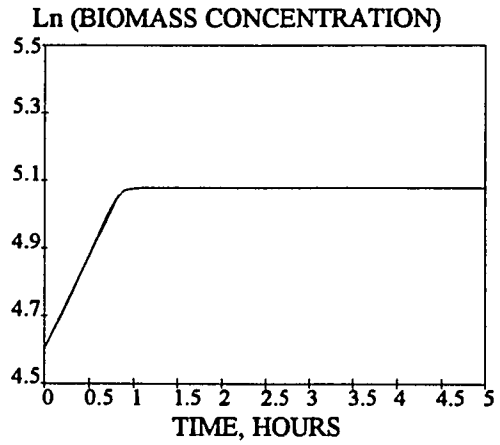

Fig 6.2: Predicted biomass concentration values versus time when b_0 = 100 g m^{-3}. Case B

the exponential phase the inoculum must be small in real experiments. It should be mentioned though that if the biomass concentration is too low, it is hard to detect its changes through optical density readings as the values fall below the minimum detectable level of the spectrophotometer. Based on these considerations it was decided to run the batch experiments with an initial biomass concentration of about 4 g m^{-3} (OD = 0.015). Furthermore, especially from Figure 6.1 it can be seen that after a certain period of time (about 2 hours for this example) there is a deviation from linearity. This deviation is an inherent feature of Andrews kinetics and suggests that not all data of the run can be considered for determining the specific growth rate.

6.1.2 Determination of the Parameters for the Specific Growth Rate Expression: For determining the parameters in the specific growth rate expression, regression of the specific growth rate values as a function of concentration to the Andrews' (or any other model) is required. Values for the specific growth rate are obtained as slopes of the linear regime of the Ln biomass versus time data. The question is whether this slope should be taken as the specific growth rate value corresponding to the substrate concentration in the

beginning of the run or to the average value of substrate concentrations in the linear regime of the Ln biomass versus time plot. To decide this, a number of numerical experiments were performed as follows. The Andrews' constants reported in the previous subsection were used and perfect biomass data were obtained and plotted as in Figure 6.1 for various initial phenol concentrations. The initial biomass concentration was assumed to be 5 g m^{-3} in all cases. The slopes were determined and attributed to either the initial phenol concentration or to the average phenol concentration of the linear regime. To further elucidate the fact that data not falling in the linear regime should not be taken into account, the procedure was repeated by using all biomass data up to the point where phenol was depleted. These generated specific growth rate values as function of phenol concentration were regressed to the Andrews model by using a non-linear regression routine based on the Gauss-Marquardt method (19). The question was which methodology would lead to values for the kinetic parameters which would be close to the originally assumed values.

Table 6.1 shows the generated data for the following cases:

Case I: Specific growth rate calculated from biomass data points in the linear regime and attributed to the initial phenol concentration.

Case II: Specific growth rate calculated from biomass data points in the linear regime and attributed to the average phenol concentration in the initial linear range.

Case III: Specific growth rate calculated from all biomass data points in the growth phase and attributed to the initial substrate concentration.

Case IV: Specific growth rate calculated using all biomass data points in the growth phase and attributed to the average substrate concentration in the growth phase.

The details of generating these data are shown in Appendix D.

Table 6.1 Substrate concentrations (initial and average) and specific growth rates

Initial Substrate concentration g m^{-3}	Average substrate concentration for the linear range g m^{-3}	Specific growth rate (initial points) h^{-1}	Average substrate concentration for all points g m^{-3}	Specific growth rate (all points) h^{-1}
20	17.287	0.5222	10.60	0.4056
25	21.925	0.5558	13.51	0.4606
30	27.04	0.5757	16.41	0.5036
35	30.40	0.5834	19.53	0.5359
40	35.35	0.5897	22.94	0.5589
60	50.86	0.5827	31.34	0.5684
80	73.12	0.5531	41.345	0.5628
100	93.73	0.5184	51.41	0.5436
125	117.28	0.4799	63.25	0.5123
150	143.15	0.4419	75.60	0.4804
200	190.87	0.3834	103.75	0.4205

The regressed kinetic parameter values for the above four cases are shown in Table 6.2

Table 6.2 Regressed Andrews parameters for cases I-IV as explained in the text

	μ^*	K_S	K_I	error in regression (%)
Actual	0.9259	11.248	141.142	-
Case I	0.982	14.60	133.85	0.18
Case II	0.924	11.043	143.93	0.17
Case III	1.19	17.99	61.429	0.57
Case IV	1.139	30.729	127.65	0.75

From Table 6.2 it can be concluded that the best estimates for the kinetic parameters are obtained when the specific growth rate is calculated using the points in the linear regime, and attributing it to the average phenol concentration in that regime. It should be also mentioned that the fit of data from cases I, III, and IV is very good as can be seen from the last entry of Table 6.2 which indicates the error in the regression. Nonetheless the values obtained are far away from the actual ones.

6.1.3 Number of Kinetic Runs: The next question which arises regarding the methodology of obtaining the kinetic parameters deals with the number of runs required for an accurate estimation of the parameters. Furthermore, since in actual experiments there is always some error involved, the sensitivity of the kinetic parameter values to the experimental error needs to be found. To answer the foregoing questions numerical experiments were again performed using the same Andrews' constants as in the previous subsections. An error was introduced in the generated perfect data and the number of assumed batch runs was also varied. Four cases were again considered.

Case Ia Error of 5% in points before the maximum of the specific growth rate curve (low phenol concentrations).

Case IIa Error of 5% in points after the maximum of the specific growth rate curve (high phenol concentrations).

Case IIIa Case Ia with fewer batch runs

Case IVa Case IIa with fewer batch runs

The data for each of these cases is shown in Appendix D. The regressed values for the biokinetic parameters for the four cases above are summarized in Table 6.3. From this table,

Table 6.3 Regressed Andrews parameters for cases Ia - IVa as explained in the text

	μ^*	K_S	K_i	error in regression (%)
Actual	0.9259	11.248	141.142	-
Case Ia	0.9132	10.834	145.369	1.66
Case IIa	0.9512	12.396	140.95	2.35
Case IIIa	0.8577	7.430	161.20	0.48
Case IVa	0.9149	11.323	163.38	0.78

it is clear that even though the error from the regression used in estimating the parameters is low, there could be a significant deviation from the actual values of the parameters. This is true especially in Case IIIa where there is a deviation of 34% in the estimation of K_S. From the foregoing considerations one can conclude that the kinetic parameters are more accurately estimated when a lot of data points are available at low substrate concentrations. For this reason, in the actual experiments, a number of low initial phenol concentrations were tried. However, at very low concentrations, the results were not satisfactory. This is due to the following: For very low initial substrate concentrations, in order to have an extended exponential growth phase, the initial biomass concentrations should be very low. The practical difficulty is that very low biomass concentrations cannot be accurately determined by the spectrophotometer.

6.1.4 Experimental Determination of Kinetic Constants: The kinetics of phenol biodegradation by *P. putida* (ATCC 17514) and *P. resinovorans* (ATCC 14235) were studied in batch experiments. A typical Ln (biomass concentration) versus time plot is shown in Fig 6.3. The yield coefficient, for each kinetic run, was determined as follows: biomass and phenol concentration were regressed to the equation $b = b_0 + Y(S_0 - S)$. The biomass versus phenol concentration data corresponding to Figure 6.3 are shown in Figure 6.4. The average of the yield coefficient values from all runs with a particular species was

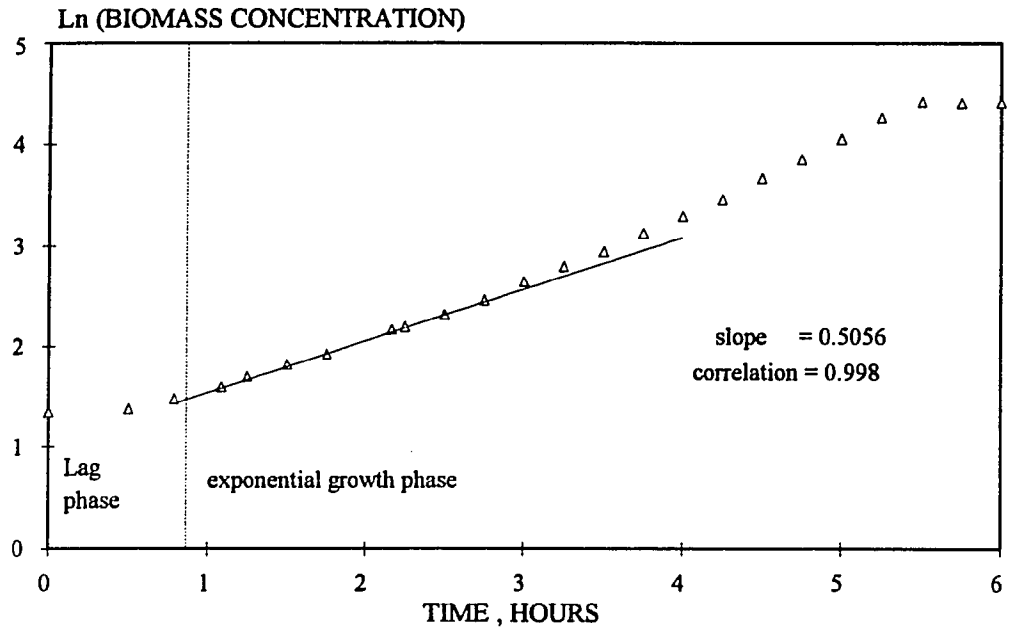

Figure 6.3 Plot of Ln biomass concentration versus time for determination of the specific growth rate of *P. resinovorans*. Run-10.

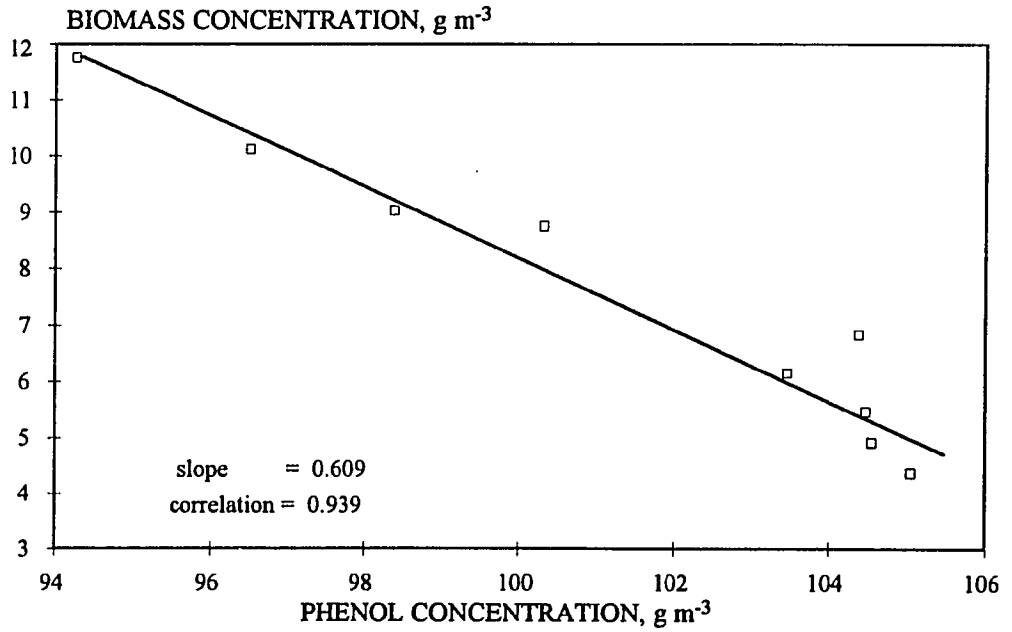

Figure 6.4 Plot of biomass concentration versus phenol concentration for the calculation of yield coefficient of *P. resinovorans*. Run-10.

taken as the yield coefficient of that species on phenol. Data and plots for the various kinetic runs with *P. resinovorans* are listed in the Appendix A (Figures A-1 to A-22). The data for *P. putida* are given in Appendix B (Figures B-1 to B-34). These data are summarized in Tables 6.4 and 6.5.

Table 6.4 Specific growth rates and yield coefficients for *P. resinovorans* (ATCC 14235)

Expt. Run	Initial Phenol Concentration g m^{-3}	Average Phenol concentration g m^{-3}	Specific growth rate, μ h^{-1}	Yield coefficient, Y (grams biomass/grams phenol)
1	19.43	16.88	0.512	0.748
2	26.85	22.71	0.567	0.589
3	37.88	34.25	0.624	0.762
4	41.08	37.81	0.644	0.804
5	57.05	52.24	0.607	0.683
6	62.38	56.56	0.5229	0.702
7	74.04	70.5	0.5875	0.685
8	92.15	83.32	0.553	0.626
9	100.24	82.95	0.4952	0.624
10	105.05	101.27	0.5056	0.609
11	150.72	144.41	0.4603	0.597

The average yield coefficient for *P. resinovorans* on phenol was 0.675 with a standard deviation of 0.075.

Table 6.5 Specific growth rates and yield coefficients for *P. putida* (ATCC 17514)

Expt. Run	Initial Phenol Concentration g m^{-3}	Average Phenol concentration g m^{-3}	Specific growth rate, μ h^{-1}	Yield coefficient, Y (grams biomass/grams phenol)
1	17.81	14.742	0.4490	0.717
2	19.31	17.796	0.5026	0.802
3	24.85	22.292	0.5518	0.786
15	26.71	19.08	0.5140	0.721
4	31.43	27.835	0.5724	0.738
5	32.86	28.024	0.5999	0.748
17	37.28	26.45	0.5711	0.724
6	41.80	34.884	0.6044	0.848
7	51.28	44.95	0.5976	0.800
8	59.40	54.645	0.5747	0.752
9	74.03	70.234	0.5978	0.781
10	77.03	74.57	0.6050	0.832
16	78.66	59.56	0.5709	0.706
11	82.64	75.45	0.5796	0.726
12	106.14	98.212	0.5495	0.812
13	124.78	122.04	0.5330	0.776
14	154.73	152.17	0.5001	0.785

The average yield coefficient for *P. putida* on phenol was 0.768 with a standard deviation of 0.042.

The specific growth rate data for the two species were regressed to the Andrews expression by using a nonlinear regression routine based on the Gauss-Marquardt method, and the values of the kinetic parameters obtained are shown in Table 6.6.

Table 6.6 Andrews parameters for *P. putida* (ATCC 17514) and *P. resinovorans* (ATCC 14235)

Species	μ^* h^{-1}	K_s $g\ m^{-3}$	K_I $g\ m^{-3}$
Pseudomonas putida (ATCC 17514)	0.897	12.204	203.678
Pseudomonas resinovorans (ATCC 14235)	1.007	12.985	117.75

The plots of the specific growth rates versus phenol concentrations are shown in Figures 6.5 and 6.6. The curves denote the predicted specific growth rate based on the kinetic parameters determined. Based on the kinetic parameters, a cross over of the two curves occurs at a single phenol concentration of 46.302 g m^{-3}. Because of the crossing of the specific growth rate curves the SFBR model predicts that if the reactor is originally inoculated with both species, coexistence of the two species is possible if the operating parameters are selected in a way such that for part of the cycle phenol concentrations favor *P. putida* and for rest of the cycle they give the competitive advantage to *P. resinovorans*.

6.2 SFBR EXPERIMENTS

6.2.1 Pure Culture Experiments: Once the kinetic parameters were determined, SFBR experiments were conducted, using only one species at a time. The conditions for the run with *P. resinovorans* (SFBR-R) were as follows

fill time	1 hour
total time	2.5 hours
Minimum volume	0.5 liters
Maximum volume	2.00 liters
Phenol concentration in feed, S_f	104.0 g m^{-3}
Initial Phenol concentration, S_0	15.11 g m^{-3}
Initial biomass concentration, b_0	62.878 g m^{-3}

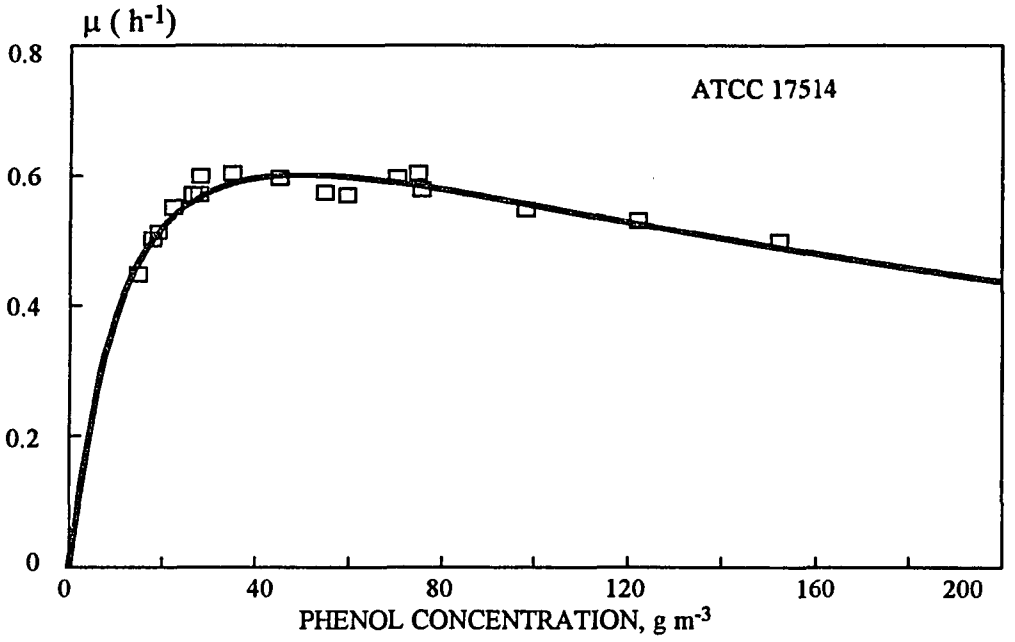

Figure 6.5 Specific growth rate curve of *P. putida* (ATCC 17514)

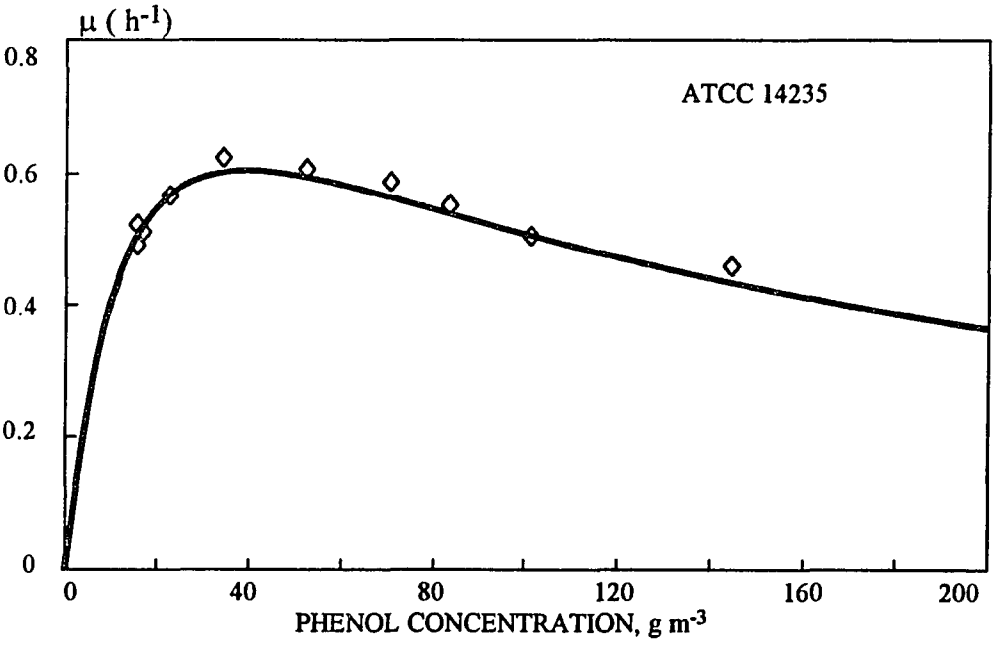

Figure 6.6 Specific growth rate curve of *P. resinovorans* (ATCC 14235)

This experiment was run for four cycles with readings taken in the first and fourth cycle. The phenol and the biomass concentration profiles for the first cycle are shown in Figures 6.7 and 6.8 respectively. The corresponding profiles for the fourth cycle are shown in Appendix C (Figures C-1 and C-2). The experimental data are also listed in the Appendix C. The curves in the plots represent model predictions based on the parameters obtained from the batch experiments and were generated by integrating equations (15)-(18) in chapter 4 with $b_2 = 0$. The integration was performed by using a fourth order Runge-Kutta method (The FORTRAN code is given in Appendix C). As can be seen from these curves there is excellent agreement between the predicted values and the observed values.

For SFBR experiments with a pure culture of *P. putida* (SFBR-P) the conditions were as follows:

fill time	0.25 hour
total time	1.5 hours
Minimum volume	2.0 liters
Maximum volume	4.0 liters
Phenol concentration in feed, S_f	61.35 g m^{-3}
Initial Phenol concentration, S_0	0.0 g m^{-3}
Initial biomass concentration, b_0	38.82 g m^{-3}

The experimental data as well as the phenol and biomass concentration profiles for the first and sixth cycle are shown in the Appendix C (Table C-2; Figures C-3 to C-6). As can be seen from these figures there is excellent agreement between the predicted and the experimentally observed values. Thus, it can be concluded that the model has the capability of predicting SFBR operation with pure cultures and that the kinetic parameters determined in batch experiments are (as expected) independent of the reactor operation mode.

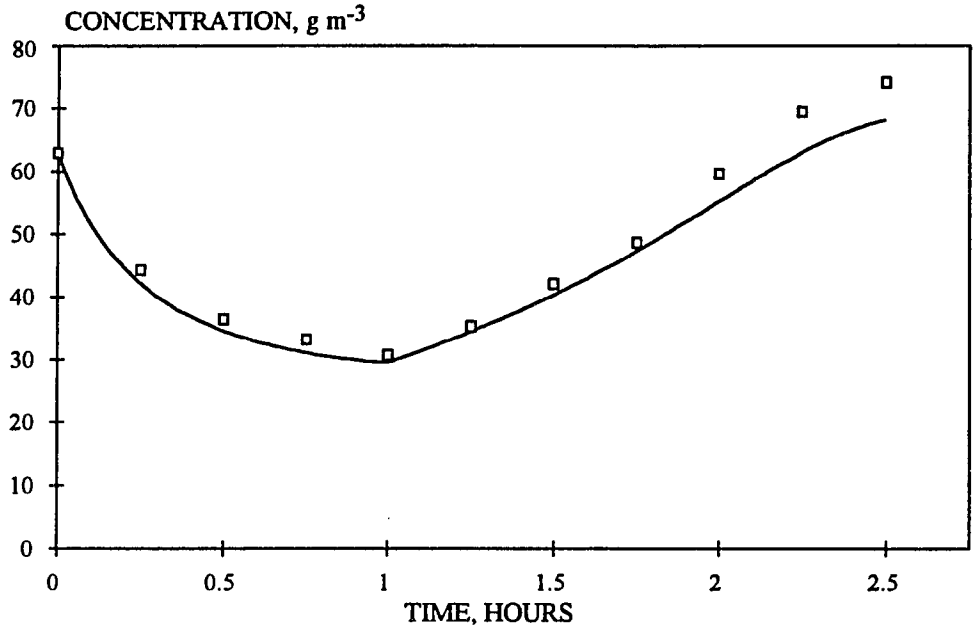

Figure 6.7 Biomass concentration profile for the first cycle of run SFBR-R with *P. resinovorans*

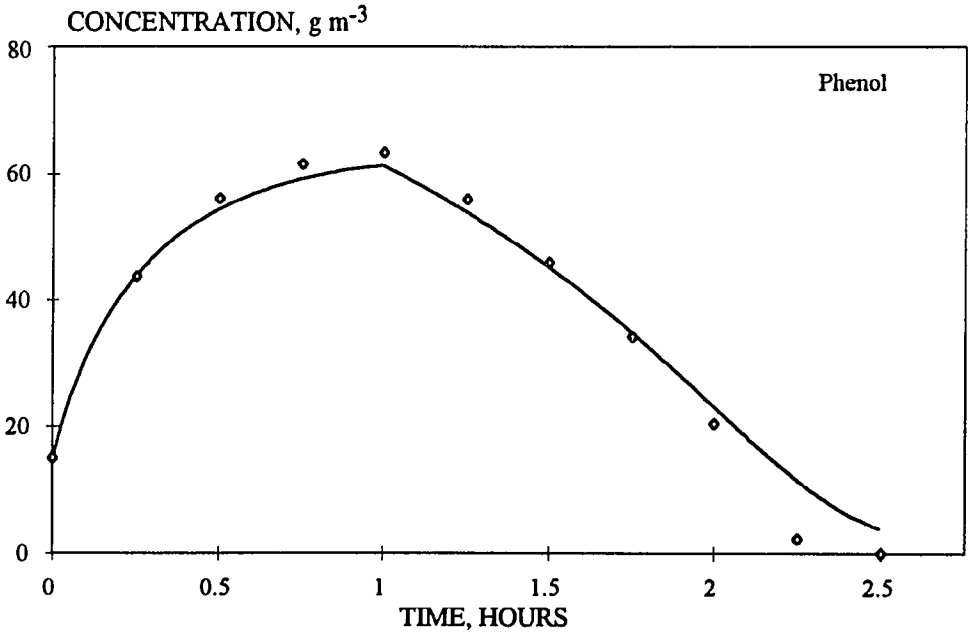

Figure 6.8 Phenol concentration profile for the first cycle of run SFBR-R with *P. resinovorans*

6.2.2 Mixed Culture Experiments

6.2.2.1 Operating Diagram: Before running SFBR experiments with mixed cultures, the model equations (15)-(18) (Chapter 4) were used in numerical studies in order to predict the various types of behavior of the system. The model contains 5 parameters (γ_1, γ_2, η, ϕ, ω) which depend on kinetics and are known, and four operating parameters (β, σ_1, δ, u_f) which can be varied freely. After some initial simulations it was found that using values of $\delta = 0.25$ and $\sigma_1 = 0.40$ would help in the experiments in the sense that in most cases biomass concentrations would not be excessive. For these values an operating diagram was prepared. This diagram, shown in Figure 6.9, indicates what will be the behavior of the SFBR under various phenol concentrations in the untreated waste (u_f) and various β-values which indicate the hydraulic residence time in the reactor. The specific parameter values used for preparing the operating diagram are ,

γ_1 = 0.059918
γ_2 = 0.103665
δ = 0.25
η = 1.137778
σ_1 = 0.40
ϕ = 1.122631
ω = 1.063995

The numerical methods used in preparing the diagram were discussed in Chapter 2. The character of each periodic state of the system in the various regions of the diagram is shown in Table 6.7. It is observed that stable coexistence of the two species is possible in regions 13, 14, 15. Thus, if the operating conditions are such that they define a point in one of these regions, the system is predicted to operate in a state of periodic coexistence. In regions 13 and 14 the coexistence state is the only one which is stable and therefore, the system will reach this state regardless of the start-up conditions. However, in region 15 multistability, i.e., more than one stable state, is observed. Therefore, depending on the

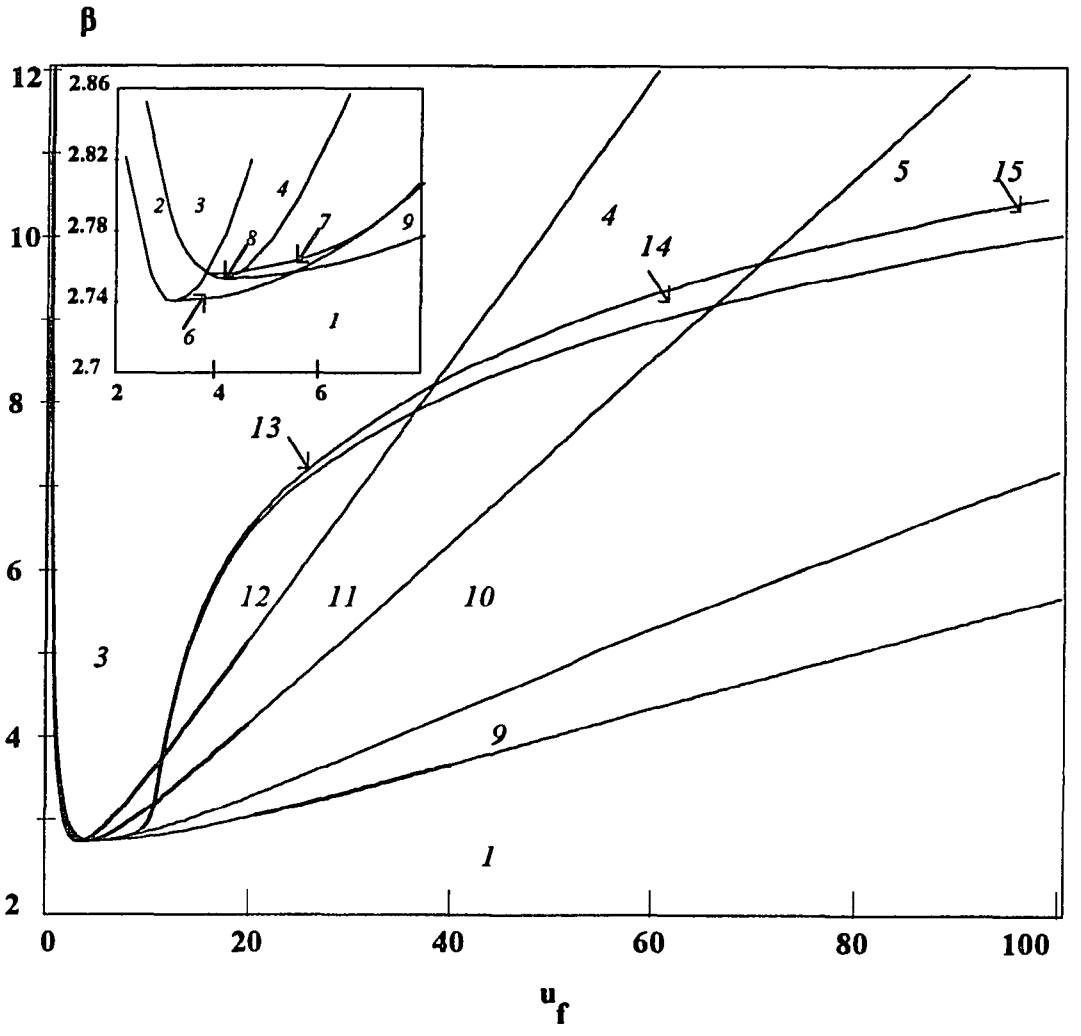

Fig 6.9 Operating diagram for the system in the β-u_f plane for σ_1=0.4 and δ = 0.25

Table 6.7 Character of each periodic state in the various regions of the operating diagram (Figure 6.9) of the system*

Region	Washout	1-state	2-state	Coexistence
1	S	-	-	-
2	D	-	S	-
3	U	D	S	-
4	D	D	S, U	-
5	S	D, D	S, U	-
6	S	-	S, D	-
7	S	S, D	S, D	-
8	D	S	S, D	-
9	S	S, D	-	-
10	S	S, D	D, U	-
11	D	S	D, U	-
12	U	S	D	-
13	U	D	D	S
14	D	D	D, U	S
15	S	D, D	D, U	S

* S: stable node or stable focus; U: unstable node or unstable focus; D: saddle (unstable). 1-state: survival of *P. Putida* only; 2-state: survival of *P. resinovorans* only.

initial conditions (start-up) the system will either reach a state of coexistence, or a state of extinction of both species (washout). Multistability is observed in other regions as well. For example in region 10, both the wash out state and the state of survival of *P. putida* only are stable. Multistability must be taken into account during operation, since some significant perturbation could move the system from one state to another.

The features of the operating diagram shown in figure 6.9 are exhibited by any system of two pure and simple competitors when both species follow Andrews' kinetics and their specific growth rate curves cross each other at a single nonzero value. It should be mentioned though that for other model parameter values, such systems have been found to have more complicated types of behavior - quasiperiodicity and chaos (52). If these curves cross each other at two values, the operating diagram is much more complex. The operating diagram is much simpler when the two curves do not cross each other. In such cases, neither coexistence nor a state where only the slower growing species survives is possible.

6.2.2.2 Description of Mixed Culture Experiments

Based on the operating diagram, regions for conducting the mixed culture experiments were selected. The basis for selecting the operating conditions for the experiments was to study all possible outcomes, i.e., survival of only one species, washout, and coexistence. The operating conditions were selected in a way which avoided very high biomass concentrations as this could lead to flocculation, oxygen limitation, mass transfer effects and possible foaming. Though these phenomena occur in real systems they were not investigated in the present study. Four experiments were performed under the conditions shown in Table 6.8 and are discussed in the following subsections.

Table 6.8 Operating conditions and initial (start-up) concentrations for mixed culture experiments

		SFBR -M1	**SFBR -M2**	**SFBR -M3**	**SFBR -M4**
fill time	t_1 (h)	1.2	1.2	1.2	2.75
"react" time	t_2 (h)	2.75	2.75	2.75	6.625
draw time	t_3 (h)	3.0	3.0	3.0	6.875
reference flow rate	Q_f^* (L h^{-1})	1.25	1.25	1.25	0.5454
phenol concentration in feed	S_f (g m^{-3})	79.15	202.76	202.76	503.26
initial phenol concentration in the reactor	S_0 (g m^{-3})	5.03	0	0	0
initial concentration of *P. putida* in the reactor	$b_{1,0}$ (g m^{-3})	10.0	20.0	10.0	25.59
initial concentration of *P. resinovorans* in the reactor	$b_{2,0}$ (g m^{-3})	59.21	56.20	10.0	16.93
minimum volume	V_0 (L)	0.5	0.5	0.5	0.5
maximum volume	V_m (L)	2.0	2.0	2.0	2.0
dimensionless feed concentration	u_f	6.4856	16.6142	16.6142	41.2373
dimensionless measure of hydraulic residence time	β	3.588	3.588	3.588	8.223
Region in Figure 6.9		3	10	10	14

Run SFBR-M1: The conditions (β and u_f) for this experiment define a point in region-3 of the operating diagram. The prediction is that the only possible steady state for the system is one in which only *P. resinovorans* (ATCC 14235) survives. The reactor was initially inoculated with both species. Figure 6.10 shows the experimental and predicted values for *P. resinovorans* concentration during the 1st, 6th, and 24th cycle of operation. The profiles for the concentration of phenol, total biomass, and biomass of *P. putida* as well as the experimental data are given in Appendix C (Table C-3; Figures C-7 to C-9). The experiment was stopped after the 24th cycle since the concentration of the total biomass was practically equal to the biomass concentration of *P. resinovorans*. As can be seen from the figures there is excellent agreement between the experimental data and theoretical predictions.

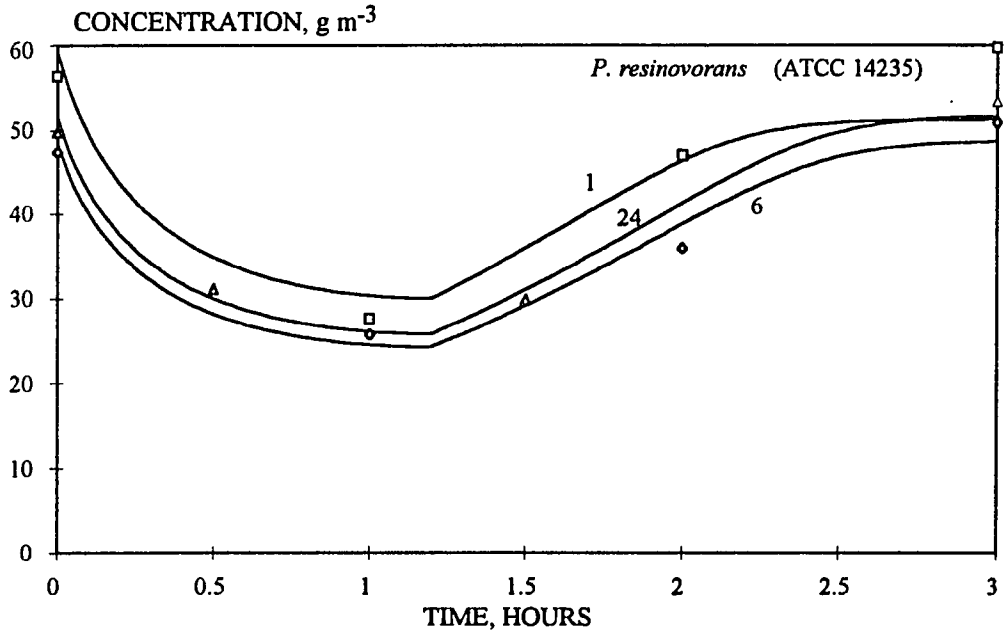

Figure 6.10 *P. resinovorans* biomass concentration profiles for the 1st, 6th, and 24th cycle of SFBR-M1. Curves indicate model predictions. The data are correspondingly represented by □, ◇, and △.

Runs SFBR-M2 and SFBR-M3: The conditions (β and u_f) for these experiments define a point in region 10 of the operating diagram. The difference between these two experiments is in the initial biomass concentrations. Depending on the start-up conditions the prediction is that the system would reach either a state where no population survives (washout), or a state where only *P. putida* survives.

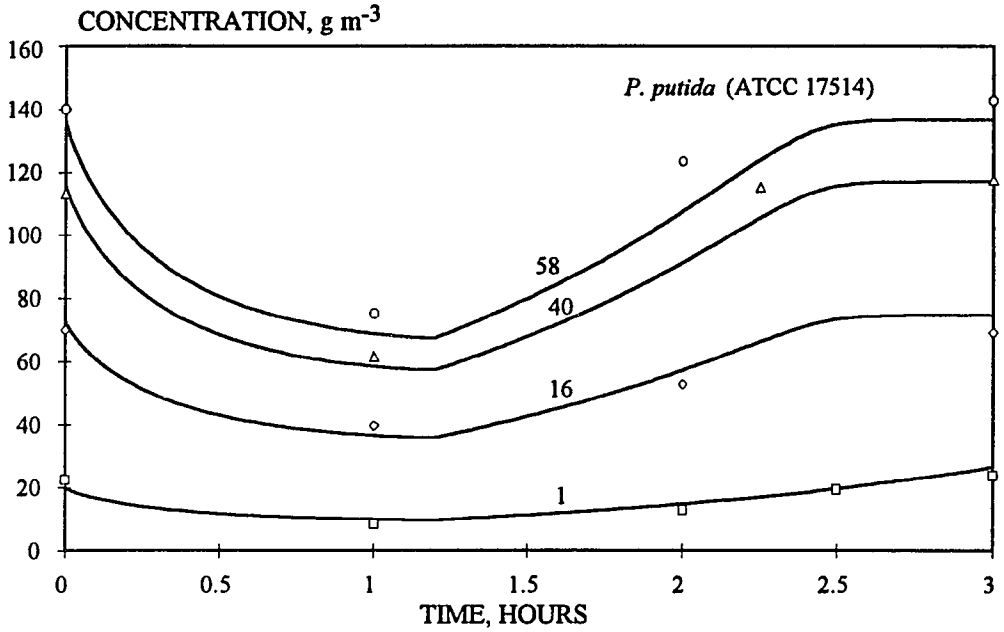

Figure 6.11 *P. putida* biomass concentration profiles for the 1st, 16th, 40th, 58th cycle of SFBR-M2. Curves represent model predictions. The data are correspondingly represented by □, ◇, △, and ○.

Under the initial biomass concentrations for SFBR-M2 the model predicted that *P. putida* would survive. The biomass concentration of *P. resinovorans* which was predicted to washout, was initially three times higher than that of *P. putida*. This was done in order to verify the model predictions under the "worst scenario". Figure 6.11 shows the experimental and the predicted values for *P. putida* for the 1st, 16th, 40th and 58th cycle. The corresponding figures for the concentrations of phenol, total biomass, and biomass of *P. resinovorans* (Figures C-10 to C-12) as well as the experimental data (Table C-4) are

given in Appendix C. The dynamics are slow but they clearly indicate the survival of *P. putida* while *P. resinovorans* moves toward complete elimination from the reactor. Again, there is excellent agreement between the data and model predictions.

For SFBR-M3, the initial biomass concentration was such that the predicted outcome was the washout of both species. The initial biomass concentrations of both species were equal. Only the total biomass concentration was measured as the predicted outcome was washout. Figure 6.12 shows the phenol concentration profiles for the 1st and 24th cycle. The experimental data (Table C-5) as well as the profiles of the total biomass (Figure C-13) are given in Appendix C. Clearly, the system is proceeding towards total biomass washout. Experiments SFBR-M2 and SFBR-M3 demonstrated that multiple outcomes are possible under the same operating conditions.

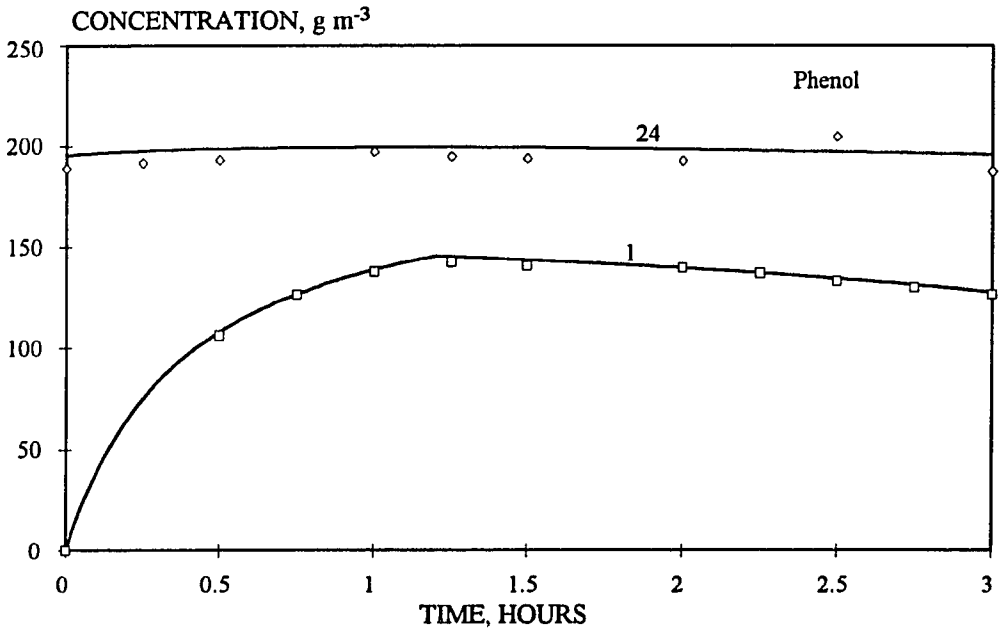

Figure 6.12 Phenol concentration profiles for the 1st and 24th cycle of run SFBR-M3. Curves represent model predictions. The data are correspondingly represented by □, and ◇.

Run SFBR-M4: This experiment was performed under conditions which fall in region 14 of the operating diagram. The theoretical prediction is that the only possible state for the system is that of coexistence of the two species. The experiment was started with very low biomass concentrations even though the prediction was that both species would achieve high concentrations in the steady cycle. The data and the model predictions for the first cycle are shown in Figures 6.13 and 6.14. The experimental data (Table C-6) as well as the concentration profiles of phenol, total biomass, biomass of *P. putida* and biomass of *P. resinovorans* (Figures C-14 to C-17) are shown in the Appendix C. Figures C-14 to C-17 show the data and model predictions for the 21st and the 28th cycle. There is a clear indication that the biomass concentration of both species increases. Furthermore, while the phenol and total biomass concentration reach the steady cycle relatively fast, the individual biomass concentrations exhibit very slow dynamics. The model predicts that it would take about 1400 cycles to reach the steady cycle. For this reason, the system was perturbed by increasing the concentration of *P. resinovorans*. This species was grown separately in pure culture, and a certain volume of this suspension was added to the mixed culture at the end of the 28th cycle. The concentrations and volumes were selected in a way such that the composition of the mixed culture would represent a point on the steady cycle. Figures C-14 to C-17 also show the data and the predicted values for the 4th and 11th cycle after the perturbation. Clearly the system reached a steady cycle of coexistence as predicted by the model.

During the initial operation of the reactor under conditions of SFBR-M4 the dissolved oxygen concentration levels fell to very low values. For this reason, oxygen was mixed with air before it entered the reactor, so that the dissolved oxygen levels were maintained above 6.8 g m^{-3}. Furthermore, the high biomass concentrations obtained in SFBR-M4 led to a higher dilution requirement for the samples before plating. This may explain why the agreement between the data and model predictions for individual biomass concentrations

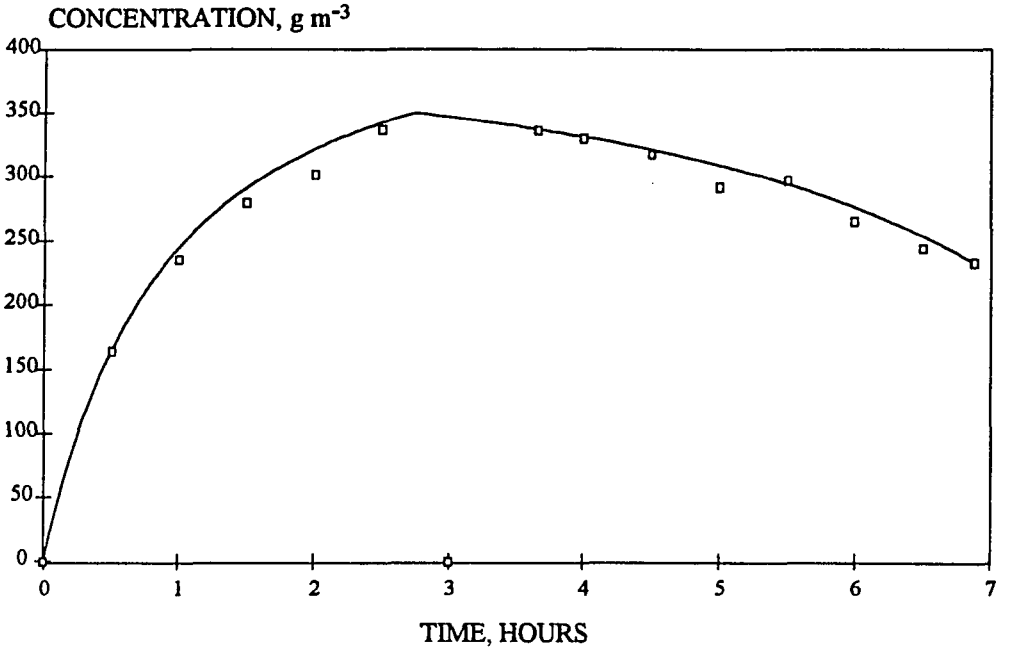

Figure 6.13 Phenol concentration profile for the 1st cycle of SFBR-M4. Curve represents model prediction

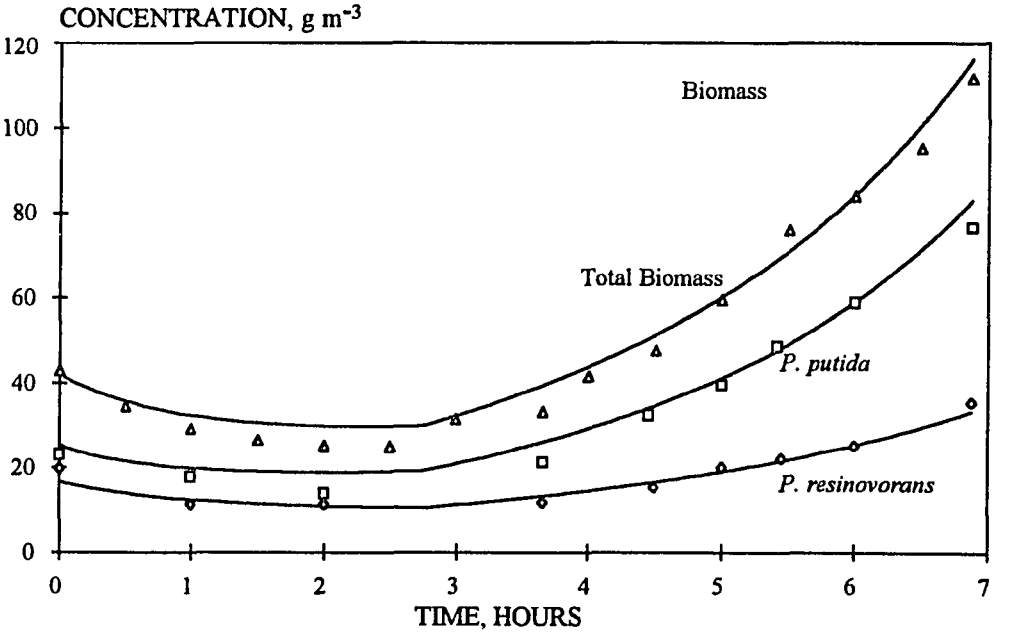

Figure 6.14 Biomass concentration profiles for the 1st cycle of SFBR-M4. Curves represent model predictions.

is not as good as in other experiments. Finally, the cycle time shown in Figures C-14 to C-17 is 4 hours even though it is reported as 6.875 hours in Table 6.8. Actually, phenol gets totally depleted in the first three hours of the cycle; for this reason after 15 cycles, the cycle time was set at 4 hours.

It can be concluded from these experiments that the model equations describe the system very well. All model predictions were experimentally validated and it should be emphasized that this is the first experimental demonstration of coexistence of two pure and simple competitors in a reactor which has periodically varying inputs.

CHAPTER 7

CONCLUSIONS AND RECOMMENDATIONS

In this dissertation the dynamics of pure and simple competition between two species in a sequencing fed-batch reactor were studied both at the theoretical and the experimental level. This study offers the first experimental demonstration of coexistence of two pure and simple competitors in a spatially homogeneous reactor having a time dependent input flowrate. A detailed model has been derived, numerically solved, and experimentally validated. Predictions of complex dynamics and multiple outcomes under certain operating conditions have been experimentally shown to actually occur. The model is primarily based on the kinetics of utilization of the substrate competed for by the two populations. Kinetic expressions were revealed from independent pure culture batch experiments and for phenol, they were found to follow Andrews' inhibitory expression.

A systematic study has been performed regarding the methodology for obtaining the kinetic parameters in the Andrews expression. The results suggest that batch experiments need to be performed with low initial biomass concentrations and for a wide spectrum of initial substrate (phenol) concentrations. The values of kinetic parameters are more sensitive to rates obtained at low concentrations, thus more experiments are needed in the non-inhibitory region rather than at high (inhibitory) concentrations. For small initial biomass concentrations an exponential growth phase can be identified (linear region on a semi-log plot). The slope is the specific growth rate corresponding to the average substrate concentration during the exponential growth phase. The common practice of attributing the specific growth rate to the initial substrate concentration seems incorrect.

Regarding coexistence, it can be concluded that it requires the crossing of the specific growth rate curves of the two competitors at least at one, non-zero, value of the substrate concentration. The crossing of the specific growth rate curves of the two

populations employed in this study occurs at S_c = 46.302 g m^{-3} (or u_c = 2.96). In the operating diagram (Figure 6.9), the region where coexistence of two populations occurs, originates from the point $u_f = 3.793 = u_c$.

The implications of the results of this dissertation for the degradation of hazardous wastes may be illustrated by the following hypothetical example. Suppose that, as is true in many cases, a mixed unidentified culture is to be used. Initial studies are performed in batch experiments to determine the kinetics of biodegradation, and the biomass is treated as a single population. These kinetics are only apparent expressions and depend on the biomass composition. Then, a pilot SFBR study is conducted in a particular region of the operating diagram, say region 11 of Figure 6.9. The biomass composition changes with time and thus, the pilot data cannot be properly explained based on small scale experiments. If the pilot unit is operated long enough, one (or some) species will washout and performance will be stabilized. If these data are used for the final design, and as a safety factor the hydraulic residence time (β) is increased, the system will find itself in another region of the operating parameter space. Assume for example that the pilot unit is run at $u_f = 35$ and $\beta = 7.5$, and that the design of the actual unit is for $u_f = 35$ and $\beta = 8.5$. The system moves from region 11 to region 3, and if the original inoculum used in the pilot and the full-scale unit is the same, the steady-cycle biomass composition differs between the two units. The significance of the resulting scale-up error depends on the difference in the biokinetic parameters of the two species

Another example where a mixed culture is actually needed is as follows. Consider a waste which contains recalcitrant pollutants, A and B. Assume that two strains, M and N are isolated or developed and have the ability to co-metabolize pollutants A and B, respectively. Co-metabolism of a compound implies that it cannot serve either as energy or carbon source for the bacteria; the transformation is a side effect of the growth of bacteria on another (primary) substrate. If the same primary substrate is used for species M and N, then they compete for it. Thus, treatment of pollutants A and B in the same vessel is

impossible unless a mixed culture of species M and N is maintained. Random selection of experimental conditions would lead to a lengthy and costly process development phase. This study indicates where (regions 13,14, and 15 of Figure 3) the experiments should really be performed.

Now that a mathematical model which has been fully validated with experiments exists, a number of further studies can be performed. One can optimize SFBR design and operation by proper selection of operating parameters such as σ_1 (indicating slow or fast fill), δ (indicating the fraction of the reactor contents which should remain in the reactor at the end of a cycle), and β (hydraulic residence time). Optimization can be performed subject to constraints, such as "maintain a mixed culture", or maintain species which can persist in Ω", where Ω is a prespecified domain of the operating parameter space. The objective function for optimization can be either based on the capital cost or on maximum throughput for a given reactor volume. These optimization studies would need development of proper computer software since most existing programs are for steady state rather than for periodic operation of a reactor.

It is believed that the present study contributes towards a fundamental understanding of SBR (or SFBR) technology. At the same time it is realized that more complex systems need now to be studied. Such systems should involve multiple substrates (i.e., mixed wastes). Mixed substrates may lead to cross-inhibitory effects or to cometabolism. Such topics are of interest and it is recommended that they be studied in the future. Furthermore, questions on oxygen limitation, flocculation, and settling of biomass should also be addressed at a fundamental level. Finally, it is recommended that a closer collaboration of engineers and microbiologists be established in order to effectively address questions such as methods for fast and easy species identification, and possible formation of stable intermediates during biodegradation of complex wastes.

APPENDIX A

Experimental Data for *Pseudomonas resinovorans* (ATCC 14235)

The experimental data for determination of the specific growth rate and yield coefficient of *Pseudomonas resinovorans* (ATCC 14235) on phenol are given in this appendix. Tables A-1 to A-11 list the experimental data for the eleven batch experiments. The odd numbered figures show the plots of Ln biomass concentration versus time for the determination of the specific growth rate. The even numbered figures show the plots of biomass concentration versus phenol concentration for the determination of the yield coefficient. Yield coefficients were determined based on the data used for determining the specific growth rate (linear regime of the Ln biomass concentration versus time plot).

Table A-1 Run-1. The exponential growth phase began at t = 1.0 h. The average phenol concentration in the linear regime was 16.88 g m^{-3}

Sample No.	Time h	Optical density	Biomass concentration g m^{-3}	Ln (Biomass concentration)	Phenol concentration g m^{-3}
1	0	0.017	4.64750	1.53633	19.43
2	0.5	0.020	5.46765	1.69885	19.39
3	0.75	0.022	6.01442	1.79416	18.76
4	1	0.024	6.56118	1.88117	18.18
5	1.25	0.027	7.38133	1.99895	16.84
6	1.5	0.031	8.47486	2.1371	15.63
7	1.833	0.039	10.66193	2.36668	12.62
8	2.25	0.048	13.12237	2.57432	9.23
9	2.533	0.061	16.67634	2.81399	3.99
10	3	0.077	21.05047	3.04692	0
11	3.25	0.076	20.77708	3.03385	0
12	3.5	0.076	20.77708	3.03385	0
13	3.75	0.076	20.77708	3.03385	0

Table A-2 Run-2. The exponential growth phase began at t = 0.8 h. The average phenol concentration in the linear regime was 22.71 g m^{-3}

Sample No.	Time h	Optical density	Biomass concentration g m^{-3}	Ln (Biomass concentration)	Phenol concentration g m^{-3}
1	0	0.012	3.28059	1.18802	27.9
2	0.25	0.012	3.28059	1.18802	27.51
3	0.5	0.013	3.55398	1.26807	26.85
4	0.8	0.014	3.82736	1.34217	26.15
5	1.033	0.0165	4.51081	1.50648	24.84
6	1.25	0.019	5.19427	1.64756	23.33
7	1.583	0.022	6.01442	1.79416	22.6
8	1.75	0.026	7.10795	1.96121	20.72
9	2	0.029	7.9281	2.07041	18.62
10	2.25	0.034	9.29501	2.22948	17
11	2.5	0.041	11.20869	2.41669	15.98
12	2.7833	0.049	13.39575	2.59494	12.46
13	3	0.062	16.94973	2.83025	8.94
14	3.25	0.073	19.95694	2.99358	4.14
15	3.5	0.088	24.05768	3.18045	0
16	3.75	0.091	24.87782	3.21398	0
17	4	0.091	24.87782	3.21398	0

Table A-3 Run-3. The exponential growth phase began at t = 1.0 h. The average phenol concentration in the linear regime was 34.25 g m^{-3}

Sample No.	Time h	Optical density	Biomass concentration g m^{-3}	Ln (Biomass concentration)	Phenol concentration g m^{-3}
1	0	0.013	3.55398	1.26807	37.88
2	0.25	0.012	3.28059	1.18802	37.94
3	0.667	0.013	3.55398	1.26807	37.38
4	1 0	0.015	4.10074	1.41117	36.48
5	1.25	0.018	4.92089	1.59349	35.62
6	1.5	0.02	5.46765	1.69885	35.15
7	2 0	0.029	7.9281	2.07041	31.93
8	2.333	0.036	9.84178	2.28664	28.99
9	2.66	0.046	12.5756	2.53176	25.78
10	3	0.059	16.12958	2.78065	20.78
11	3.33	0.079	21.59723	3.07257	13.37
12	3.833	0.124	33.89945	3.5234	0
13	4.25	0.124	33.89945	3.5234	0

Table A-4 Run-4. The exponential growth phase began at t = 0.833 h. The average phenol concentration in the linear regime was 37.81 g m^{-3}

Sample No.	Time h	Optical density	Biomass concentration g m^{-3}	Ln (Biomass concentration)	Phenol concentration g m^{-3}
1	0	0.013	3.55398	1.26807	43.79
2	0.25	0.015	4.10074	1.41117	43.93
3	0.5	0.0165	4.51081	1.50648	43.42
4	0.833	0.018	4.92089	1.59349	41.08
5	1	0.0205	5.60435	1.72354	40.96
6	1.333	0.026	7.10795	1.96121	40.07
7	1.583	0.03	8.20148	2.10431	38.3
8	1.75	0.033	9.02163	2.19962	37.06
9	2	0.038	10.38854	2.3407	34.87
10	2.25	0.046	12.5756	2.53176	32.34
11	2.55	0.058	15.8562	2.76356	27.67
12	2.75	0.069	18.86341	2.93722	23.66
13	3.05	0.087	23.78429	3.16903	16.93
14	3.25	0.1	27.33827	3.30829	11.84
15	3.5	0.123	33.62607	3.5153	3.32
16	3.75	0.141	38.54696	3.65188	0
17	4	0.143	39.09373	3.66596	0
18	4.5	0.141	38.54696	3.65188	0

Table A-5 Run-5. The exponential growth phase began at t = 0.75 h. The average phenol concentration in the linear regime was 52.24 g m^{-3}

Sample No	Time h	Optical density	Biomass concentration g m^{-3}	Ln (Biomass concentration)	Phenol concentration g m^{-3}
1	0	0.011	3.00721	1.10101	57.09
2	0.25	0.011	3.00721	1.10101	58.13
3	0.5	0.011	3.00721	1.10101	56.57
4	0.75	0.011	3.00721	1.10101	57.05
5	1	0.013	3.55398	1.26807	56.75
6	1.25	0.015	4.10074	1.41117	55.92
7	1.75	0.019	5.19427	1.64756	54.12
8	2.0833	0.023	6.2878	1.83861	53.03
9	2.4167	0.029	7.9281	2.07041	49.2
10	2.75	0.038	10.38854	2.3407	48.1
11	3	0.044	12.02884	2.48731	43.78
12	3.25	0.055	15.03605	2.71045	40.32
13	3.5833	0.073	19.95694	2.99358	33.93
14	4.0833	0.108	29.52533	3.38525	20.2
15	4.4166	0.158	43.19447	3.76571	2.93
16	4.75	0.175	47.84197	3.8679	0
17	5	0.175	47.84197	3.8679	0

Table A-6 Run-6. The exponential growth phase began at t = 0.75 h. The average phenol concentration in the linear regime was 56.56 g m^{-3}

Sample No.	Time h	Optical density	Biomass concentration g m^{-3}	Ln (Biomass concentration)	Phenol concentration g m^{-3}
1	0	0.0125	3.41728	1.22885	62.38
2	0.25	0.013	3.55398	1.26807	61.67
3	0.5	0.0135	3.69067	1.30587	61.8
4	0.75	0.015	4.10074	1.41117	61.34
5	1	0.016	4.37412	1.47571	60.58
6	1.25	0.018	4.92089	1.59349	59.6
7	1.5	0.02	5.46765	1.69885	58.68
8	1.75	0.023	6.2878	1.83861	57.76
9	2	0.026	7.10795	1.96121	56.31
10	2.25	0.029	7.9281	2.07041	55.12
11	2.5	0.033	9.02163	2.19962	53.06
12	2.75	0.038	10.38854	2.3407	51.4
13	3	0.045	12.3022	2.50978	49.22
14	3.25	0.053	14.48928	2.67341	46.15
15	3.5	0.061	16.67634	2.81399	42.82
16	3.75	0.069	18.86341	2.93722	38.16
17	4	0.079	21.59723	3.07257	33.27
18	4.25	0.097	26.51812	3.27783	26.83
19	4.5	0.118	32.25916	3.4738	18.31
20	4.75	0.138	37.72681	3.63037	11
21	5	0.174	47.56859	3.86217	0
22	5.25	0.178	48.66212	3.8849	0
23	6	0.178	48.66212	3.8849	0

Table A-7 Run-7.The exponential growth phase began at t = 0.5 h. The average phenol concentration in the linear regime was 70.50 g m^{-3}

Sample No.	Time h	Optical density	Biomass concentration g m^{-3}	Ln (Biomass concentration)	Phenol concentration g m^{-3}
1	0	0.011	3.00721	1.10101	74.2
2	0.25	0.0135	3.69067	1.30581	73.52
3	0.5	0.0125	3.41728	1.22885	74.04
4	0.75	0.0145	3.96405	1.37727	73.09
5	1	0.016	4.37412	1.47571	71.95
6	1.333	0.02	5.46765	1.69885	69.73
7	1.583	0.023	6.2878	1.83861	70.38
8	1.85	0.027	7.38133	1.99895	68.06
9	2.0833	0.032	8.74825	2.16885	66.27
10	2.4167	0.041	11.20869	2.41669	62.99
11	2.5	0.051	13.94252	2.63494	59.13
12	3	0.062	16.94973	2.83025	55.27
13	3.25	0.074	20.23032	3.00718	50.92
14	3.5	0.092	25.15121	3.22491	44.98
15	3.75	0.108	29.52533	3.38525	37.17
16	4	0.135	36.90667	3.60839	29.3
17	4.25	0.165	45.10815	3.80906	17.75
18	4.5	0.212	57.95713	4.0597	1.065
19	5.25	0.223	60.96434	4.11029	0
20	6	0.222	60.69096	4.10579	0

Table A-8 Run-8. The exponential growth phase began at t = 1.0 h. The average phenol concentration in the linear regime was 83.52 g m^{-3}

Sample No.	Time h	Optical density	Biomass concentration g m^{-3}	Ln (Biomass concentration)	Phenol Concentration g m^{-3}
1	0.0	0.013	3.55397	1.26806	93.51
2	0.25	0.015	4.10074	1.41117	93.29
3	0.566	0.017	4.64751	1.53633	91.91
4	0.75	0.018	4.92089	1.59349	92.15
5	1	0.02	5.46765	1.69885	90.78
6	1.25	0.023	6.2878	1.83861	89.83
7	1.5	0.026	7.10795	1.96121	89.64
8	1.75	0.029	7.9281	2.07041	87.89
9	2	0.032	8.74825	2.16885	85.09
10	2.25	0.038	10.38854	2.3407	82.68
11	2.5	0.044	12.02884	2.48731	81.23
12	2.833	0.054	14.76267	2.6921	76.83
13	3	0.061	16.67634	2.81399	73.65
14	3.333	0.076	20.77708	3.03385	66.65
15	3.5	0.085	23.23753	3.14577	63.26
16	3.75	0.101	27.61165	3.31824	54.28
17	4.066	0.127	34.7196	3.5473	45.65
18	4.25	0.152	41.55417	3.727	36.01
19	4.5	0.192	52.48948	3.96061	21.55
20	4.75	0.23	62.87802	4.1412	7.59
21	5	0.267	72.99318	4.29037	0
22	5.25	0.264	72.17303	4.27907	0
23	5.75	0.264	72.17303	4.27907	0

Table A-9 Run-9. The exponential growth phase began at t = 0.75 h. The average phenol concentration in the linear regime was 82.95 g m^{-3}

Sample No.	Time h	Optical density	Biomass concentration g m^{-3}	Ln (Biomass concentration)	Phenol concentration g m^{-3}
1	0	0.012	3.28059	1.18802	100.24
2	0.25	0.013	3.55398	1.26807	99.56
3	0.5	0.014	3.82736	1.34218	98.17
4	0.75	0.015	4.10074	1.41117	98.19
5	1	0.016	4.37412	1.47571	97.48
6	1.25	0.018	4.92089	1.59349	96.6
7	1.5	0.02	5.46765	1.69885	95.74
8	1.75	0.023	6.2878	1.83861	94.4
9	2	0.025	6.83457	1.92199	93.56
10	2.25	0.029	7.9281	2.07041	91.19
11	2.5	0.032	8.74825	2.16885	90.35
12	2.75	0.0355	9.70509	2.27265	88.37
13	3	0.04	10.93531	2.392	86.08
14	3.25	0.045	12.30222	2.50978	82.69
15	3.5	0.052	14.2159	2.65436	79.95
16	3.75	0.061	16.67634	2.81399	74.35
17	4	0.07	19.13679	2.95161	72.52
18	4.25	0.079	21.59723	3.07257	67.09
19	4.5	0.09	24.60444	3.20293	61.94
20	4.75	0.103	28.15842	3.33785	54.96
21	5	0.116	31.71239	3.45671	47.26
22	5.25	0.137	37.45343	3.6231	38.1
23	5.5	0.159	43.46785	3.77202	27.86
24	5.75	0.201	54.94992	4.00642	13.13
25	6	0.242	66.15861	4.19206	0
26	6.25	0.257	70.25935	4.25219	0
27	6.5	0.259	70.80612	4.25995	0
28	7	0.257	7025935	4.25219	0

Table A-10 Run-10. The exponential growth phase began at t = 0.75 h. The average phenol concentration in the linear regime was 101.27 g m^{-3}

Sample No.	Time h	Optical density	Biomass concentration g m^{-3}	Ln (Biomass concentration)	Phenol concentration g m^{-3}
1	0	0.014	3.82736	1.34217	106.62
2	0.5	0.0145	3.96405	1.37727	106.88
3	0.783	0.016	4.37412	1.47571	105.05
4	1.083	0.018	4.92089	1.59349	104.55
5	1.25	0.02	5.46765	1.69885	104.48
6	1.5	0.0225	6.15111	1.81663	103.47
7	1.75	0.025	6.83457	1.92199	104.39
8	2.166	0.032	8.74825	2.16885	100.32
9	2.25	0.033	9.02163	2.19962	98.39
10	2.5	0.037	10.11516	2.31404	96.51
11	2.75	0.043	11.75546	2.46432	94.27
12	3	0.052	14.2159	2.65436	91.5
13	3.25	0.0605	16.53965	2.80576	88.74
14	3.5	0.07	19.13679	2.95161	83.75
15	3.75	0.084	22.96415	3.13393	78.2
16	4	0.099	27.06489	3.29824	72.7
17	4.25	0.117	31.98577	3.46529	65.08
18	4.5	0.144	39.36711	3.67293	56.09
19	4.75	0.173	47.2952	3.85641	45.26
20	5	0.212	57.95713	4.0597	27.6
21	5.25	0.261	71.35288	4.26764	9.06
22	5.5	0.306	83.6551	4.4267	0.08
23	5.75	0.302	82.56157	4.41354	0
24	6	0.304	83.10834	4.42015	0

Table A-11 Run-11. The exponential growth phase began at t = 0.75 h. The average phenol concentration in the linear regime was 144.41 g m^{-3}

Sample No.	Time h	Optical Density	Biomass concentration g m^{-3}	Ln (Biomass concentration)	Phenol concentration g m^{-3}
1	0	0.012	3.28059	1.18802	152.1
2	0.3	0.013	3.55398	1.26807	151.42
3	0.583	0.014	3.82736	1.34217	151.68
4	0.75	0.014	3.82736	1.34217	152.09
5	1	0.014	3.82736	1.34217	150.72
6	1.25	0.015	4.10074	1.41117	150.51
7	1.5	0.017	4.64751	1.53633	151.44
8	1.75	0.019	5.19427	1.64756	148.67
9	2	0.021	5.74104	1.74764	148.14
10	2.25	0.0235	6.42449	1.86012	146.8
11	2.5	0.026	7.10795	1.96121	144.79
12	2.75	0.03	8.20148	2.10431	143.33
13	3	0.034	9.29501	2.22948	141.04
14	3.25	0.038	10.38854	2.3407	139.3
15	3.5	0.043	11.75546	2.46432	136.02
16	3.916	0.0525	14.35259	2.66393	132.25
17	4.25	0.064	17.49649	2.862	126.75
18	4.5	0.074	20.23032	3.00718	122.51
19	4.75	0.086	23.51091	3.15746	118.48
20	5	0.099	27.06489	3.29824	111.31
21	5.25	0.111	30.34548	3.41265	103.05
22	5.5	0.132	36.08651	3.58592	95.72
23	5.75	0.153	41.82755	3.73356	83.66
24	6	0.185	50.5758	3.92347	70.1
25	6.25	0.221	60.41758	4.10128	54.76
26	6.583	0.268	73.26656	4.2941	30.48
27	6.75	0.298	81.46804	4.40021	11.37
28	7	0.356	97.32424	4.57805	0
29	7.333	0.35	95.68394	4.56105	0
30	8	0.345	94.31702	4.54666	0

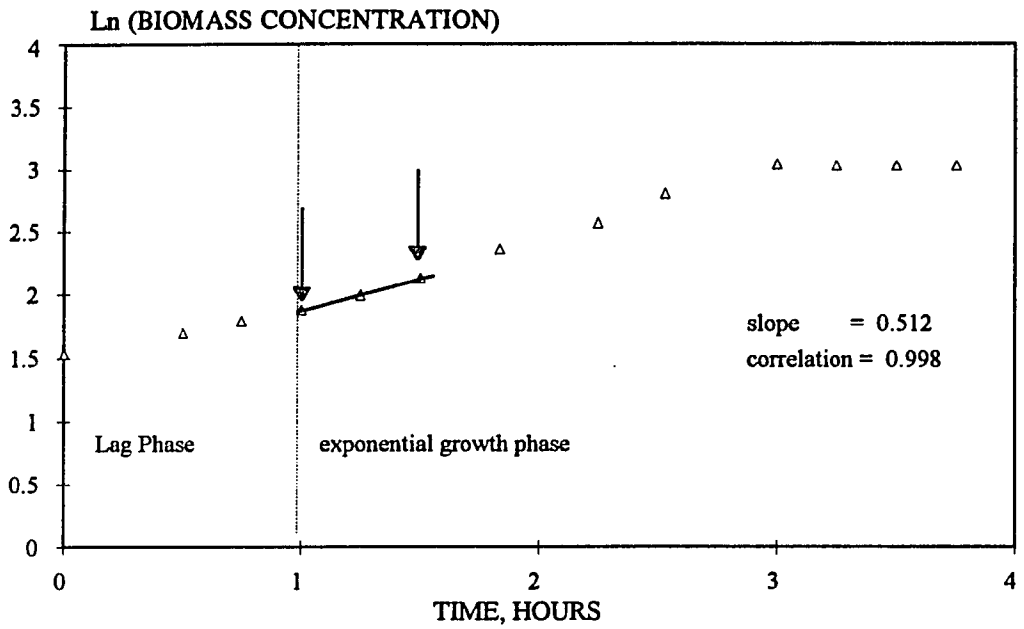

Figure A-1 Plot of Ln biomass concentration versus time for determination of the specific growth rate. Run-1.

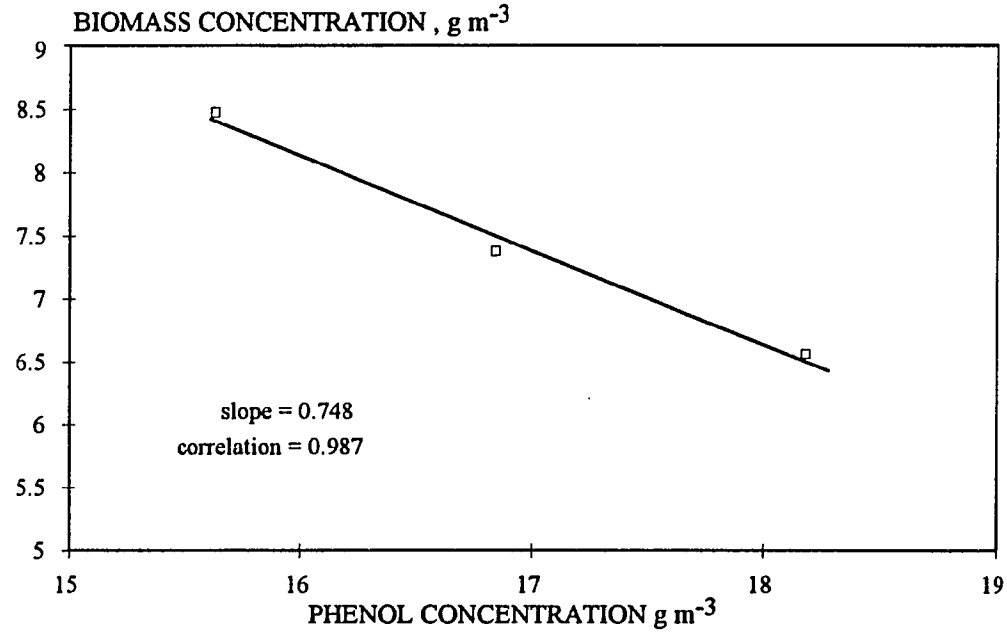

Figure A-2 Plot of biomass concentration versus phenol concentration for the determination of the yield coefficient. Run-1

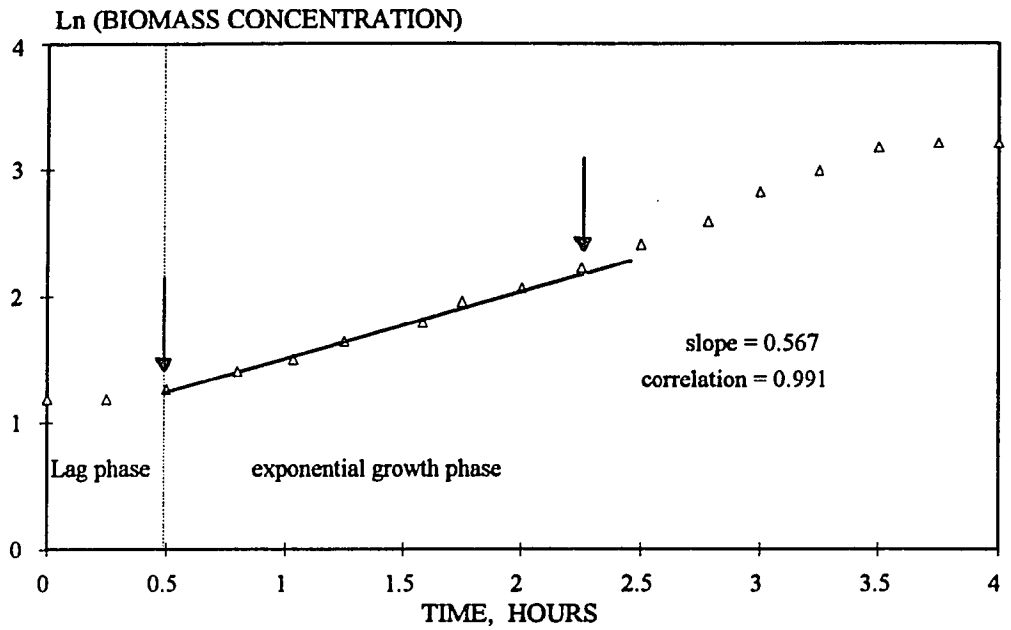

Figure A-3 Plot of Ln biomass concentration versus time for determination of the specific growth rate. Run-2

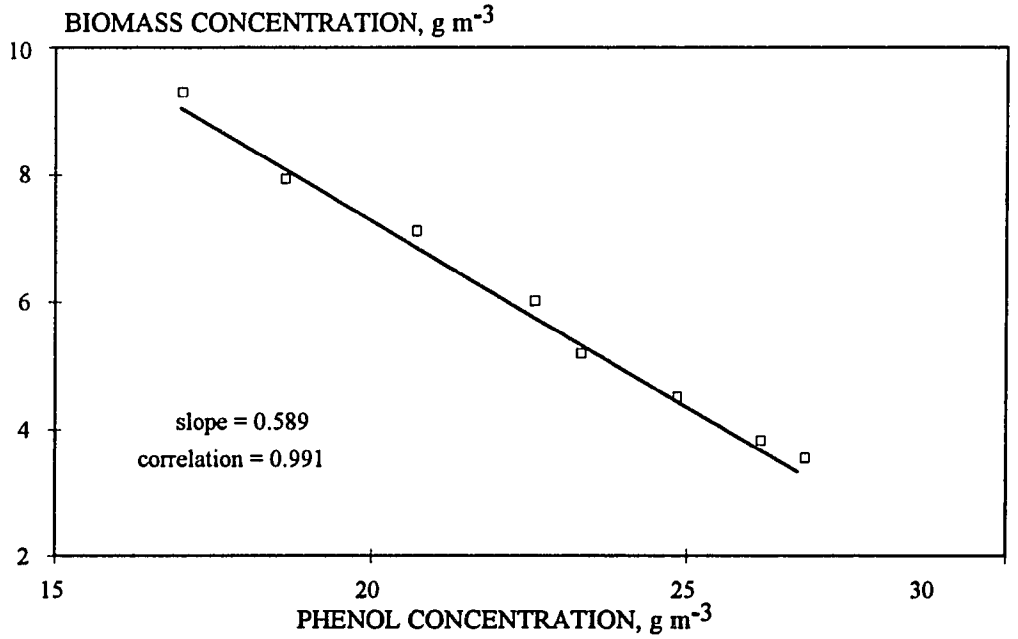

Figure A-4 Plot of biomass concentration versus phenol concentration for the determination of the yield coefficient. Run-2

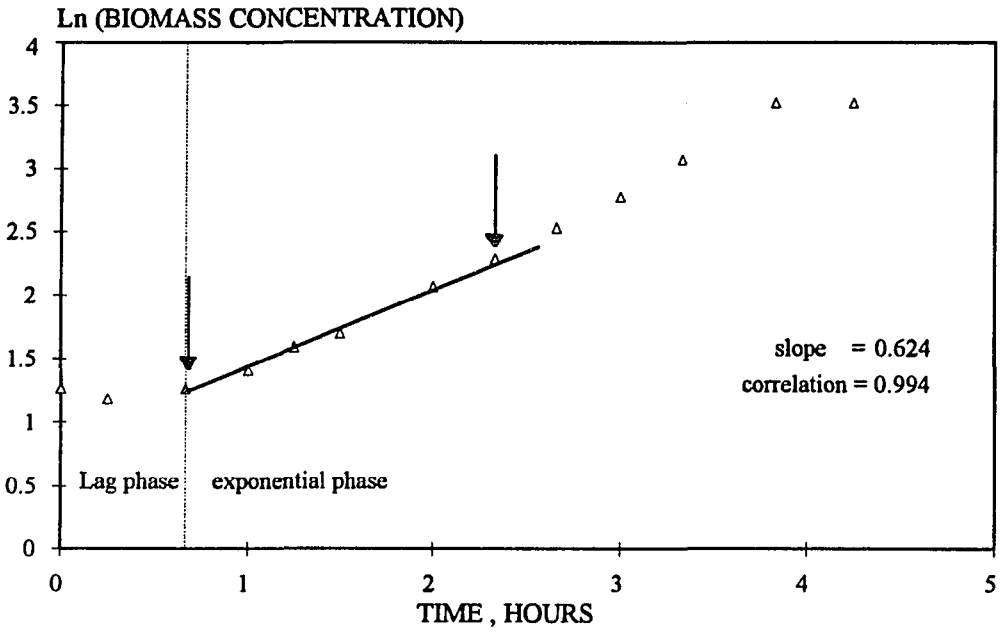

Figure A-5 Plot of Ln biomass concentration versus time for determination of the specific growth rate. Run-3.

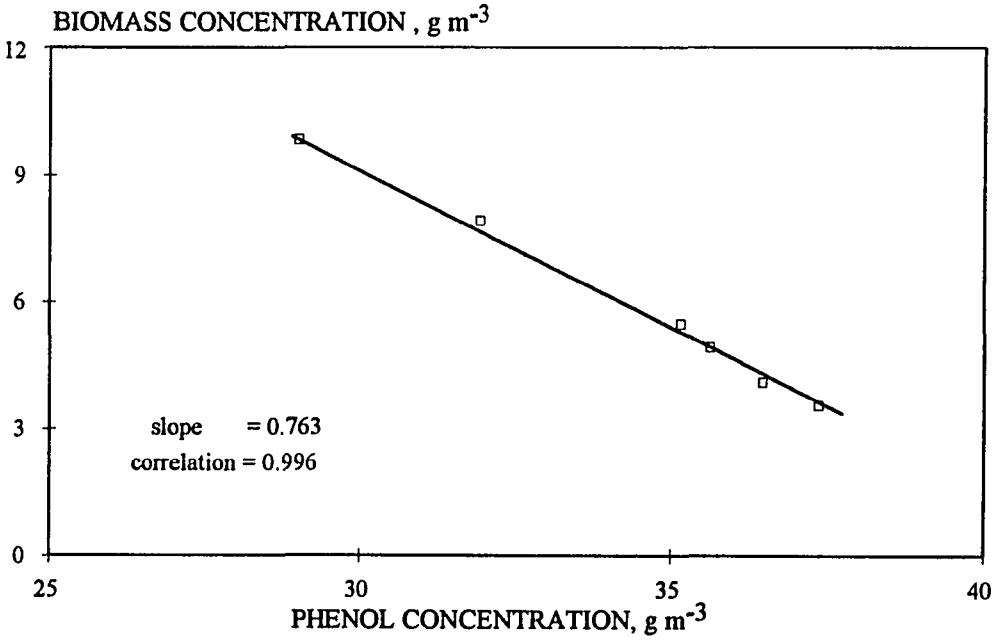

Figure A-6 Plot of biomass concentration versus phenol concentration for the determination of the yield coefficient. Run-3

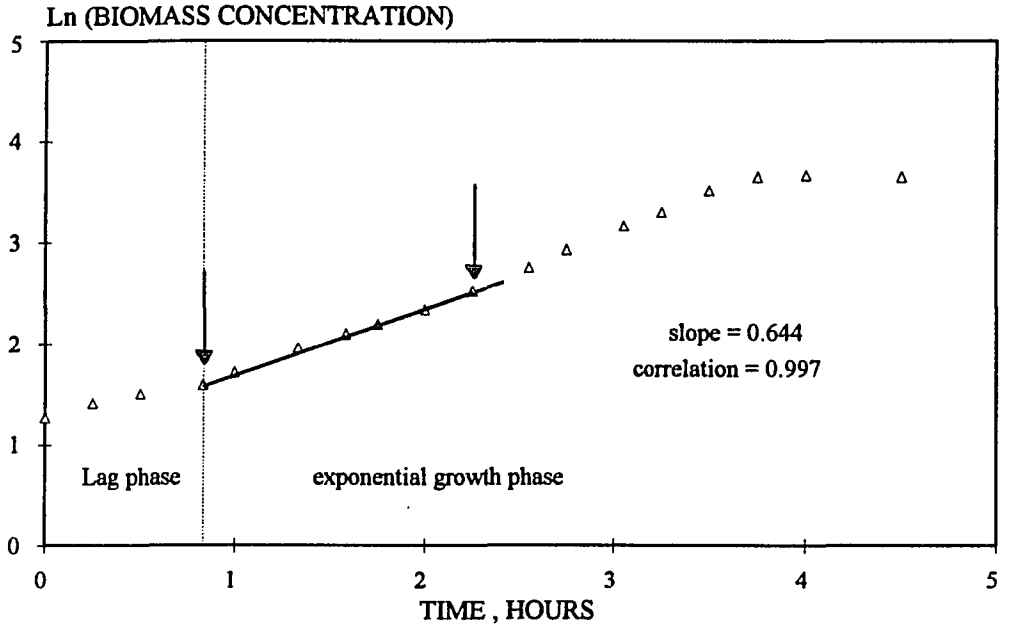

Figure A-7 Plot of Ln biomass concentration versus time for determination of the specific growth rate. Run-4.

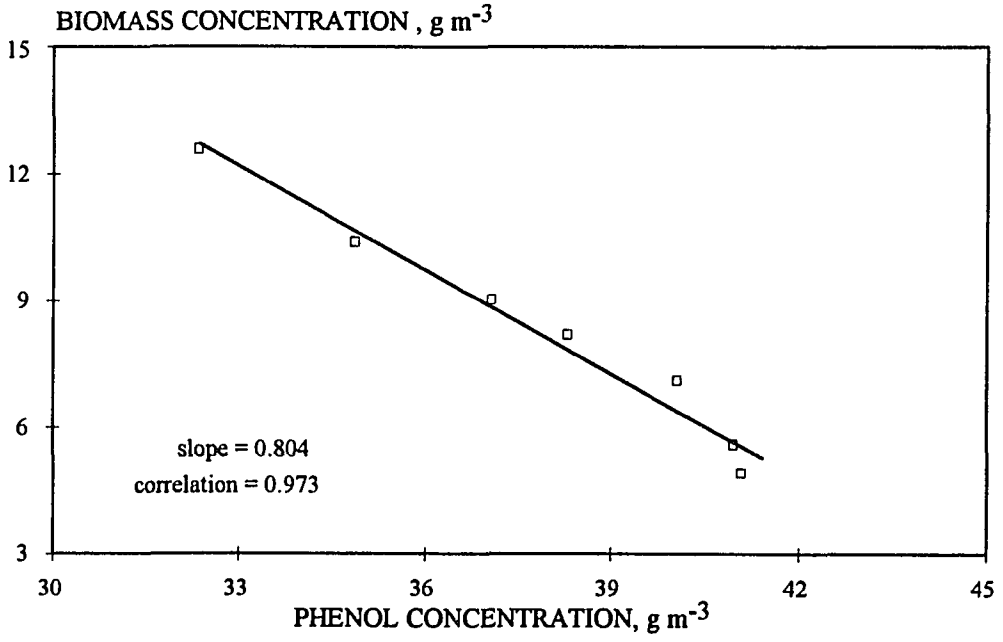

Figure A-8 Plot of biomass concentration versus phenol concentration for the determination of the yield coefficient. Run-4

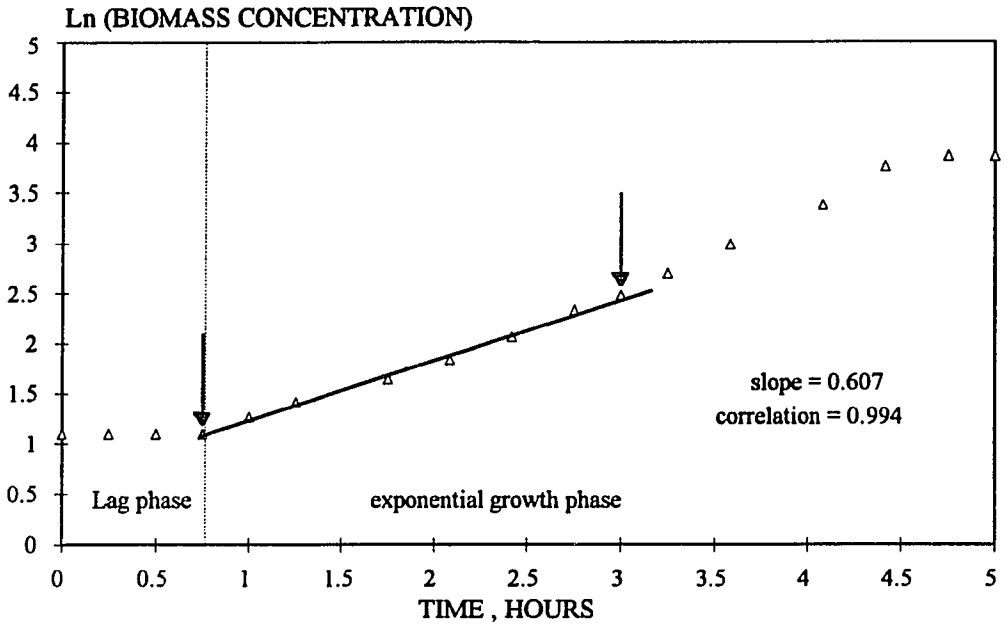

Figure A-9 Plot of Ln biomass concentration versus time for determination of the specific growth rate. Run-5.

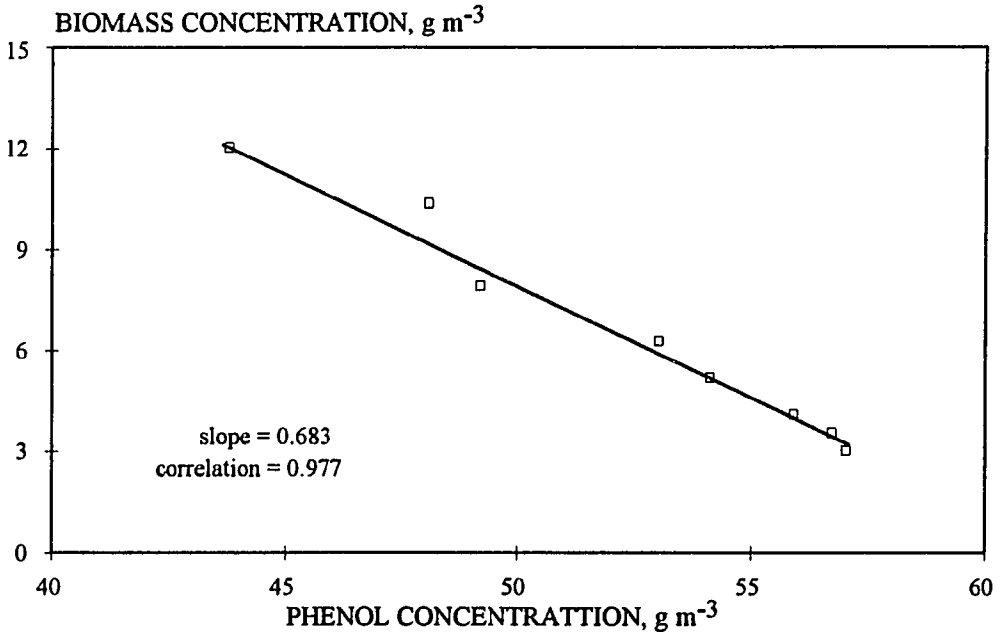

Figure A-10 Plot of biomass concentration versus phenol concentration for the determination of the yield coefficient. Run-5

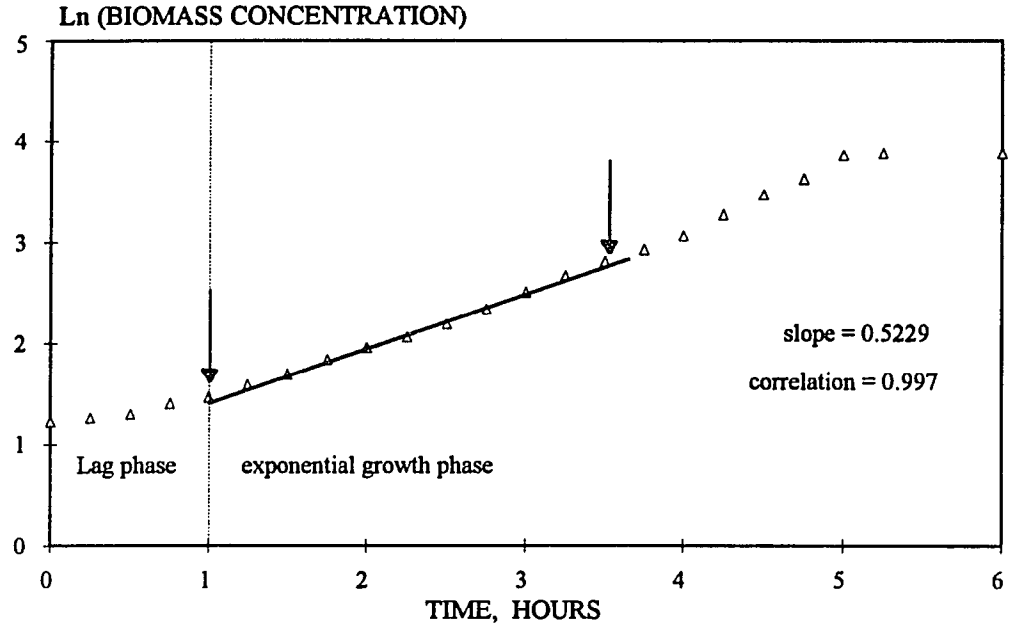

Figure A-11 Plot of Ln biomass concentration versus time for determination of the specific growth rate. Run-6.

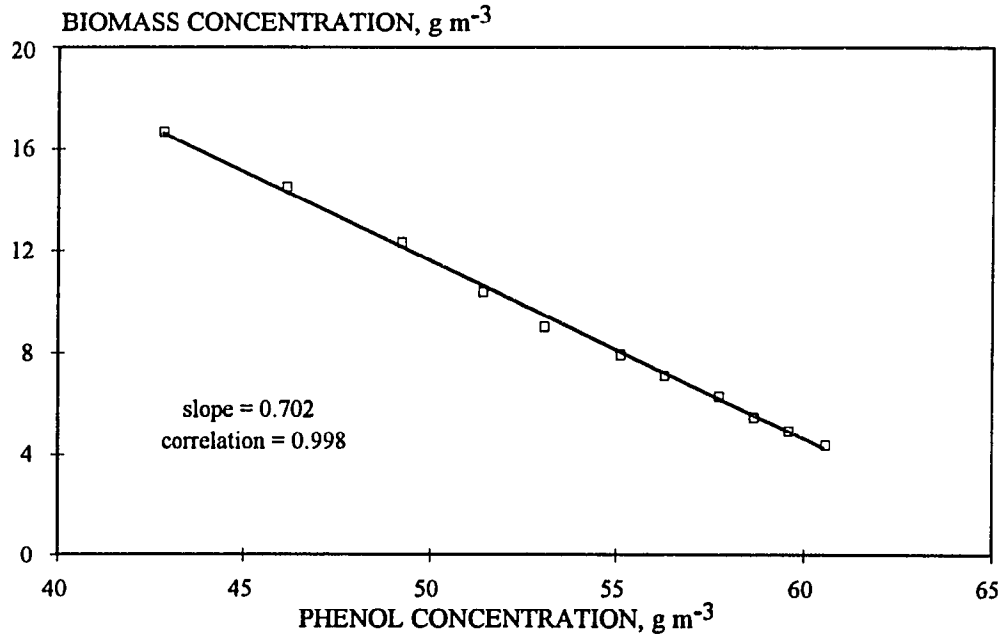

Figure A-12 Plot of biomass concentration versus phenol concentration for the determination of the yield coefficient. Run-6

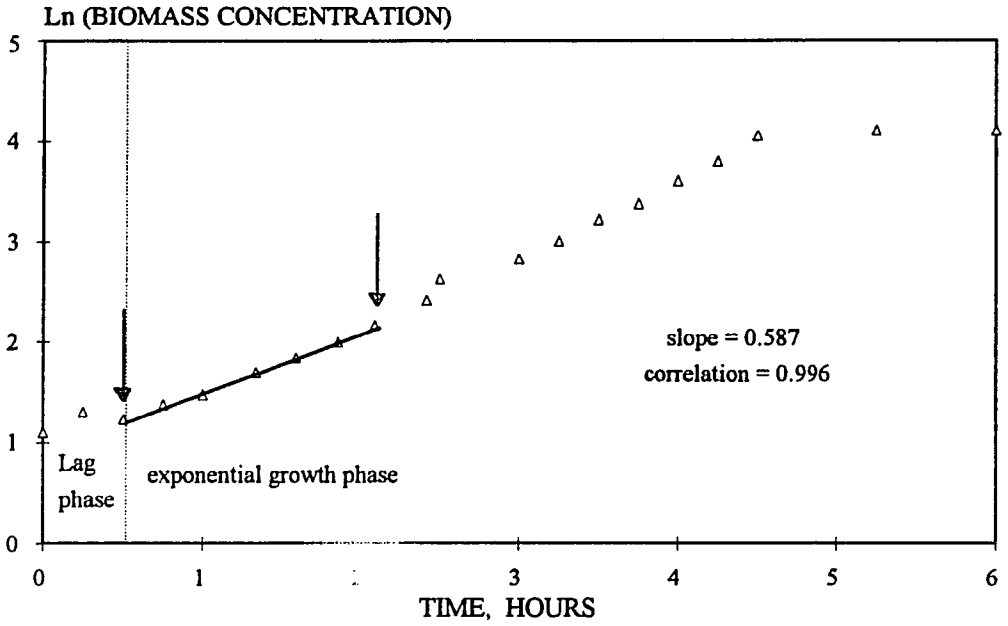

Figure A-13 Plot of Ln biomass concentration versus time for determination of the specific growth rate. Run-7.

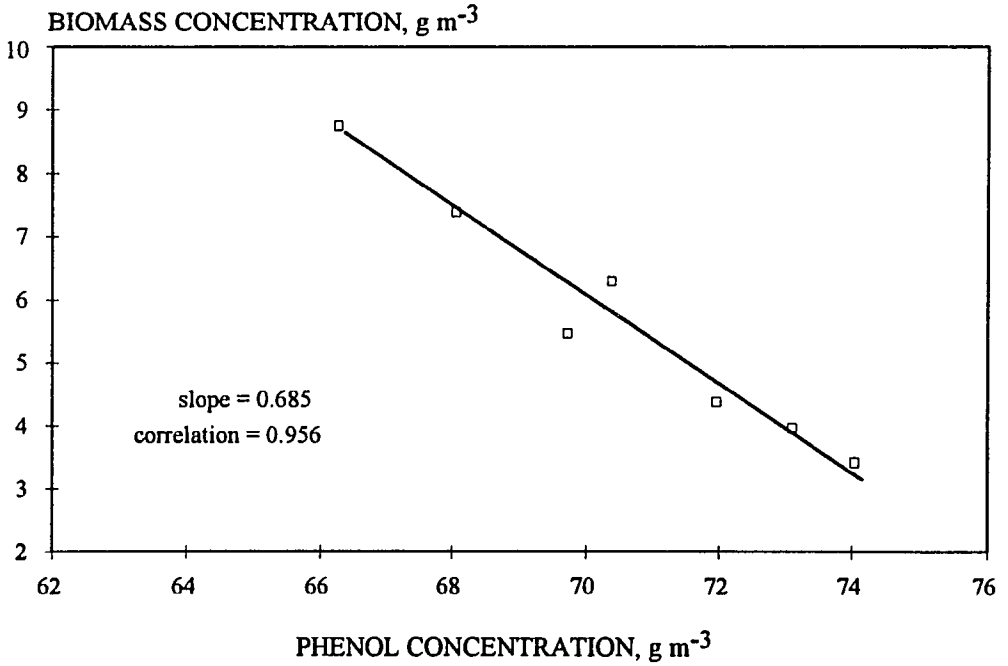

Figure A-14 Plot of biomass concentration versus phenol concentration for the determination of the yield coefficient. Run-7

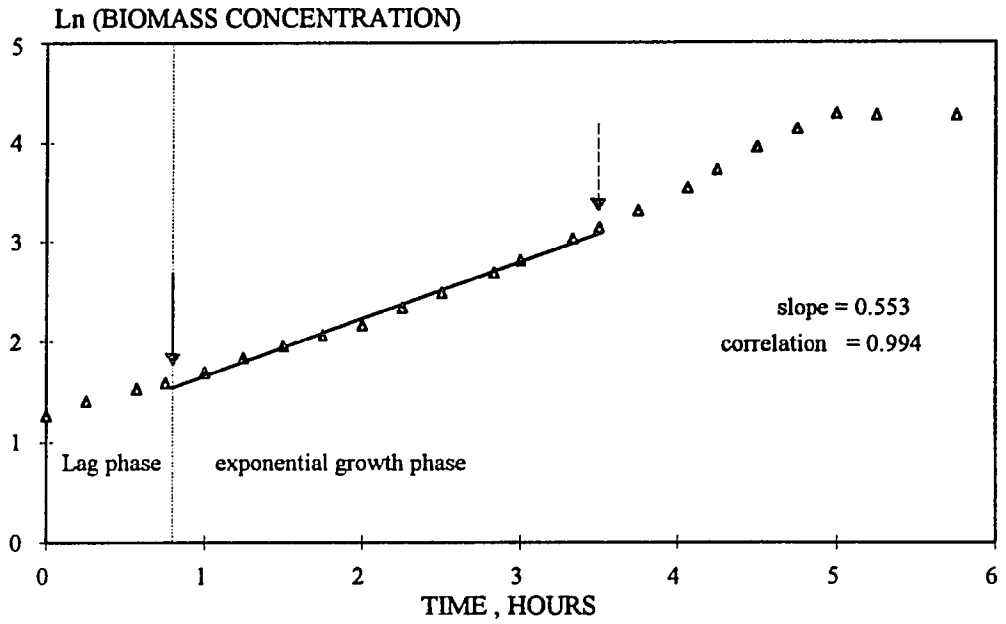

Figure A-15 Plot of Ln biomass concentration versus time for determination of the specific growth rate. Run-8.

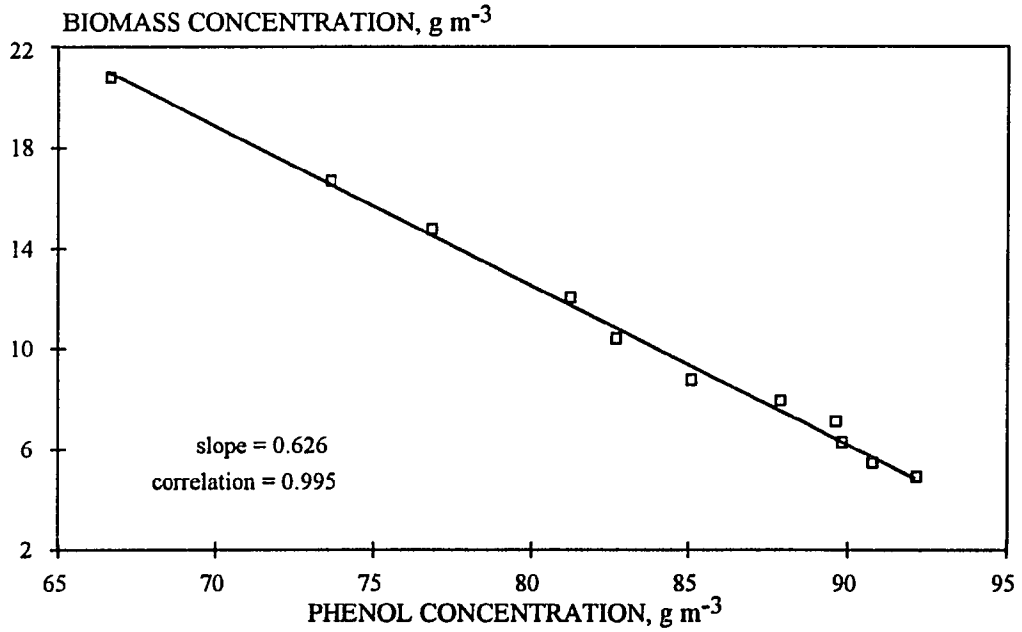

Figure A-16 Plot of biomass concentration versus phenol concentration for the determination of the yield coefficient. Run-8

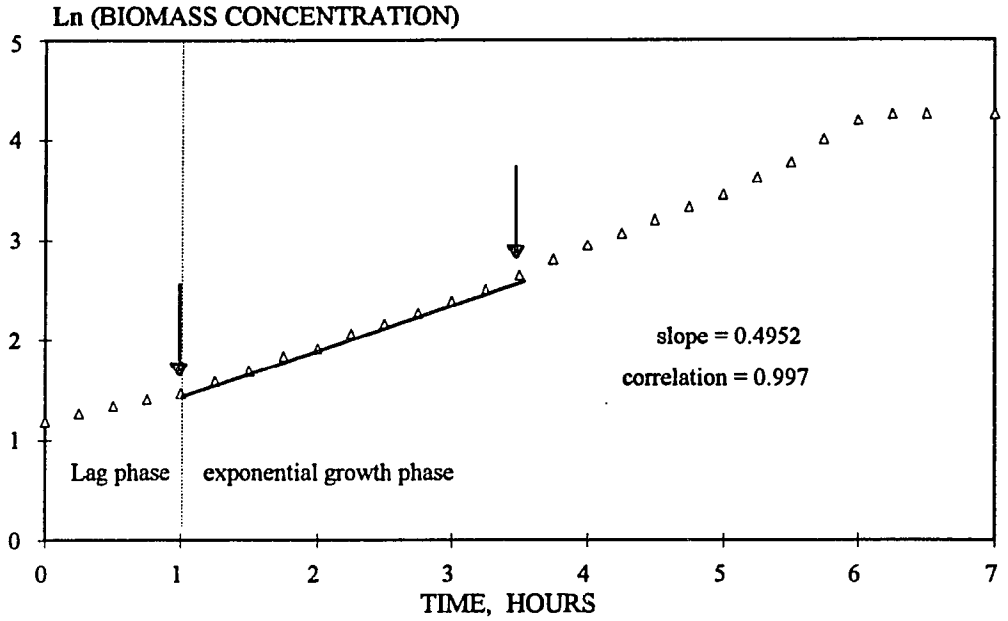

Figure A-17 Plot of Ln biomass concentration versus time for determination of the specific growth rate. Run-9.

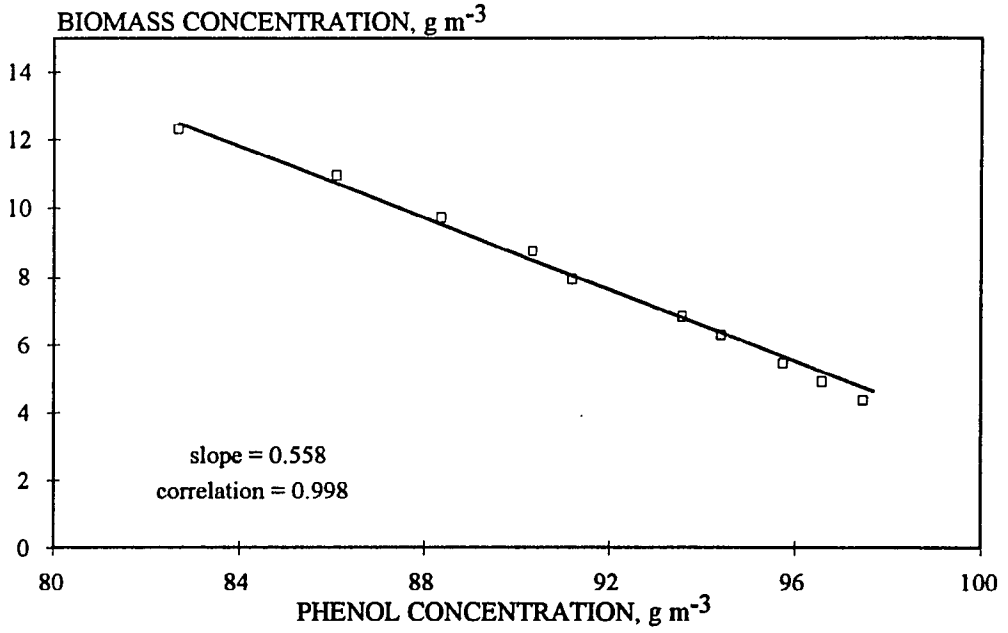

Figure A-18 Plot of biomass concentration versus phenol concentration for the determination of the yield coefficient. Run-9

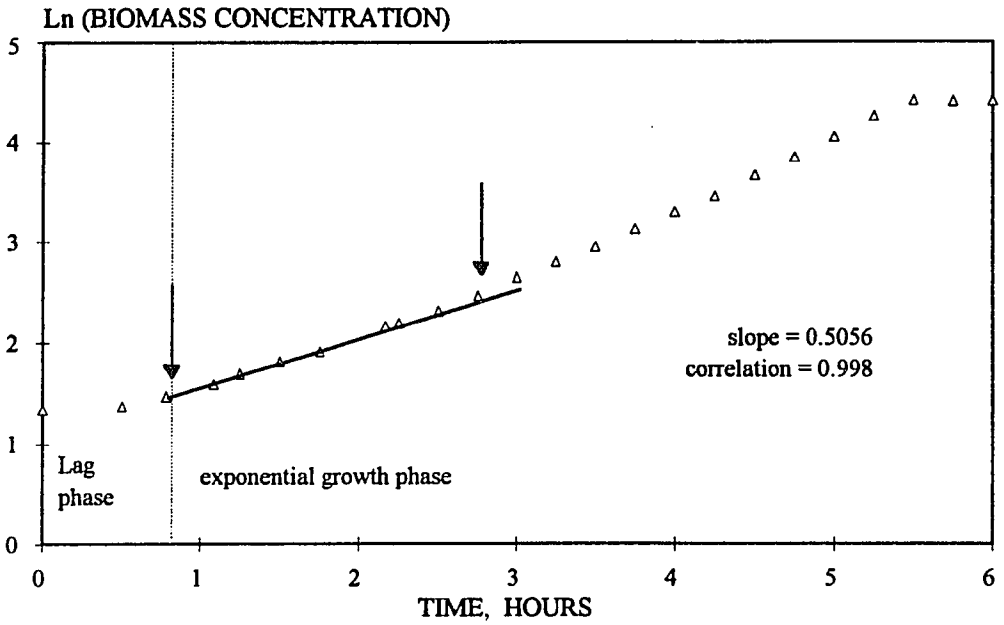

Figure A-19 Plot of Ln biomass concentration versus time for determination of the specific growth rate. Run-10.

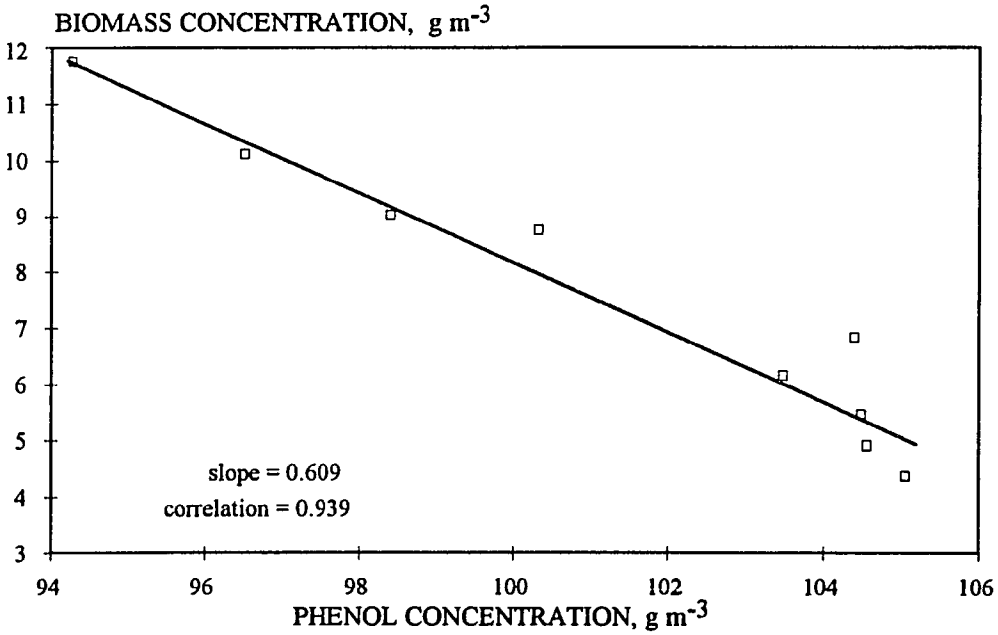

Figure A-20 Plot of biomass concentration versus phenol concentration for the determination of the yield coefficient. Run-10

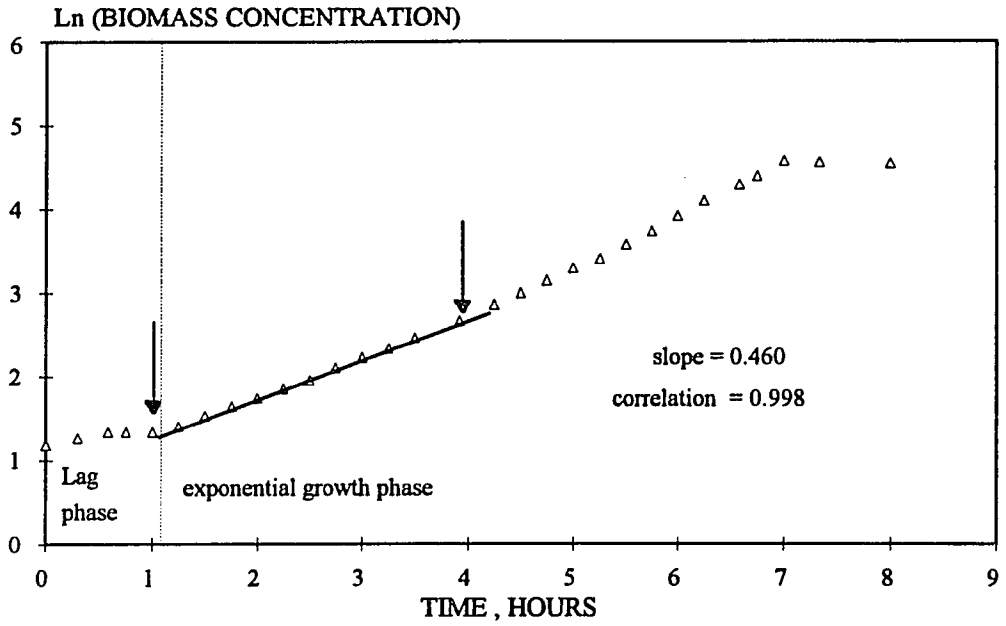

Figure A-21 Plot of Ln biomass concentration versus time for determination of the specific growth rate. Run-11.

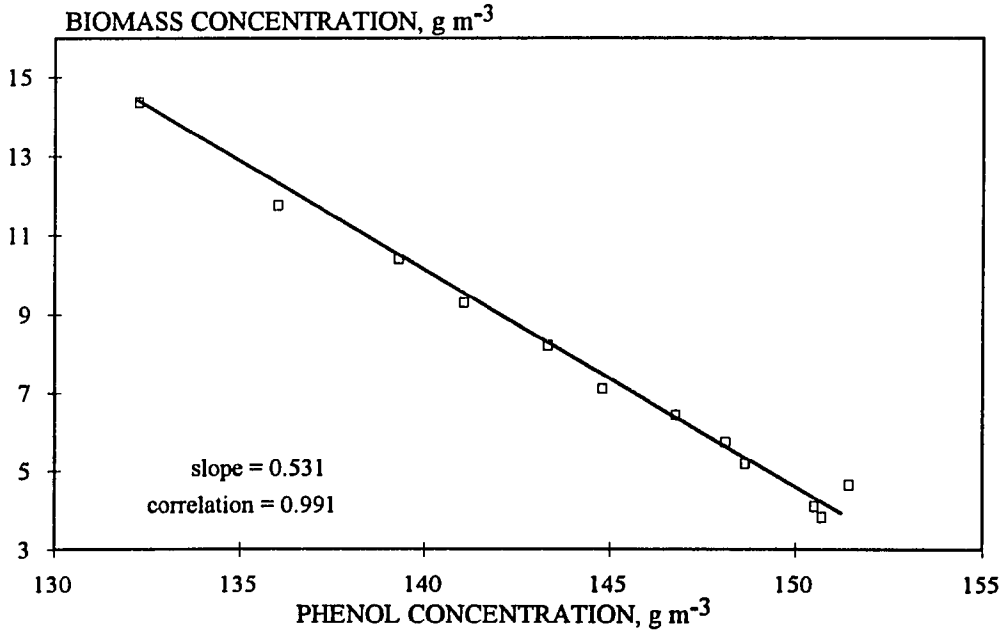

Figure A-22 Plot of biomass concentration versus phenol concentration for the determination of the yield coefficient. Run-11

APPENDIX B

Experimental Data for *Pseudomonas putida* (ATCC 17514)

The experimental data for determination of the specific growth rate and yield coefficient of *Pseudomonas putida* (ATCC 17514) on phenol are given in this appendix. Tables B-1 to B-17 list the experimental data for the seventeen batch experiments. The odd numbered figures show the plots of Ln biomass concentration versus time for the determination of the specific growth rate. The even numbered figures show the plots of biomass concentration versus phenol concentration for the determination of the yield coefficient. Yield coefficients were determined based on the data used for determining the specific growth rate (linear regime of the Ln biomass concentration versus time plot).

Table B-1 Run-1. The exponential growth phase began t = 0.5 h. The average phenol concentration in the linear regime was 14.74 g m^{-3}

Sample No.	Time h	Optical density	Biomass concentration g m^{-3}	Ln (Biomass concentration)	Phenol concentration g m^{-3}
1	0	0.015	4.10074	1.41117	17.81
2	0.25	0.016	4.37412	1.47571	17.37
3	0.5	0.017	4.64751	1.53633	16.86
4	0.75	0.019	5.19427	1.64756	16.22
5	1	0.021	5.74104	1.74764	15.48
6	1.25	0.023	6.2878	1.83861	14.57
7	1.5	0.0265	7.24464	1.98026	13.37
8	1.75	0.03	8.20148	2.10431	11.95
9	2	0.035	9.56839	2.25847	10.31
10	2.25	0.042	11.48207	2.44079	7.91
11	2.5	0.05	13.66914	2.61514	4.98
12	2.75	0.059	16.12958	2.78065	1.71
13	3	0.068	18.59002	2.92263	0
14	3.25	0.067	18.31664	2.90781	0
15	3.5	0.0068	1.859	0.62004	0

Table B-2 Run-2. The exponential growth phase began at t = 0.5 h. The average phenol concentration in the linear regime was 17.79 g m^{-3}

Sample No.	Time h	Optical density	Biomass concentration g m^{-3}	Ln (Biomass concentration)	Phenol concentration g m^{-3}
1	0	0.013	3.55398	1.26807	20.24
2	0.25	0.014	3.82736	1.34217	19.71
3	0.5	0.015	4.10074	1.41117	19.31
4	0.75	0.017	4.64751	1.53633	18.59
5	1	0.019	5.19427	1.64756	18.1
6	1.25	0.0215	5.87773	1.77117	17.05
7	1.5	0.025	6.83457	1.92199	15.93
8	1.75	0.029	7.9281	2.07041	14.45
9	2	0.033	9.02163	2.19962	12.74
10	2.25	0.039	10.66193	2.36668	10.09
11	2.5	0.046	12.5756	2.53176	7.51
12	2.75	0.055	15.03605	2.71045	3.76
13	3	0.068	18.59002	2.92263	0
14	3.25	0.073	19.95694	2.99358	0
15	3.5	0.072	19.68355	2.97978	0
16	4	0.072	19.68355	2.97978	0

Table B-3 Run-3. The exponential growth phase began at t = 0.0 h. The average phenol concentration in the linear regime was 22.29 g m^{-3}

Sample No.	Time h	Optical density	Biomass concentration g m^{-3}	Ln (Biomass concentration)	Phenol concentration g m^{-3}
1	0	0.015	4.10074	1.41117	24.85
2	0.25	0.017	4.64751	1.53633	24.13
3	0.5	0.019	5.19427	1.64756	23.06
4	0.75	0.022	6.01442	1.79416	21.98
5	1	0.022	6.01442	1.79416	21.98
6	1.25	0.0255	6.97126	1.9418	20.87
7	1.667	0.039	10.66193	2.36668	15.6
8	1.75	0.042	11.48207	2.44079	14.43
9	2	0.049	13.39575	2.59494	11.66
10	2.25	0.059	16.12958	2.78065	7.85
11	2.5	0.071	19.41017	2.9658	3.64
12	2.75	0.085	23.23753	3.14577	0
13	3	0.085	23.23753	3.14577	0
14	3.25	0.085	23.23753	3.14577	0

Table B-4 Run-4. The exponential growth phase began at t = 1.25 h. The average phenol concentration in the linear regime was 19.08 g m^{-3}

Sample No.	Time h	Optical density	Biomass concentration g m^{-3}	Ln (Biomass concentration)	Phenol concentration g m^{-3}
1	0	0.017	4.64751	1.53633	29.50
2	0.25	0.017	4.64751	1.53633	29.46
3	0.5	0.018	4.92089	1.59349	28.67
4	0.75	0.02	5.46765	1.69885	28.04
5	1	0.022	6.01442	1.79416	27.64
6	1.25	0.0235	6.42449	1.86012	26.71
7	1.5	0.026	7.10795	1.96121	24.17
8	1.75	0.029	7.9281	2.07041	22.56
9	2	0.032	8.74825	2.16885	20.83
10	2.25	0.036	9.84178	2.28664	19.56
11	2.5	0.042	11.48207	2.44079	18.67
12	2.75	0.05	13.66914	2.61514	16.23
13	3	0.057	15.58281	2.74617	13.19
14	3.25	0.064	17.49649	2.862	9.81
15	3.5	0.075	20.5037	3.02061	5.83
16	3.75	0.091	24.87783	3.21398	0.55
17	4	0.096	26.24474	3.26747	0
18	4.25	0.094	25.69797	3.24641	0
19	4.5	0.094	25.69797	3.24641	0

Table B-5 Run-5. The exponential growth phase began at t = 1.0 h. The average phenol concentration in the linear regime was 28.02 g m^{-3}

Sample No.	Time h	Optical density	Biomass concentration g m^{-3}	Ln (Biomass concentration)	Phenol concentration g m^{-3}
1	0	0.013	3.55398	1.26807	32.86
2	0.25	0.0135	3.69067	1.30581	32.21
3	0.5	0.0145	3.96405	1.37727	31.85
4	0.75	0.016	4.37412	1.47571	31.2
5	1	0.018	4.92089	1.59349	30.32
6	1.25	0.021	5.74104	1.74764	29.58
7	1.5	0.024	6.56118	1.88117	28.33
8	1.75	0.028	7.65472	2.03532	26.95
9	2	0.033	9.02163	2.19962	24.94
10	2.25	0.04	10.93531	2.392	22.5
11	2.5	0.048	13.12237	2.57432	20.05
12	2.75	0.056	15.30943	2.72847	16.3
13	3	0.067	18.31664	2.90781	12.25
14	3.25	0.082	22.41738	3.10984	6.64
15	3.5	0.01	2.73383	1.0057	0
16	3.75	0.111	30.34548	3.41265	0
17	4	0.111	30.34548	3.41265	0

Table B-6 Run-6. The exponential growth phase began at t = 0.5 h. The average phenol concentration in the linear regime was 27.83 g m^{-3}

Sample No.	Time h	Optical density	Biomass concentration g m^{-3}	Ln (Biomass concentration)	Phenol concentration g m^{-3}
1	0	0.013	3.55398	1.26807	32.93
2	0.25	0.015	4.10074	1.41117	32.37
3	0.5	0.017	4.64751	1.53633	31.43
4	0.75	0.019	5.19427	1.64756	30.74
5	1	0.022	6.01442	1.79416	29.85
6	1.25	0.025	6.83457	1.92199	28.54
7	1.5	0.029	7.9281	2.07041	27
8	1.75	0.034	9.29501	2.22948	24.79
9	2	0.04	10.93531	2.392	22.5
10	2.25	0.048	13.12237	2.57432	19.44
11	2.5	0.058	15.8562	2.76356	15.63
12	2.75	0.069	18.86341	2.93722	11.1
13	3	0.085	23.23753	3.14577	4.93
14	3.25	0.105	28.70518	3.35708	0
15	3.5	0.107	29.25195	3.37595	0
16	3.75	0.107	29.25195	3.37595	0

Table B-7 Run-7. The exponential growth phase began at t = 1.0 h. The average phenol concentration in the linear regime was 34.88 g m^{-3}

Sample No.	Time h	Optical density	Biomass concentration g m^{-3}	Ln (Biomass concentration)	Phenol concentration g m^{-3}
1	0	0.015	4.10074	1.41117	41.80
2	0.25	0.015	4.10074	1.41117	40.91
3	0.5	0.017	4.64751	1.53633	40.54
4	0.75	0.019	5.19427	1.64756	39.84
5	1.0	0.021	5.74104	1.74764	39.22
6	1.25	0.024	6.56118	1.88117	37.98
7	1.5	0.027	7.38133	1.99895	37.11
8	1.75	0.031	8.47486	2.1371	35.46
9	2	0.036	9.84178	2.28664	33.71
10	2.25	0.043	11.75546	2.46432	31.69
11	2.5	0.053	14.48928	2.67341	29.02
12	2.75	0.065	17.76987	2.8775	25.47
13	3	0.079	21.59723	3.07257	20.88
14	3.25	0.093	25.42459	3.23572	15.68
15	3.5	0.0109	2.97987	1.09188	9.67
16	3.75	0.134	36.63328	3.60096	0.61
17	4	0.148	40.46064	3.70033	0
18	4.25	0.48	131.2237	4.8769	0

Table B-8 Run-8. The exponential growth phase began at t = 1.25 h. The average phenol concentration in the linear regime was 26.45 g m^{-3}

Sample No.	Time h	Optical density	Biomass concentration g m^{-3}	Ln (Biomass concentration)	Phenol concentration g m^{-3}
1	0	0.019	5.19427	1.64756	42.56
2	0.25	0.0205	5.60435	1.72354	42.54
3	0.5	0.023	6.2878	1.83861	41.54
4	0.75	0.025	6.83457	1.92199	41.12
5	1	0.027	7.38133	1.99895	39.96
6	1.25	0.029	7.9281	2.07041	37.28
7	1.5	0.0315	8.61156	2.1531	35.87
8	1.75	0.035	9.56839	2.25847	33.27
9	2	0.04	10.93531	2.392	31.09
10	2.25	0.046	12.5756	2.53176	28.46
11	2.5	0.052	14.2159	2.65436	24.97
12	2.75	0.059	16.12958	2.78065	21.12
13	3	0.072	19.68355	2.97978	16.35
14	3.25	0.083	22.69076	3.12196	10.68
15	3.5	0.099	27.06489	3.29824	3.42
16	3.75	0.115	31.43901	3.44805	0
17	4	0.13	35.53975	3.57065	0
18	4.25	0.13	35.53975	3.57065	0
19	4.5	0.13	35.53975	3.57065	0
20	4.75	0.129	35.26637	3.56293	0

Table B-9 Run-9. The exponential growth phase began at t = 1.0 h. The average phenol concentration in the linear regime was 44.95 g m^{-3}

Sample No.	Time h	Optical density	Biomass concentration g m^{-3}	Ln (Biomass concentration)	Phenol concentration g m^{-3}
1	0	0.017	4.64751	1.53633	51.28
2	0.25	0.017	4.64751	1.53633	51.18
3	0.5	0.017	4.64751	1.53633	49.98
4	0.75	0.0185	5.05758	1.62089	49.28
5	1	0.02	5.46765	1.69885	47.94
6	1.25	0.023	6.2878	1.83861	47.32
7	1.5	0.026	7.10795	1.96121	46.24
8	1.75	0.031	8.47486	2.1371	44.77
9	2	0.036	9.84178	2.28664	42.9
10	2.25	0.042	11.48207	2.44079	40.53
11	2.5	0.05	13.66914	2.61514	38.11
12	2.75	0.0585	15.99289	2.77214	33.62
13	3	0.069	18.86341	2.93722	29.52
14	3.25	0.085	23.23753	3.14577	23.57
15	3.5	0.102	27.88503	3.32809	17.14
16	3.75	0.123	33.62607	3.5153	9
17	4	0.155	42.37432	3.74654	0
18	4.25	0.161	44.01461	3.78452	0
19	4.5	0.165	45.10815	3.80906	0
20	5	0.165	45.10815	3.80906	0

Table B-10 Run-10. The exponential growth phase began at t = 1.0 h. The average phenol concentration in the linear regime was 54.64 g m^{-3}

Sample No.	Time h	Optical density	Biomass concentration g m^{-3}	Ln (Biomass concentration)	Phenol concentration g m^{-3}
1	0	0.0195	5.33096	1.67353	62.56
2	0.25	0.022	6.01442	1.79416	61.53
3	0.5	0.023	6.2878	1.83861	60.68
4	0.75	0.026	7.10795	1.96121	60.52
5	1	0.0295	8.06479	2.08751	59.4
6	1.25	0.033	9.02163	2.19962	58.22
7	1.5	0.037	10.11516	2.31404	56.43
8	1.75	0.044	12.02884	2.48731	54.02
9	2	0.051	13.94252	2.63494	51.38
10	2.25	0.059	16.12958	2.78065	48.42
11	2.5	0.072	19.68355	2.97978	44.59
12	2.75	0.085	23.23753	3.14577	39.53
13	3	0.1	27.33827	3.30829	33.76
14	3.25	0.123	33.62607	3.5153	26.27
15	3.5	0.149	40.73402	3.70706	16.54
16	3.75	0.183	50.02903	3.9126	4.46
17	4	0.212	57.95713	4.0597	0
18	4.25	0.212	57.95713	4.0597	0
19	4.5	0.212	57.95713	4.0597	0

Table B-11 The exponential growth phase began at t = 0.75 h. The average phenol concentration in the linear regime was 70.23 g m^{-3}

Sample No.	Time h	Optical density	Biomass concentration g m^{-3}	Ln (Biomass concentration)	Phenol concentration g m^{-3}
1	0	0.012	3.28059	1.18802	76.5
2	0.25	0.013	3.55398	1.26807	74.88
3	0.5	0.015	4.10074	1.41117	74.83
4	0.75	0.017	4.64751	1.53633	74.03
5	1	0.0195	5.33096	1.67353	73.18
6	1.25	0.022	6.01442	1.79416	72.01
7	1.5	0.025	6.83457	1.92199	70.68
8	1.8	0.03	8.20148	2.10431	69.04
9	2	0.0355	9.70509	2.27265	67.27
10	2.25	0.042	11.48207	2.44079	65.43
11	2.5	0.051	13.94252	2.63494	61.52
12	2.75	0.0605	16.53965	2.80576	58.38
13	3	0.072	19.68355	2.97978	54.21
14	3.25	0.085	23.23753	3.14577	48.69
15	3.5	0.103	28.15842	3.33785	41.29
16	3.75	0.127	34.7196	3.5473	32.21
17	4	0.154	42.10093	3.74007	21.76
18	4.25	0.193	52.76286	3.96581	7.11
19	4.5	0.226	61.78449	4.12365	0
20	4.75	0.227	62.05787	4.12807	0
21	5	0.227	62.05787	4.12807	0

Table B-12 Run-12. The exponential growth phase began at t = 0.833 h. The average phenol concentration in the linear regime was 74.57 g m^{-3}

Sample No.	Time h	Optical density	Biomass concentration g m^{-3}	Ln (Biomass concentration)	Phenol concentration g m^{-3}
1	0	0.012	3.28059	1.18802	78.14
2	0.25	0.014	3.82736	1.34217	78.22
3	0.5	0.016	4.37412	1.47571	77.98
4	0.833	0.018	4.92089	1.59349	77.03
5	1	0.02	5.46765	1.69885	76.5
6	1.3	0.024	6.56118	1.88117	75.3
7	1.5	0.027	7.38133	1.99895	74.85
8	1.75	0.0315	8.61156	2.15311	72.63
9	2	0.0365	9.97847	2.30043	71.12
10	2.25	0.043	11.75546	2.46432	68.99
11	2.5	0.052	14.2159	2.65436	66.11
12	2.75	0.061	16.67634	2.81399	62.97
13	3	0.073	19.95694	2.99358	58.46
14	3.25	0.088	24.05768	3.18045	53.32
15	3.5	0.11	30.0721	3.4036	46.47
16	3.75	0.13	35.53975	3.57065	38.86
17	4	0.156	42.6477	3.75297	27.47
18	4.25	0.193	52.76286	3.96581	12.78
19	4.5	0.243	66.43199	4.19618	0
20	5	0.255	69.71259	4.24438	0
21	5.5	0.255	69.71259	4.24438	0

Table B-13 Run-13. The exponential growth phase began at t = 1.5 h. The average phenol concentration in the linear regime was 75.45 g m^{-3}

Sample No.	Time h	Optical density	Biomass concentration g m^{-3}	Ln (Biomass concentration)	Phenol concentration g m^{-3}
1	0	0.015	4.10074	1.41117	82.64
2	0.25	0.015	4.10074	1.41117	82.76
3	0.5	0.016	4.37412	1.47571	81.43
4	0.75	0.017	4.64751	1.53633	80.61
5	1	0.019	5.19427	1.64756	80.11
6	1.25	0.021	5.74104	1.74764	80.28
7	1.5	0.023	6.2878	1.83861	81.04
8	1.75	0.026	7.10795	1.96121	78.91
9	2	0.0295	8.06479	2.08751	77.38
10	2.25	0.0335	9.15832	2.21466	76.04
11	2.5	0.0395	10.79862	2.37942	74.25
12	2.75	0.0475	12.98568	2.56385	72.12
13	3	0.054	14.76267	2.6921	68.41
14	3.25	0.065	17.76987	2.8775	65.61
15	3.5	0.0755	20.64039	3.02725	61.98
16	3.75	0.091	24.87782	3.21398	56.69
17	4	0.104	28.4318	3.34751	50.41
18	4.25	0.131	35.81313	3.57831	42.54
19	4.5	0.157	42.92109	3.75936	33.07
20	4.833	0.199	54.40316	3.99642	17.39
21	5	0.237	64.7917	4.17118	5.09
22	5.25	0.268	73.26656	4.2941	0
23	5.5	0.268	73.26656	4.2941	0

Table B-14 Run-14. The exponential growth phase began at t = 1.5 h. The average phenol concentration in the linear regime was 59.56 g m^{-3}

Sample No.	Time h	Optical density	Biomass concentration g m^{-3}	Ln (Biomass concentration)	Phenol concentrtation g m^{-3}
1	0	0.019	5.19427	1.64756	84.44
2	0.25	0.021	5.74104	1.74764	83.93
3	0.5	0.022	6.01442	1.79416	83.66
4	0.75	0.023	6.2878	1.83861	82.62
5	1	0.026	7.10795	1.96121	81.27
6	1.25	0.029	7.9281	2.07041	79.97
7	1.5	0.032	8.74825	2.16885	78.66
8	1.75	0.037	10.11516	2.31404	76.89
9	2	0.041	11.20869	2.41669	75.57
10	2.25	0.046	12.5756	2.53176	73.39
11	2.5	0.051	13.94252	2.63494	71.07
12	2.75	0.06	16.40296	2.79476	68.3
13	3	0.07	19.13679	2.95161	64.33
14	3.25	0.081	22.144	3.09757	60.13
15	3.5	0.094	25.69797	3.24641	55.35
16	3.75	0.111	30.34548	3.41265	49.94
17	4	0.129	35.26637	3.56293	42.61
18	4.25	0.15	41.00741	3.71375	33.95
19	4.5	0.176	48.11536	3.8736	22.32
20	4.75	0.218	59.59743	4.08761	7.75
21	5	0.253	69.16582	4.23651	0
22	5.25	0.261	71.35288	4.26764	0
23	5.5	0.254	69.43921	4.24045	0
24	6	0.254	69.43921	4.24045	0

Table B-15 Run-15. The exponential growth phase began at t = 1.0 h. The average phenol concentration in the linear regime was 98.21 g m^{-3}

Sample No.	Time h	Optical density	Biomass concentration g m^{-3}	Ln (Biomass concentration)	Phenol concentration g m^{-3}
1	0	0.014	3.82736	1.34217	106.14
2	0.25	0.016	4.37412	1.47571	104.26
3	0.5	0.019	5.19427	1.64756	105.11
4	0.75	0.021	5.74104	1.74764	103.78
5	1	0.023	6.2878	1.83861	104.82
6	1.25	0.027	7.38133	1.99895	104.73
7	1.5	0.03	8.20148	2.10431	103.55
8	1.75	0.034	9.29501	2.22948	102.13
9	2	0.038	10.38854	2.3407	100.96
10	2.25	0.044	12.02884	2.48731	98.73
11	2.5	0.051	13.94252	2.63494	97.67
12	2.75	0.058	15.8562	2.76356	93.61
13	3	0.069	18.86341	2.93722	89.73
14	3.25	0.082	22.41738	3.10984	86.19
15	3.5	0.096	26.24474	3.26747	80.82
16	3.75	0.112	30.61886	3.42162	74.03
17	4	0.136	37.18005	3.61577	65.93
18	4.25	0.167	45.65491	3.82111	57.3
19	4.5	0.2	54.67654	4.00143	44.89
20	4.833	0.244	66.70538	4.20029	27.5
21	5	0.297	81.19466	4.39685	7.4
22	5.25	0.339	92.67673	4.52912	0
23	5.5	0.343	93.77026	4.54085	0
24	5.75	0.343	93.77026	4.54085	0

Table B-16 Run-16. The exponential growth phase began at t = 0.75 h. The average phenol concentration in the linear regime was 122.04 g m^{-3}

Sample No.	Time h	Optical density	Biomass concentration g m^{-3}	Ln (Biomass concentration)	Phenol concentration g m^{-3}
1	0	0.014	3.82736	1.34217	126.43
2	0.25	0.015	4.10074	1.41117	125.05
3	0.5	0.016	4.37412	1.47571	125.22
4	0.75	0.017	4.64751	1.53633	124.78
5	1	0.019	5.19427	1.64756	125.63
6	1.25	0.022	6.01442	1.79416	124.35
7	1.5	0.025	6.83457	1.92199	123.59
8	1.75	0.029	7.9281	2.07041	122.31
9	2	0.033	9.02163	2.19962	120.14
10	2.25	0.037	10.11516	2.31404	118.61
11	2.5	0.043	11.75546	2.46432	116.94
12	2.75	0.051	13.94252	2.63494	114.34
13	3	0.06	16.40296	2.79746	112.99
14	3.25	0.072	19.68355	2.97978	108.09
15	3.5	0.084	22.96415	3.13393	103.71
16	3.75	0.101	27.61165	3.31824	99.71
17	4	0.122	33.35269	3.50714	92.39
18	4.25	0.146	39.91387	3.68672	84.44
19	4.5	0.18	49.20889	3.89607	72.44
20	4.75	0.216	59.05066	4.0784	60.51
21	5	0.264	72.17303	4.27907	44.52
22	5.25	0.32	87.48246	4.47144	23.72
23	5.5	0.402	109.8998	4.69957	0
24	5.75	0.419	114.5474	4.74099	0
25	6	0.419	114.5474	4.74099	0

Table B-17 Run-17. The exponential growth phase began at t = 1.0 h. The average phenol concentration in the linear regime was 152.17 g m^{-3}

Sample No	Time h	Optical density	Biomass concentration g m^{-3}	Ln (Biomass concentration)	Phenol concentration g m^{-3}
1	0	0.011	3.00721	1.10101	156.55
2	0.25	0.011	3.00721	1.10101	154.39
3	0.5	0.012	3.28059	1.18802	154.19
4	0.75	0.013	3.55398	1.26807	154.57
5	1	0.014	3.82736	1.34217	154.73
6	1.25	0.016	4.37412	1.47571	155.02
7	1.5	0.018	4.92089	1.59349	152.93
8	1.75	0.02	5.46765	1.69885	152.93
9	2	0.023	6.2878	1.83861	151.83
10	2.25	0.0265	7.24464	1.98026	150.37
11	2.5	0.03	8.20148	2.10431	149.8
12	2.75	0.035	9.56839	2.25847	147.4
13	3	0.041	11.20869	2.41669	147.52
14	3.25	0.047	12.84899	2.55326	144.23
15	3.583	0.058	15.8562	2.76356	141.96
16	3.75	0.065	17.76987	2.8775	137.71
17	4	0.076	20.77708	3.03385	135.38
18	4.25	0.091	24.87782	3.21398	130.36
19	4.633	0.115	31.43901	3.44805	125.2
20	5	0.153	41.82755	3.73356	110.81
21	5.25	0.182	49.75565	3.90712	98.56
22	5.55	0.231	63.1514	4.14553	83.81
23	5.75	0.268	73.26656	4.2941	68.92
24	6	0.337	92.12997	4.5232	45.33
25	6.25	0.391	106.8926	4.67182	20.39
26	6.5	0.469	128.2165	4.85372	0
27	6.75	0.489	133.6841	4.89548	0
28	7	0.489	133.6841	4.89548	0
29	7.5	0.489	133.6841	4.89548	0

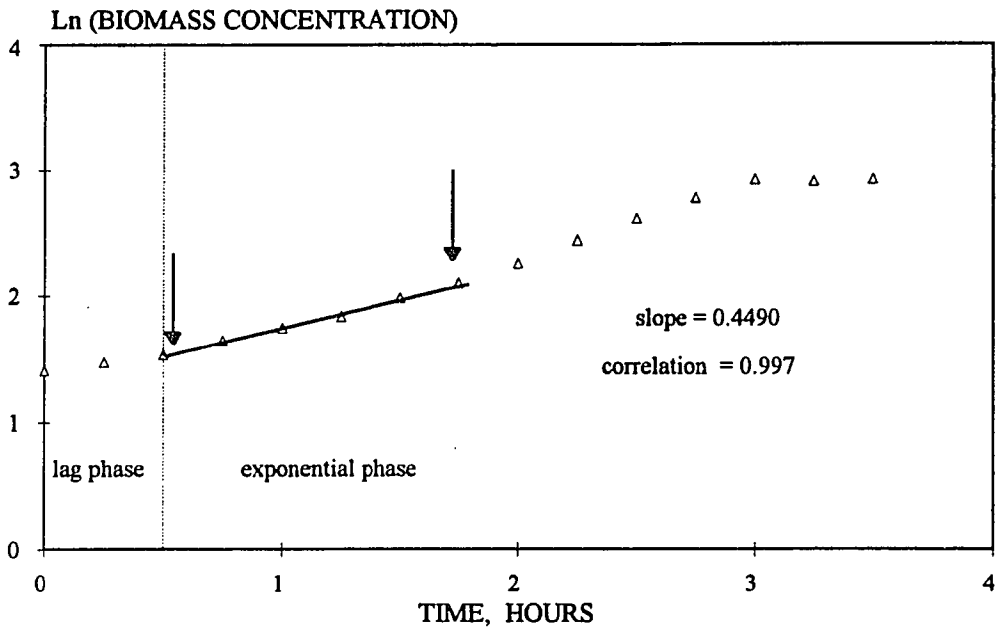

Figure B-1 Plot of Ln biomass concentration versus time for determination of the specific growth rate. Run-1.

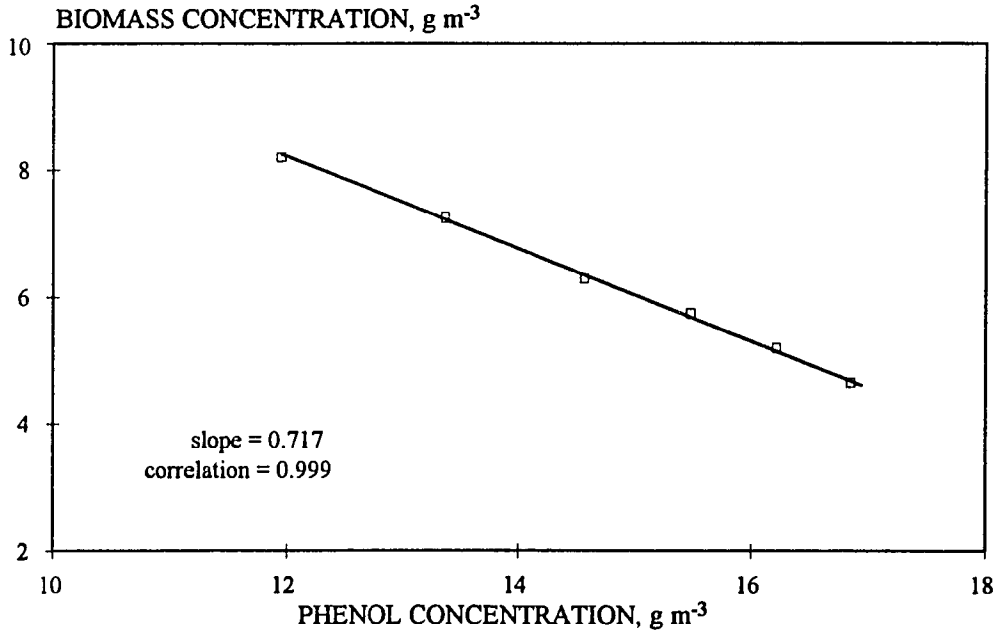

Figure B-2 Plot of biomass concentration versus phenol concentration for the determination of the yield coefficient. Run-1

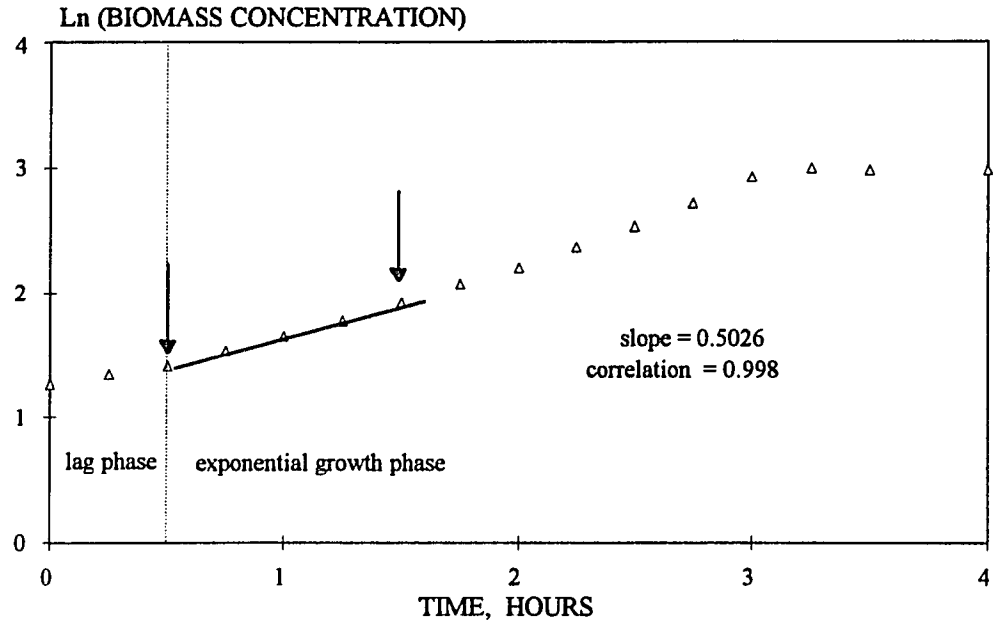

Figure B-3 Plot of Ln biomass concentration versus time for determination of the specific growth rate. Run-2.

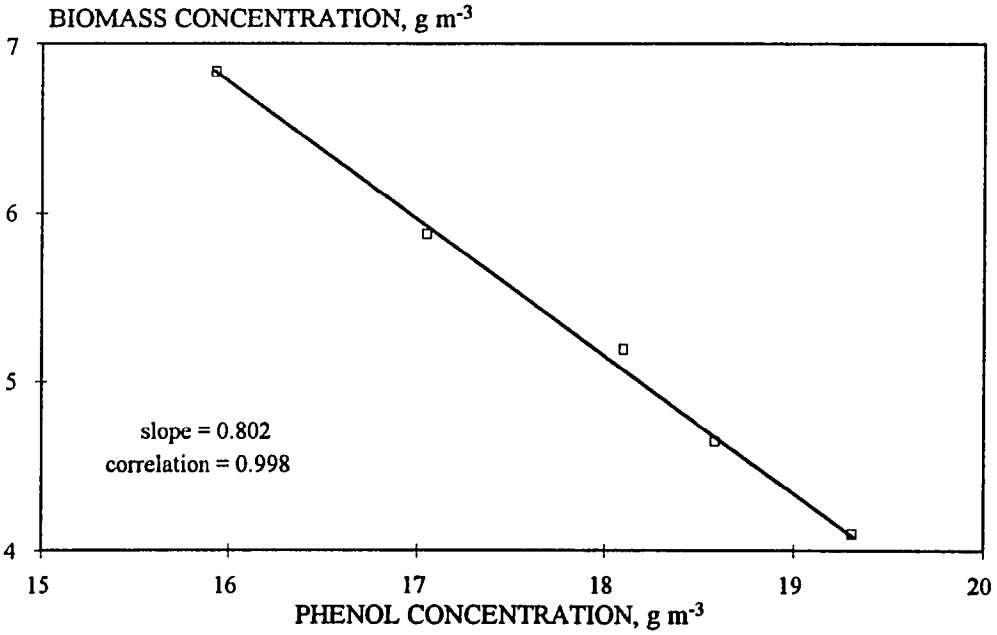

Figure B-4 Plot of biomass concentration versus phenol concentration for the determination of the yield coefficient. Run-2

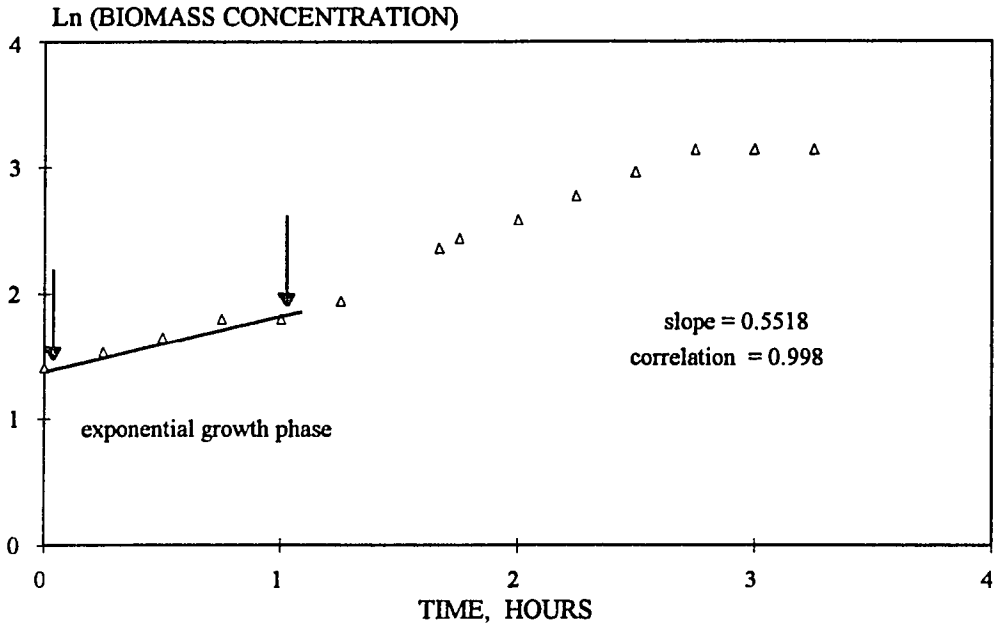

Figure B-5 Plot of Ln biomass concentration versus time for determination of the specific growth rate. Run-3.

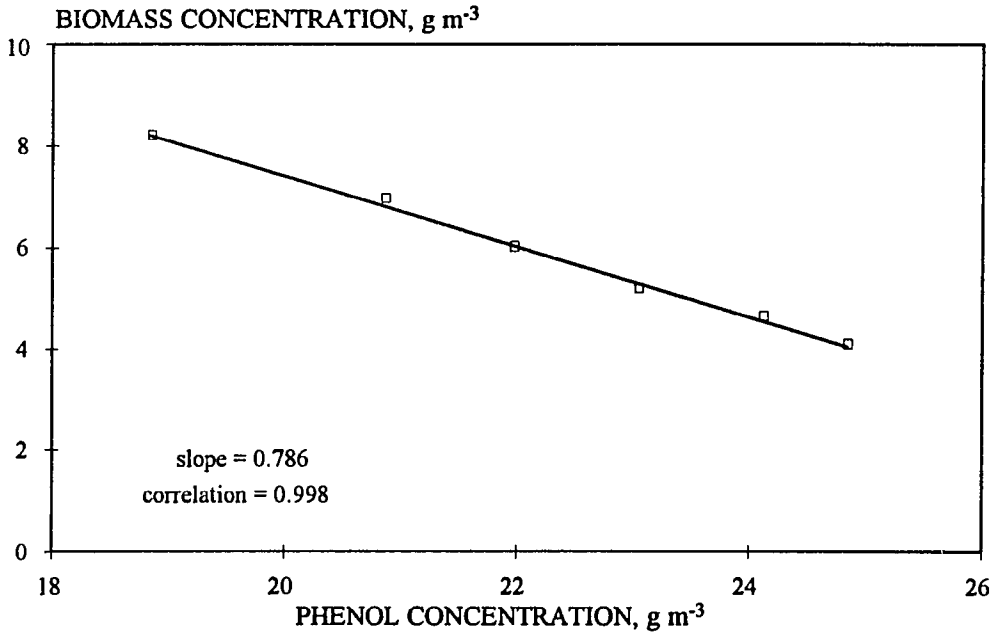

Figure B-6 Plot of biomass concentration versus phenol concentration for the determination of the yield coefficient. Run-3

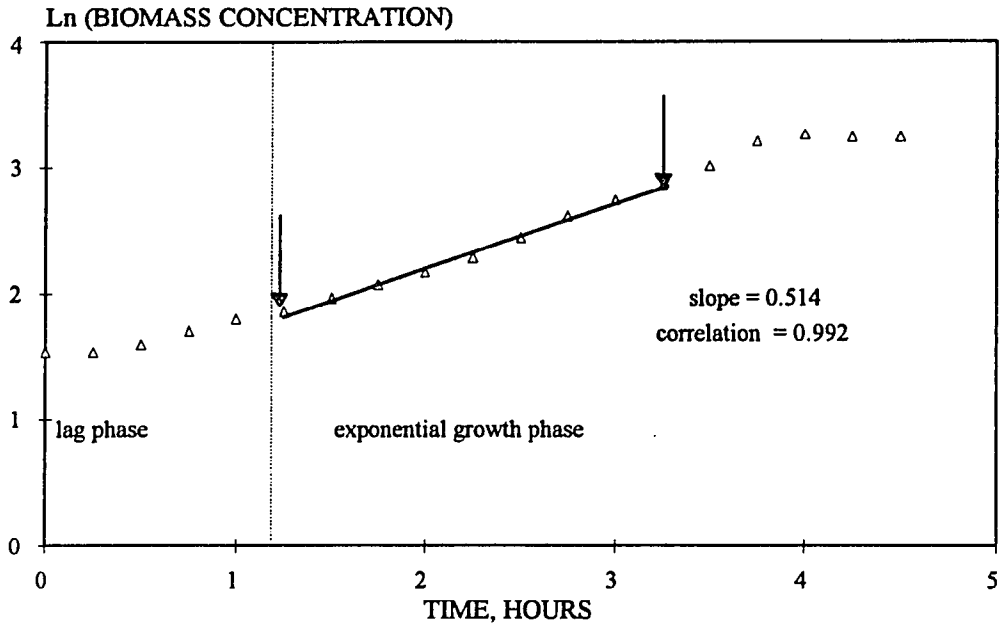

Figure B-7 Plot of Ln biomass concentration versus time for determination of the specific growth rate. Run-4.

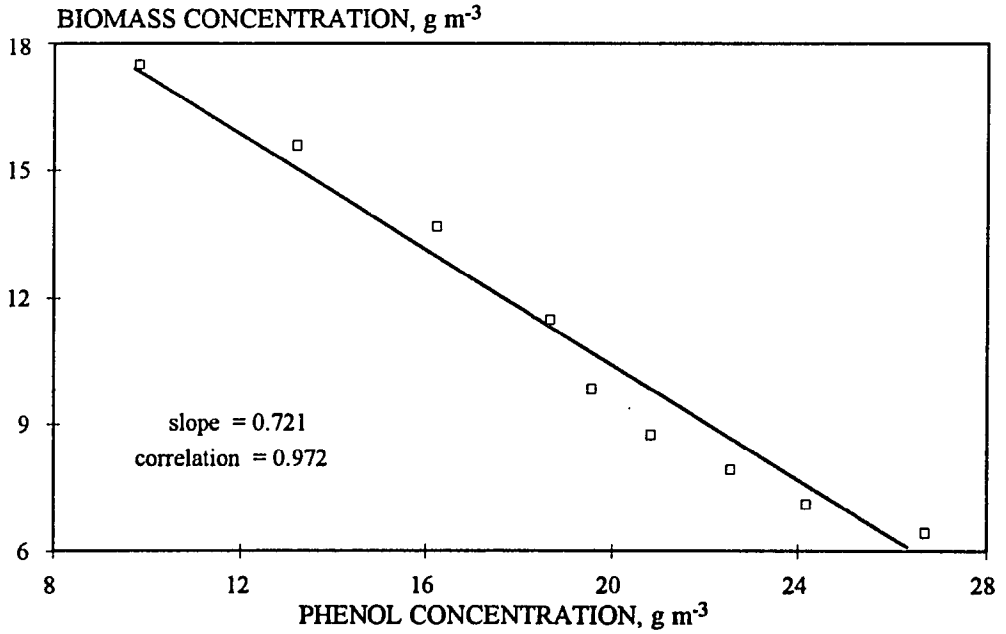

Figure B-8 Plot of biomass concentration versus phenol concentration for the determination of the yield coefficient. Run-4

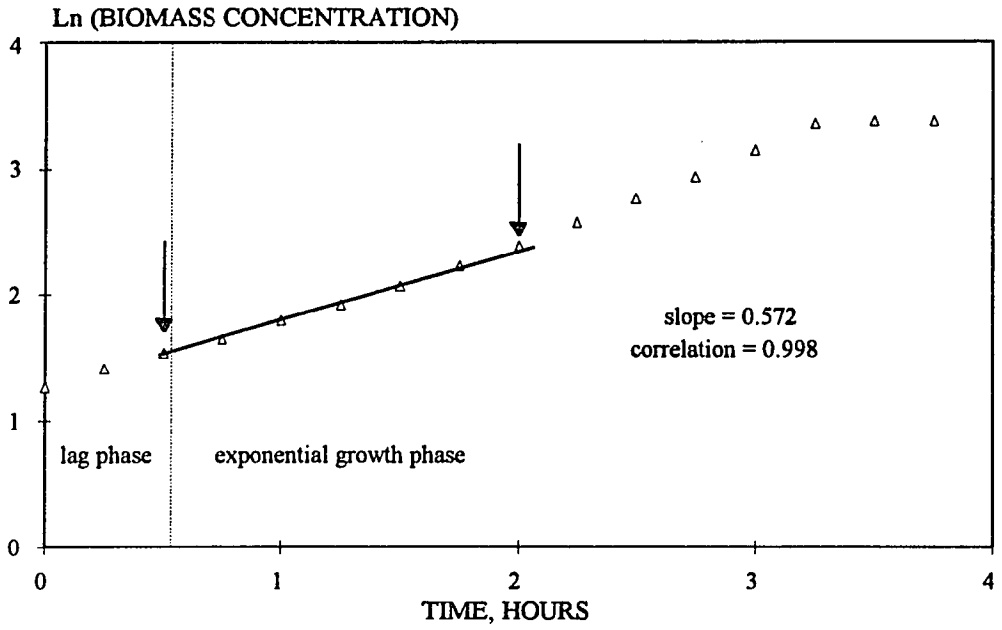

Figure B-9. Plot of Ln biomass concentration versus time for determination of the specific growth rate. Run-5.

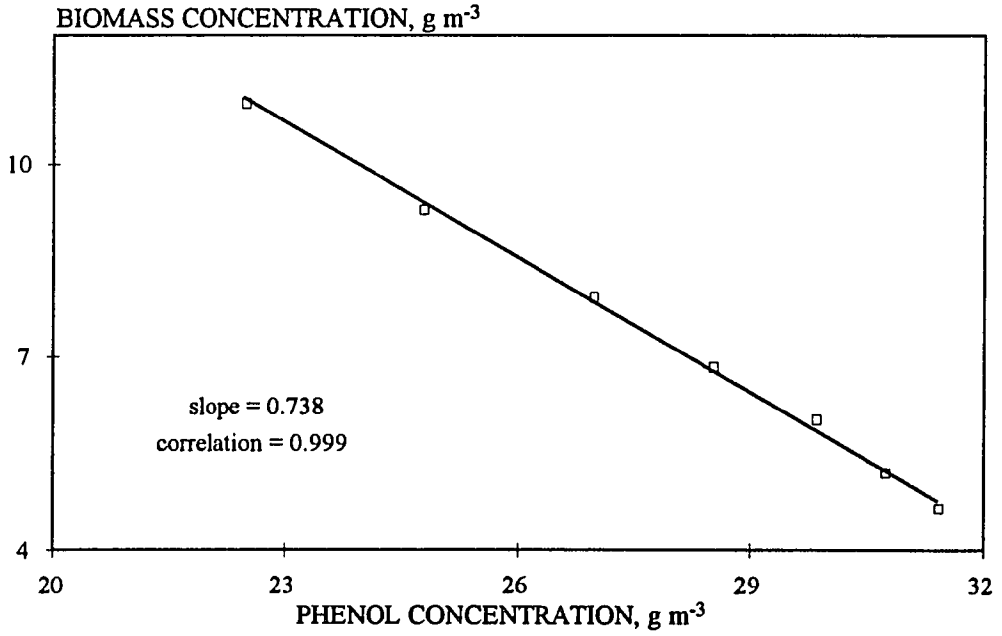

Figure B-10 Plot of biomass concentration versus phenol concentration for the determination of the yield coefficient. Run-5

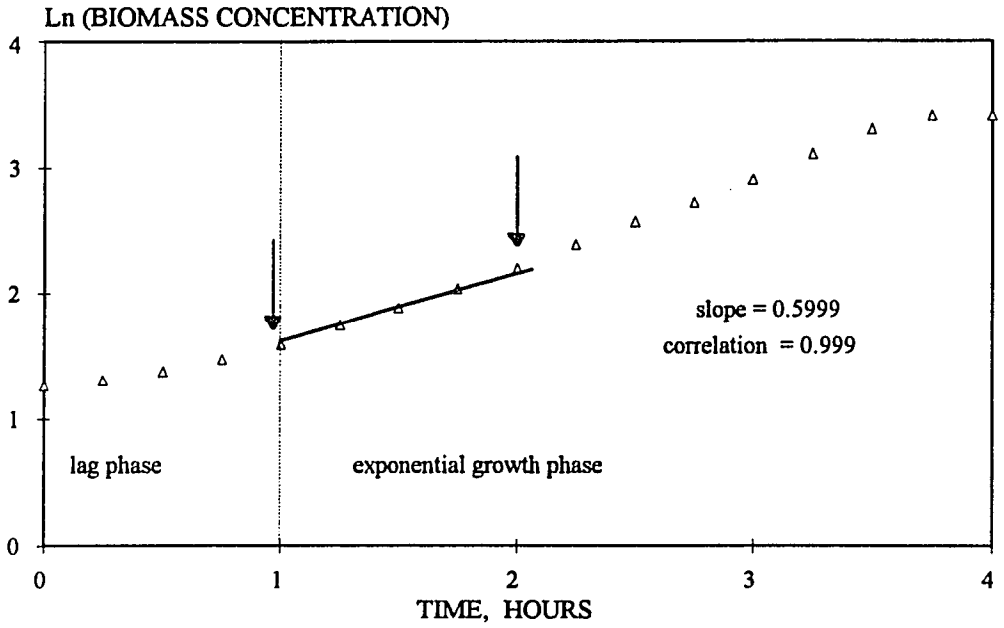

Figure B-11 Plot of Ln biomass concentration versus time for determination of the specific growth rate. Run-6.

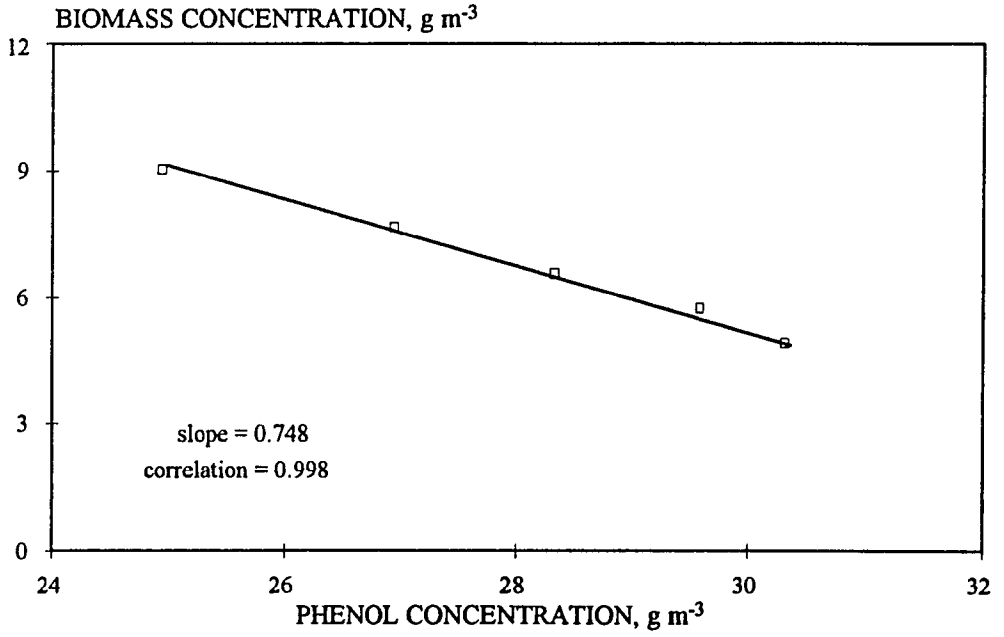

Figure B-12 Plot of biomass concentration versus phenol concentration for the determination of the yield coefficient. Run-6

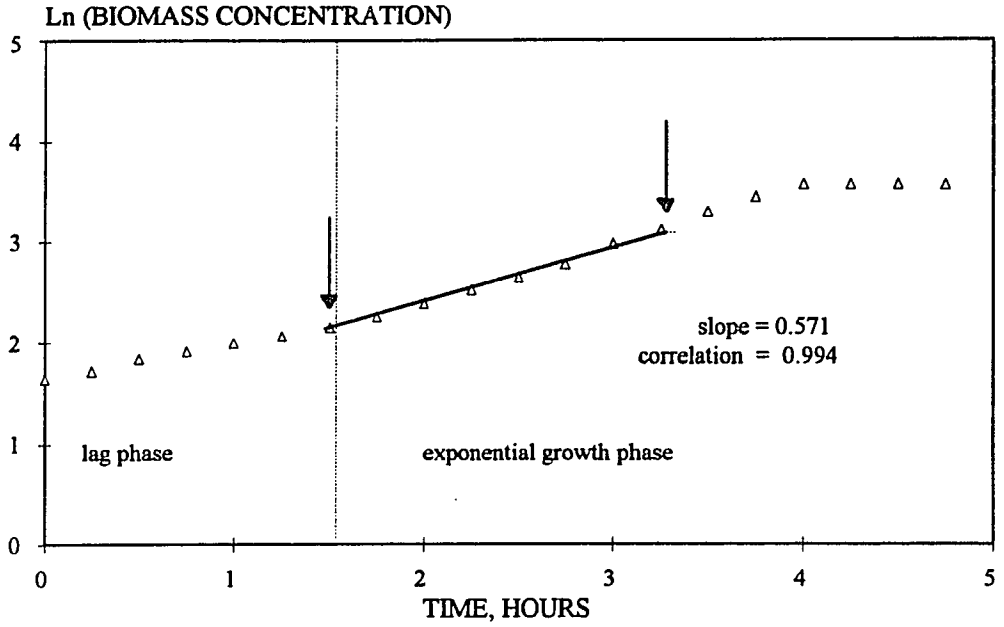

Figure B-13. Plot of Ln biomass concentration versus time for determination of the specific growth rate. Run-7.

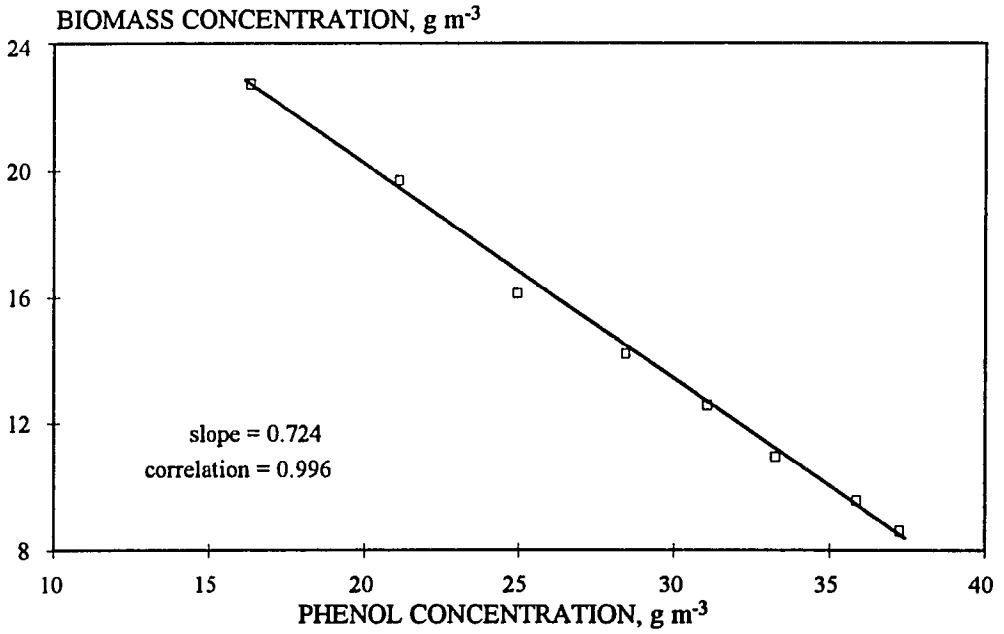

Figure B-14 Plot of biomass concentration versus phenol concentration for the determination of the yield coefficient. Run-7

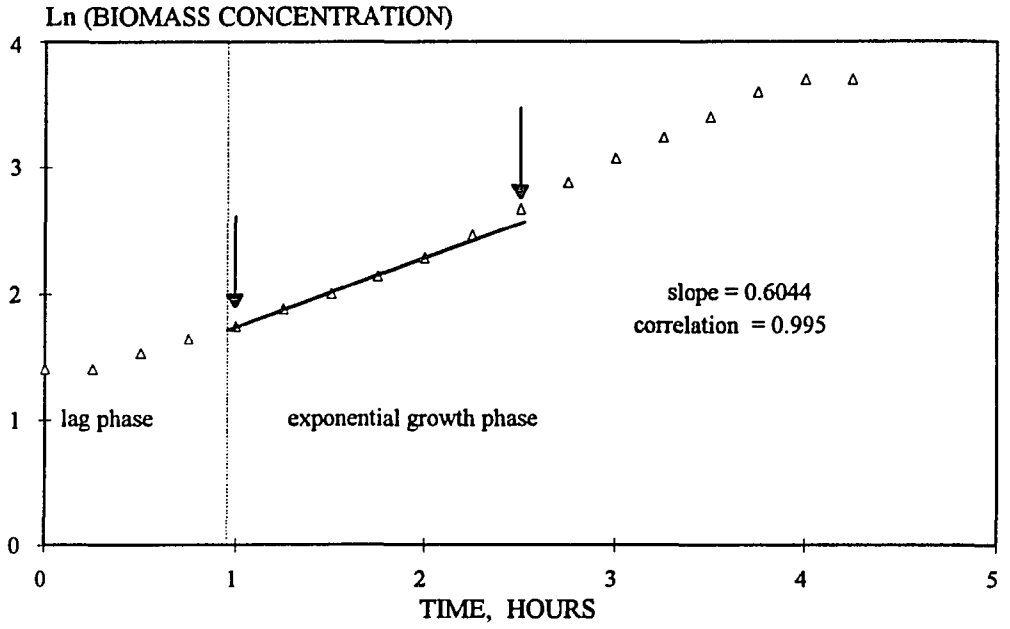

Figure B-15 Plot of Ln biomass concentration versus time for determination of the specific growth rate. Run-8.

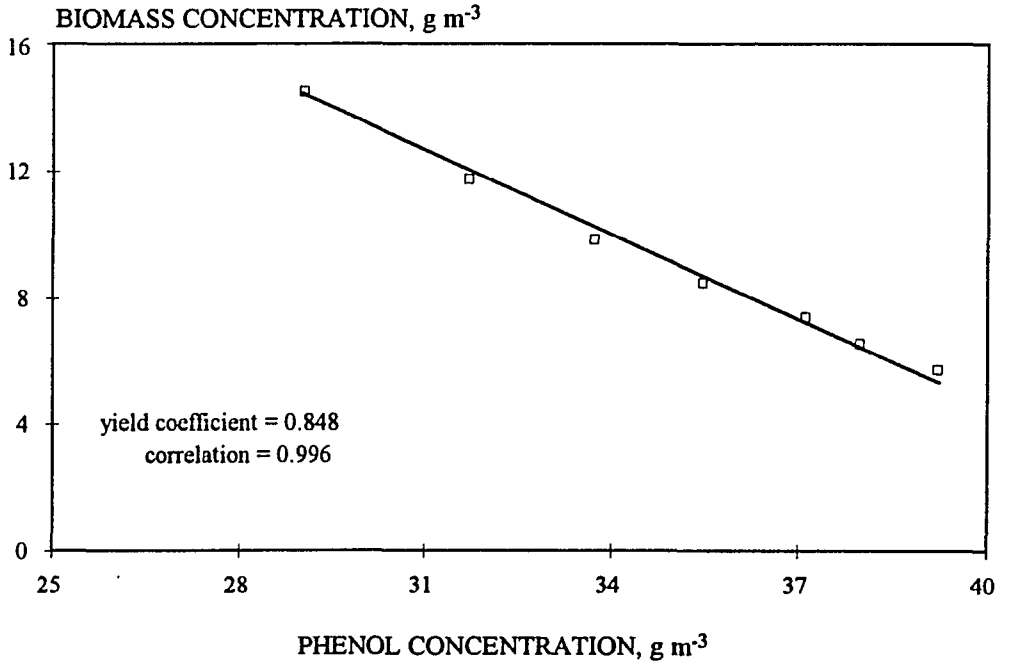

Figure B-16 Plot of biomass concentration versus phenol concentration for the determination of the yield coefficient. Run-8

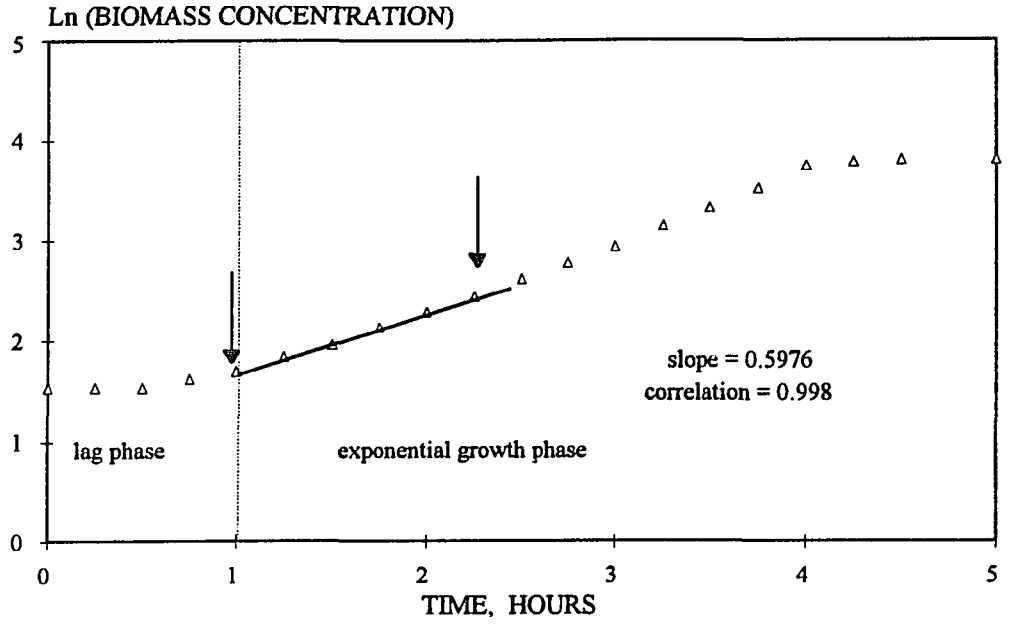

Figure B-17 Plot of Ln biomass concentration versus time for determination of the specific growth rate. Run-9.

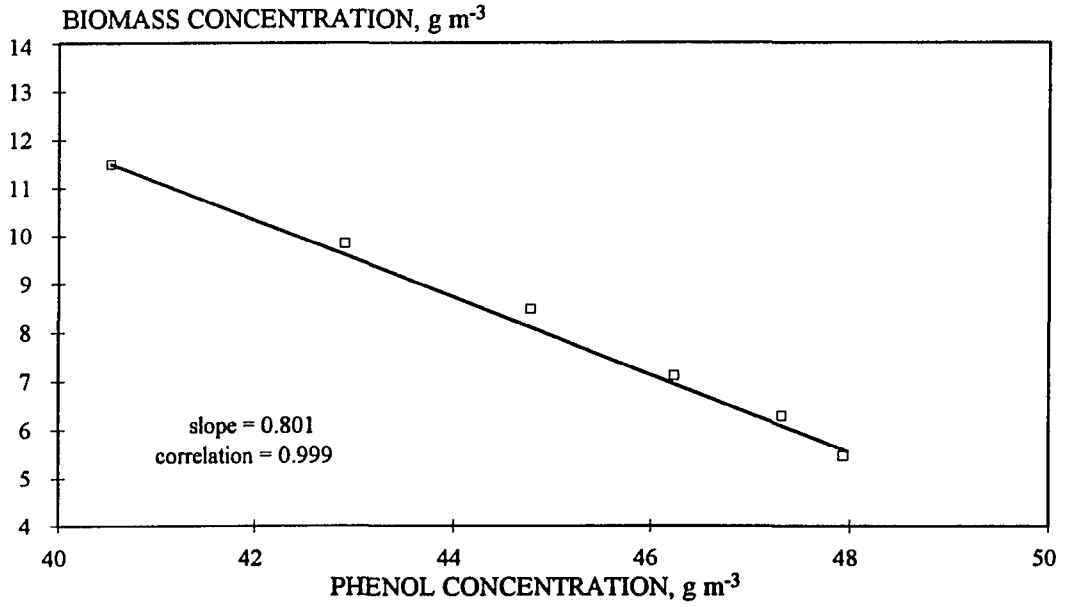

Figure B-18 Plot of biomass concentration versus phenol concentration for the determination of the yield coefficient. Run-9

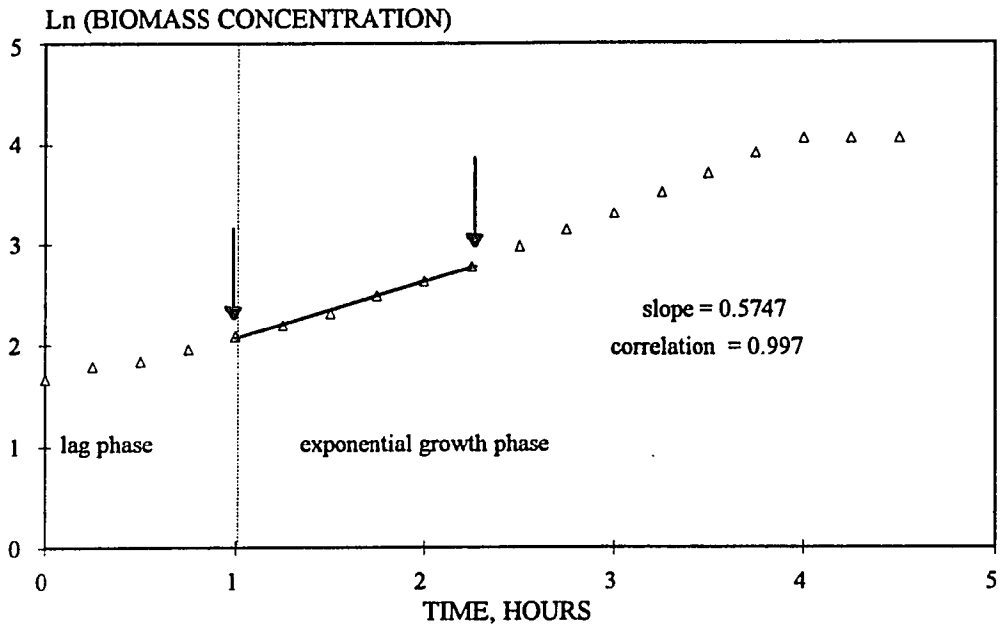

Figure B-19 Plot of Ln biomass concentration versus time for determination of the specific growth rate. Run-10.

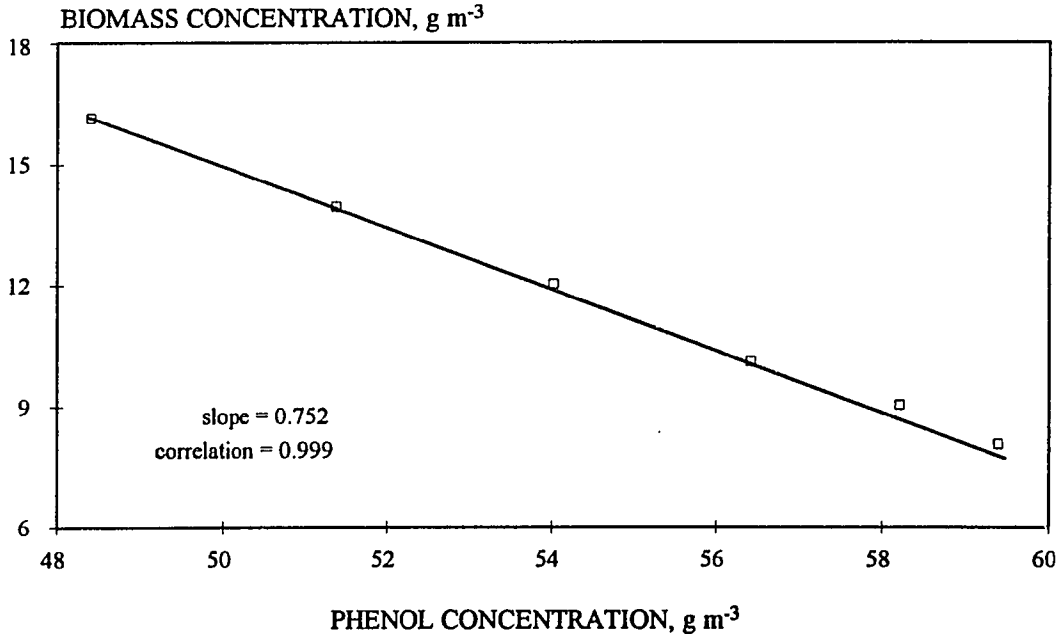

Figure B-20 Plot of biomass concentration versus phenol concentration for the determination of the yield coefficient. Run-10

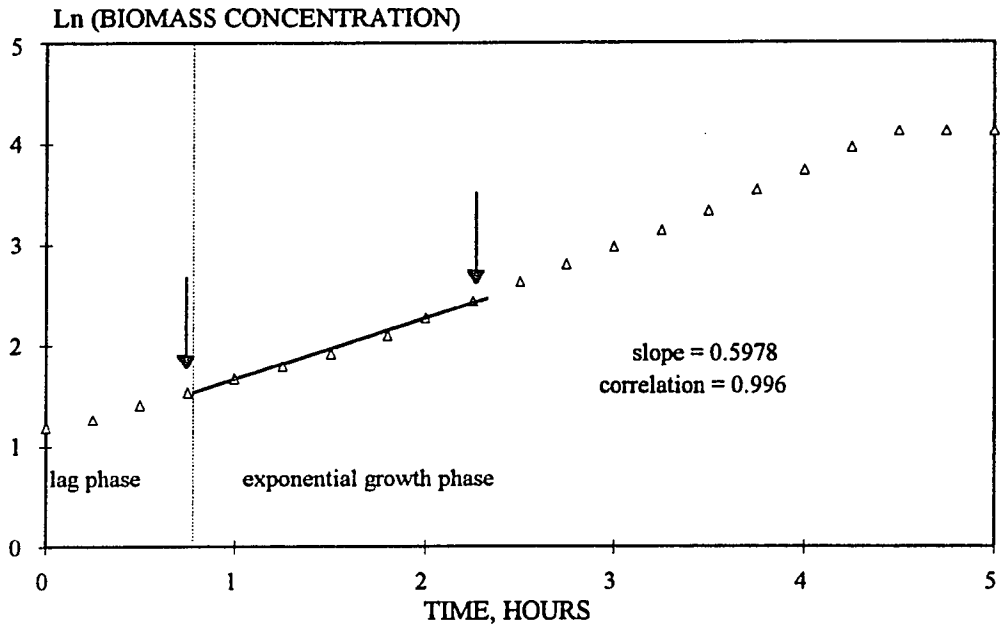

Figure B-21 Plot of Ln biomass concentration versus time for determination of the specific growth rate. Run-11.

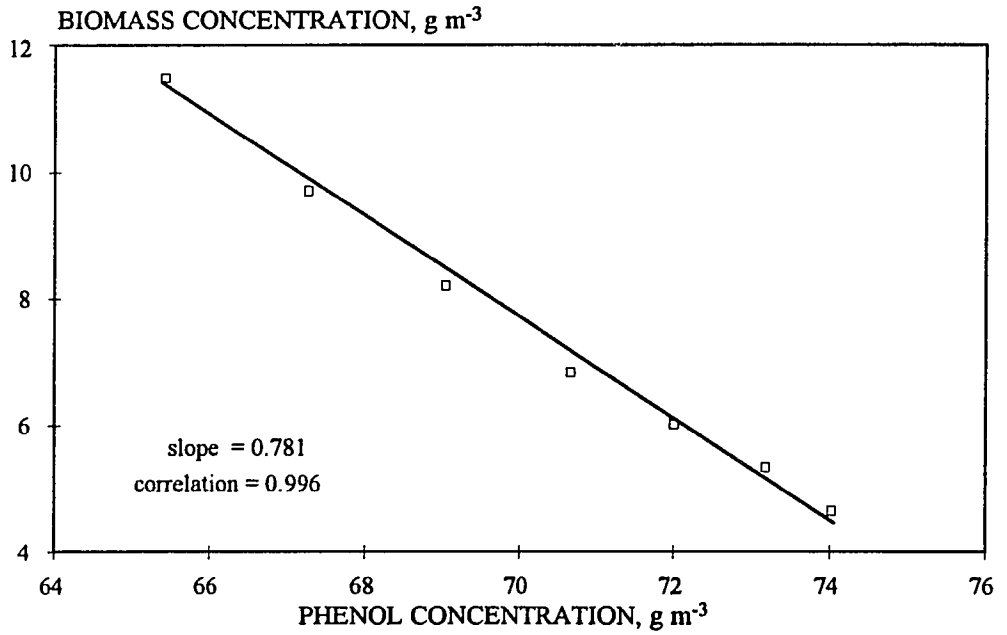

Figure B-22 Plot of biomass concentration versus phenol concentration for the determination of the yield coefficient. Run-11

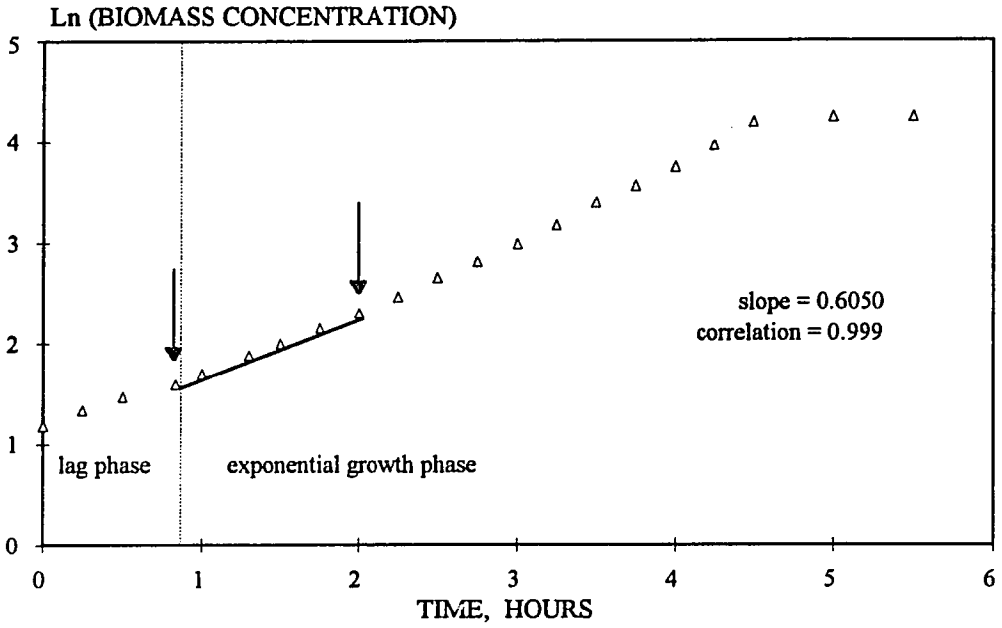

Figure B-23 Plot of Ln biomass concentration versus time for determination of the specific growth rate. Run-12.

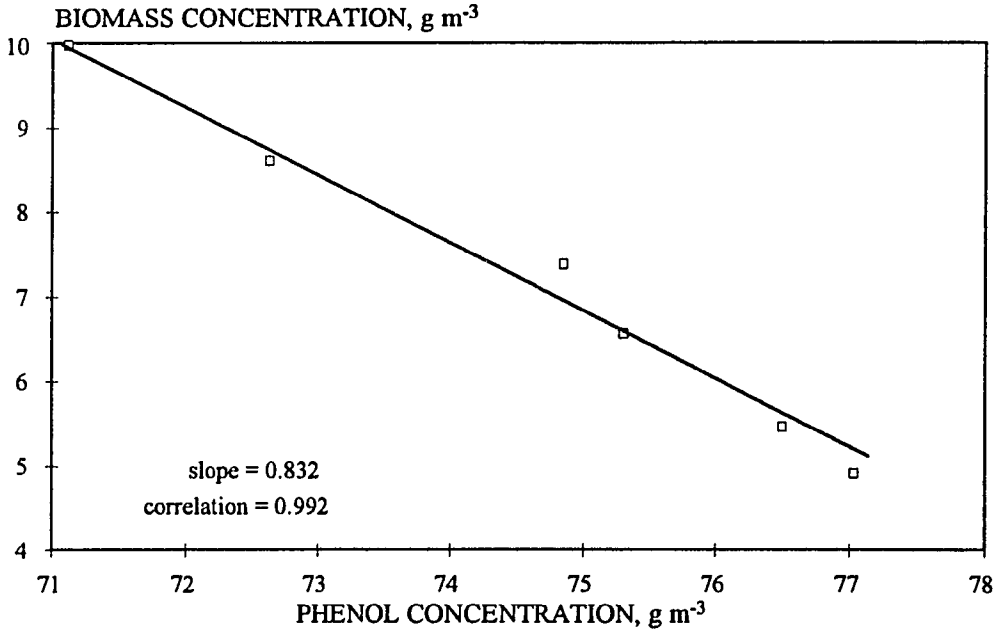

Figure B-24 Plot of biomass concentration versus phenol concentration for the determination of the yield coefficient. Run-12

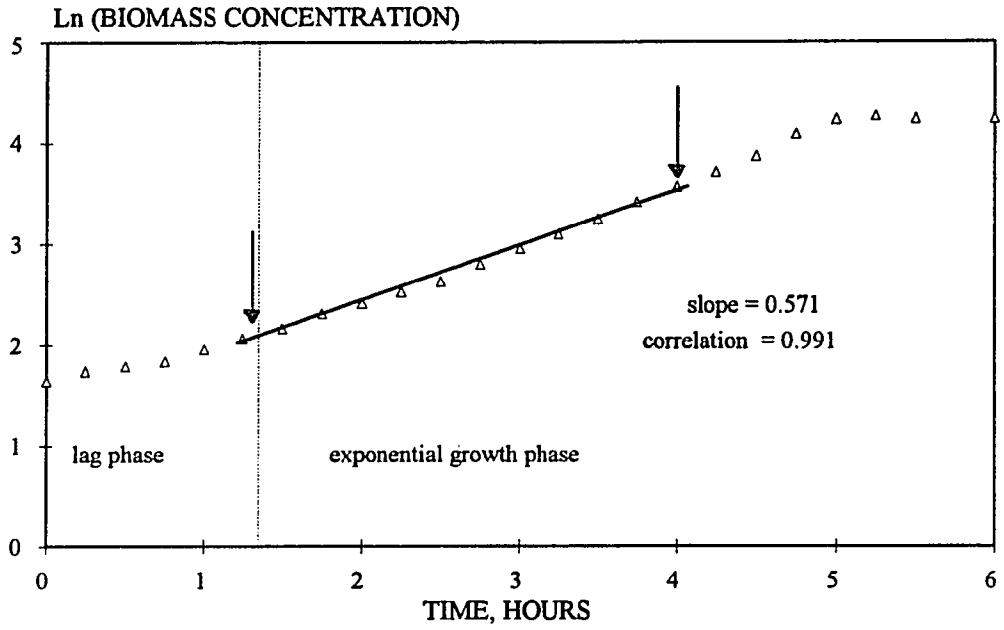

Figure B-25 Plot of Ln biomass concentration versus time for determination of the specific growth rate. Run-13.

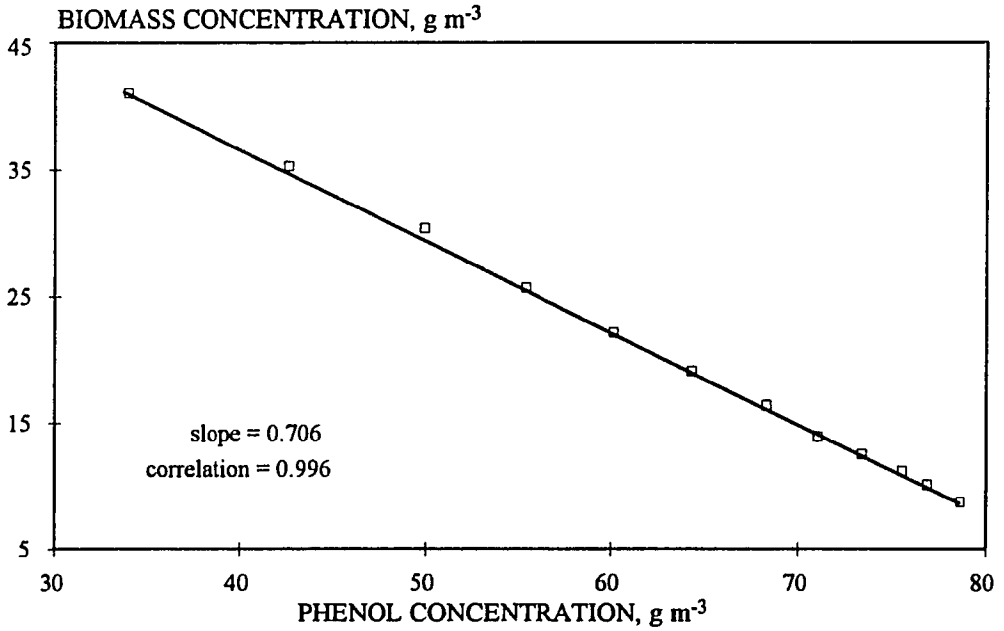

Figure B-26 Plot of biomass concentration versus phenol concentration for the determination of the yield coefficient. Run-13

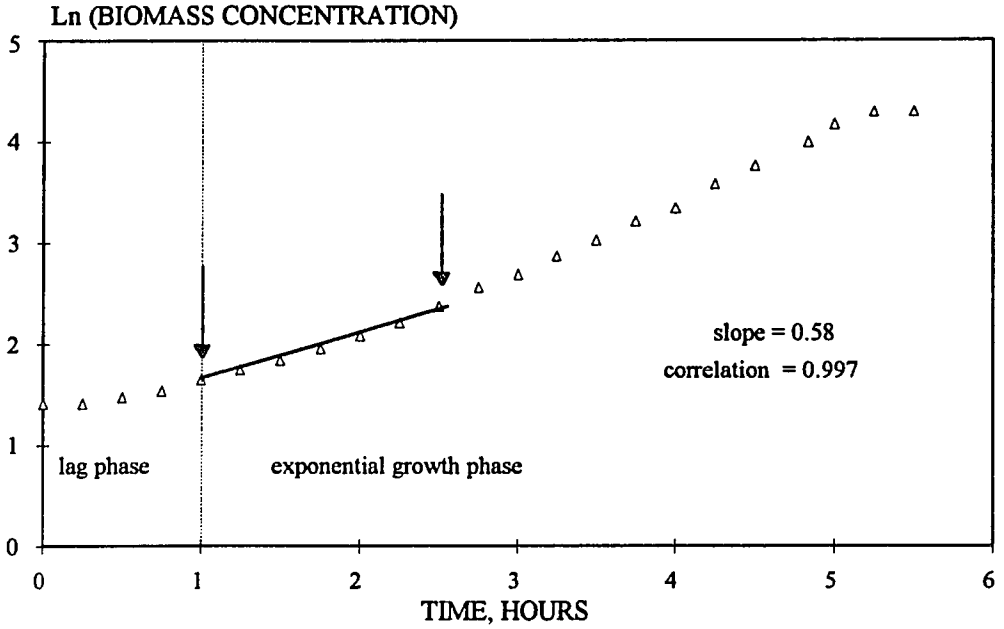

Figure B-27 Plot of Ln biomass concentration versus time for determination of the specific growth rate. Run-14.

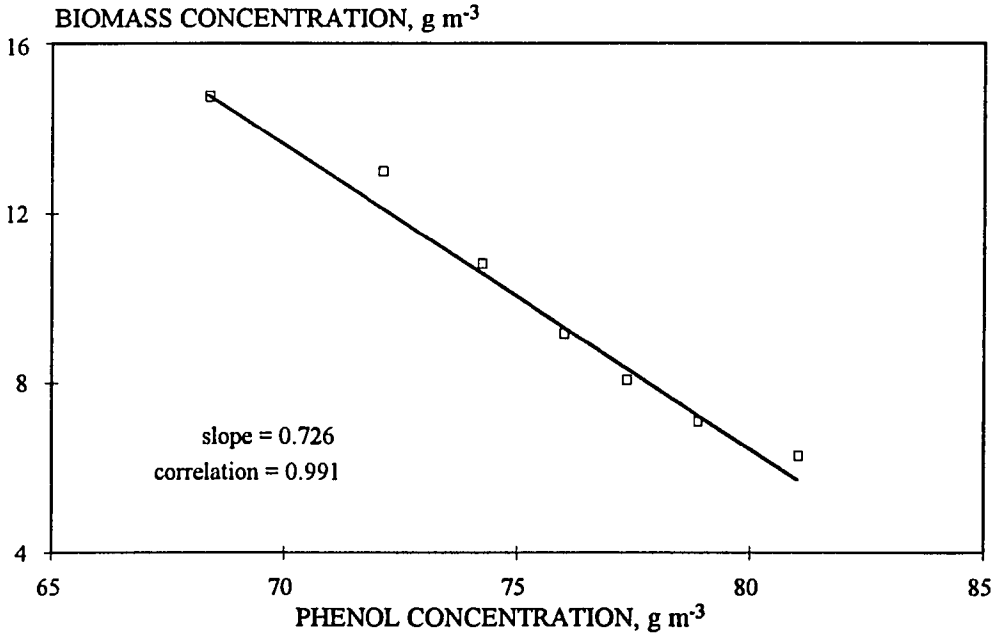

Figure B-28 Plot of biomass concentration versus phenol concentration for the determination of the yield coefficient. Run-14

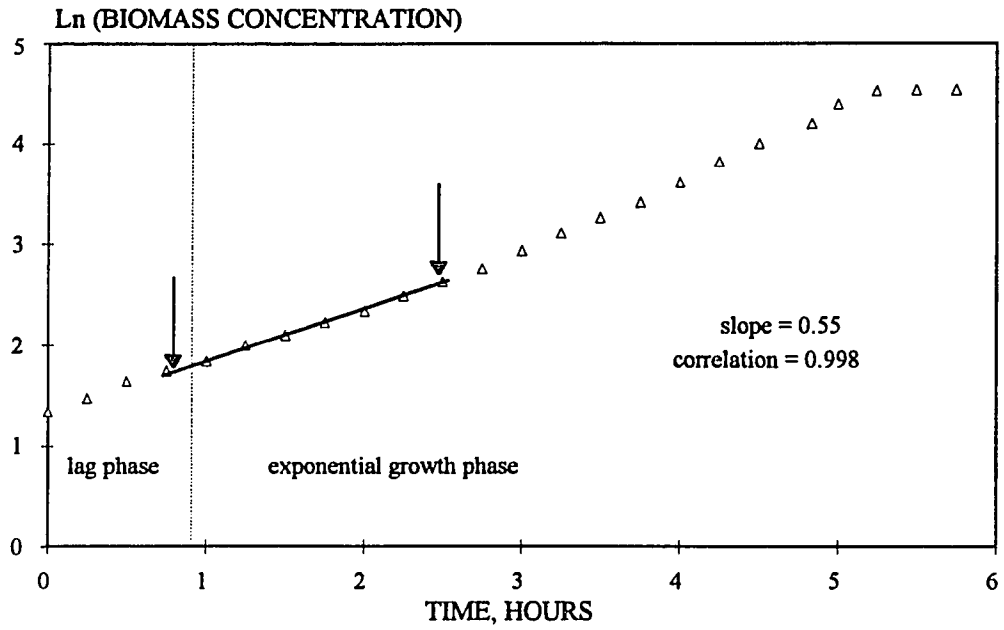

Figure B-29 Plot of Ln biomass concentration versus time for determination of the specific growth rate. Run-15.

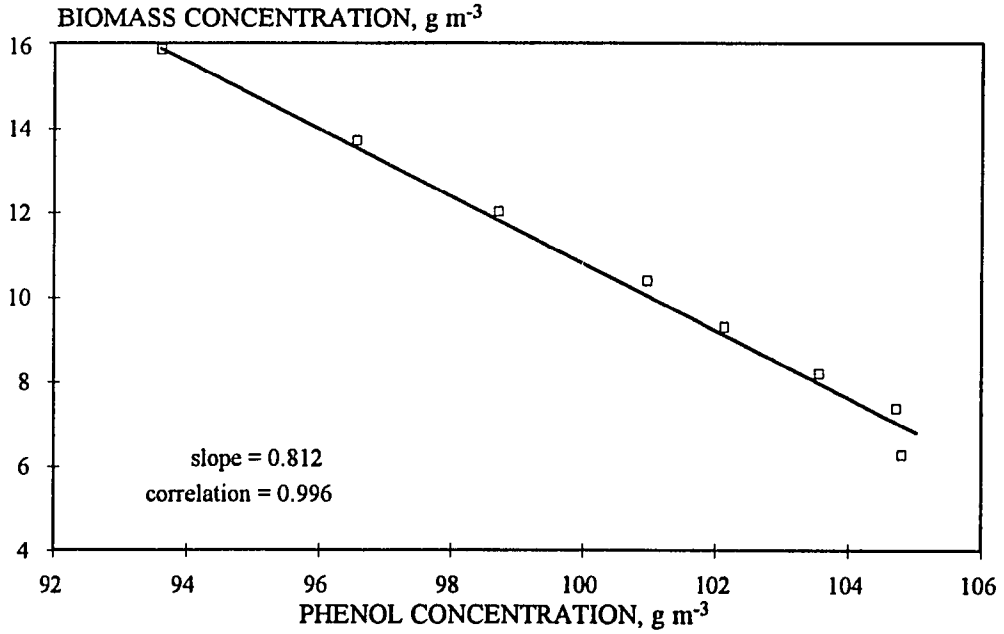

Figure B-30 Plot of biomass concentration versus phenol concentration for the determination of the yield coefficient. Run-15

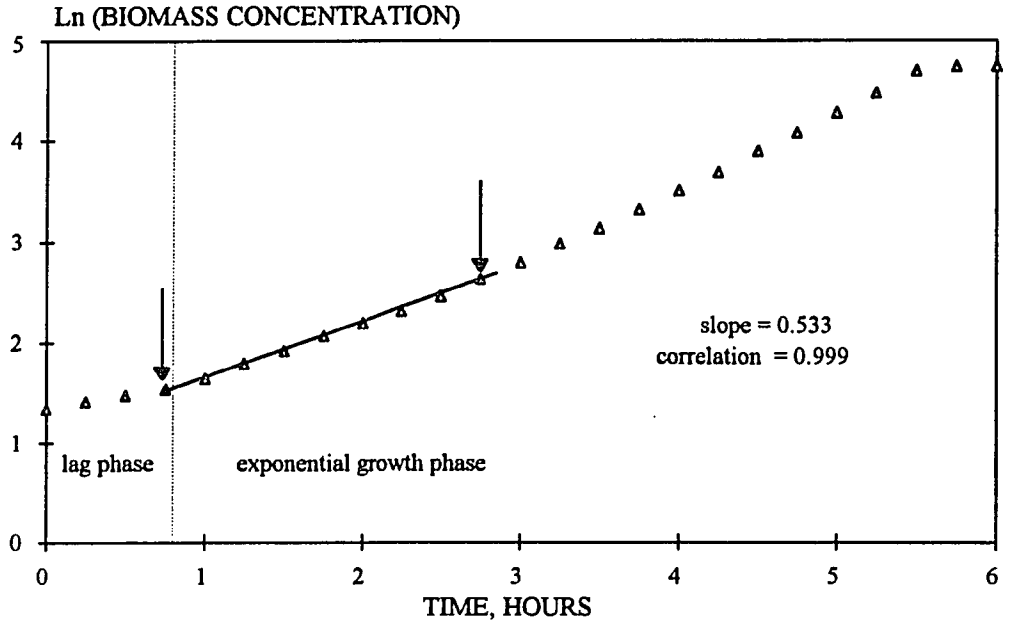

Figure B-31 Plot of Ln biomass concentration versus time for determination of the specific growth rate. Run-16.

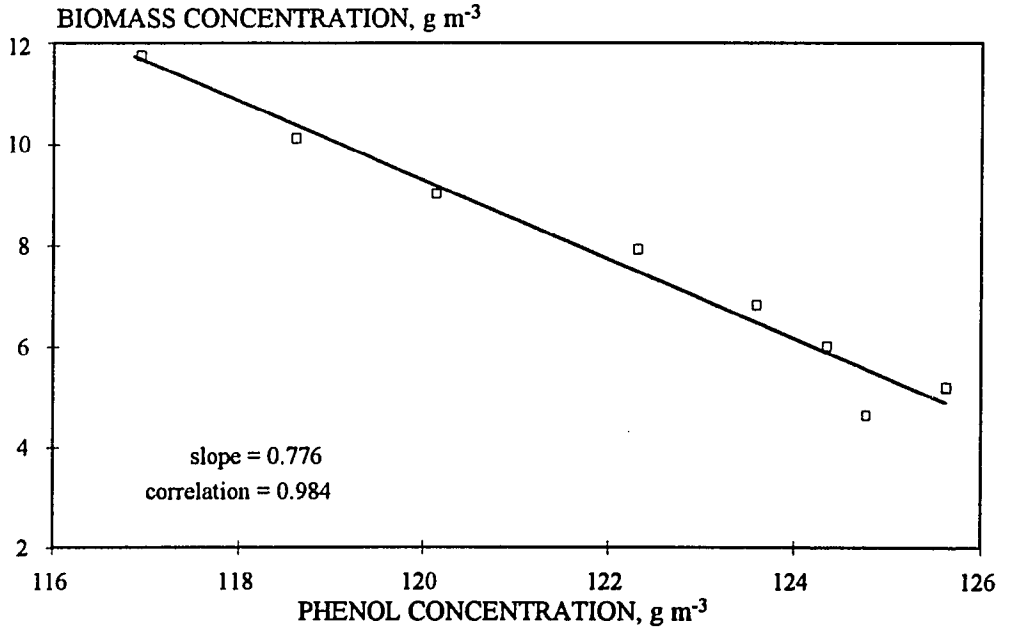

Figure B-32 Plot of biomass concentration versus phenol concentration for the determination of the yield coefficient. Run-16

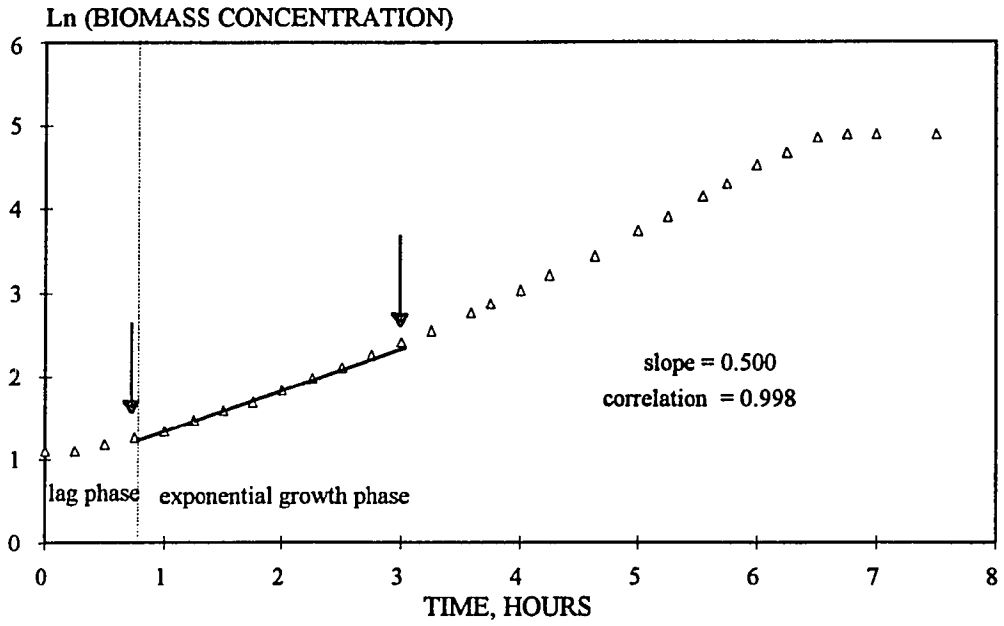

Figure B-33 Plot of Ln biomass concentration versus time for determination of the specific growth rate. Run-17.

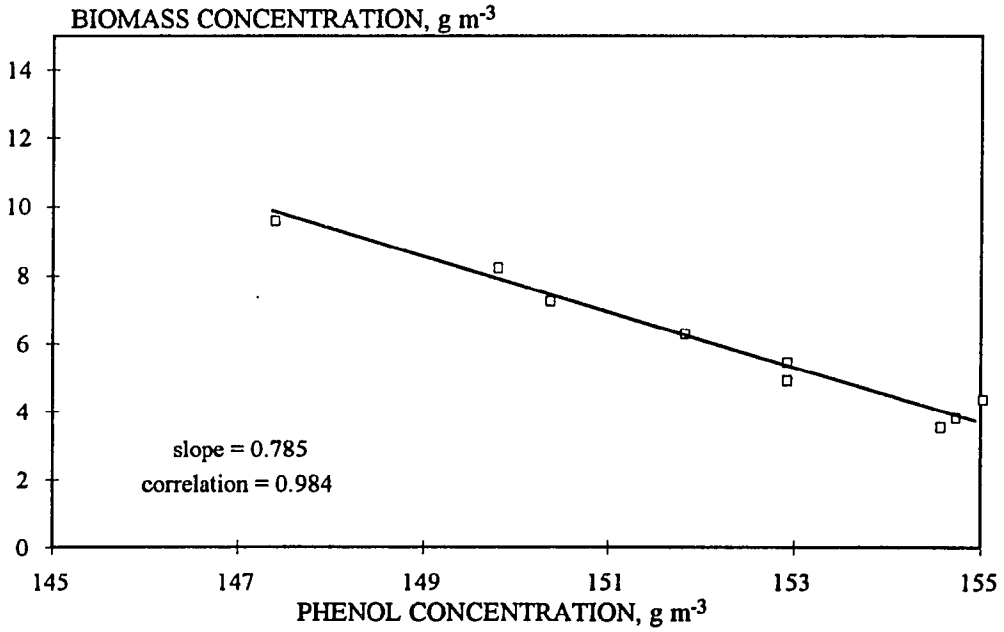

Figure B-34 Plot of biomass concentration versus phenol concentration for the determination of the yield coefficient. Run-17

APPENDIX C

Experimental data from SFBR experiments

The experimental data from the SFBR experiments are given in this appendix. Table C-1 and Figures C-1 and C-2 are for pure culture runs using *Pseudomonas resinovorans* (ATCC 14235). Table C-2 and Figures C-3 and C-4 are for pure culture runs using *Pseudomonas putida* (ATCC 17514). Tables C-3 to C-6 list the experimental data for the mixed culture experiments. The concentration profiles for the mixed culture experiments are shown in Figures C-5 to C-17. Some of the profiles are given in the main body of the dissertation (see Chapter 6). The FORTRAN code for the integration of the mass balance equations using fourth order Runge-Kutta method is also given.

Table C-1 Experimental data from an SFBR run (SFBR-R) with *P. resinovorans*

	Cycle 1			Cycle 4		
Time h	Optical density	Biomass concentration g m^{-3}	Phenol concentration g m^{-3}	Optical density	Biomass concentration g m^{-3}	Phenol concentration g m^{-3}
0	0.230	62.878	15.11	0.270	73.813	0
0.25	0.162	44.288	43.81	0.177	48.389	34.54
0.5	0.133	36.360	56.14	0.140	38.274	49.81
0.75	0.121	33.079	61.56	0.121	33.079	56.79
1	0.112	30.619	63.42	0.113	30.892	60.92
1.25	0.129	35.266	55.99	0.131	35.813	52.57
1.5	0.154	42.101	45.98	0.159	43.468	41.3
1.75	0.178	48.662	34.23	0.182	51.123	28.51
2	0.218	59.597	20.49	0.228	62.331	12.86
2.25	0.254	69.439	2.29	0.268	73.267	0
2.5	0.271	74.097	0	0.268	73.267	0

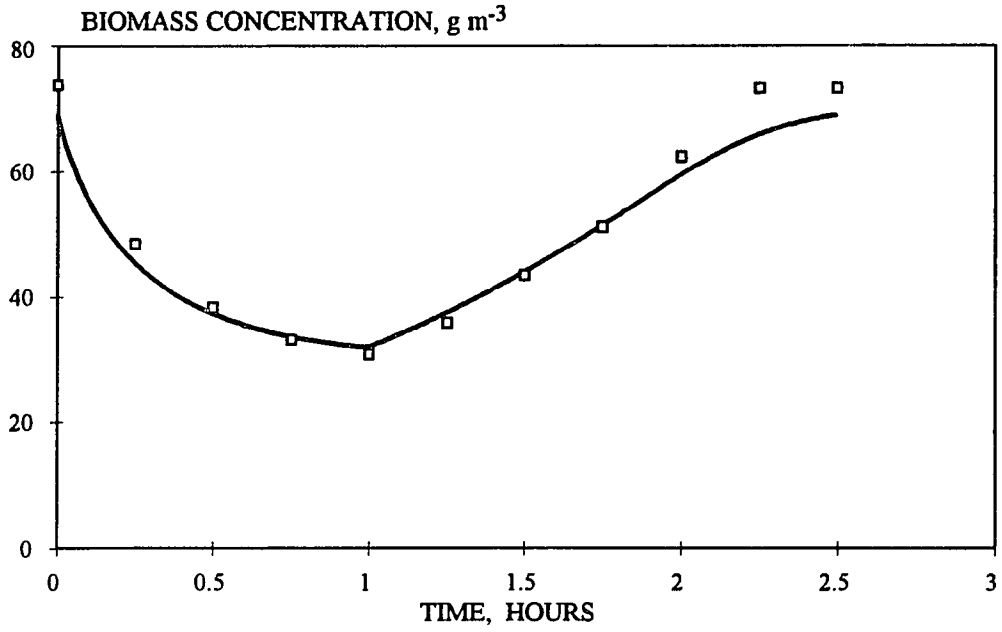

Figure C-1 Biomass concentration profile for the fourth cycle of the SFBR run with *P. resinovorans* - (SFBR-R). The curve indicates model predictions

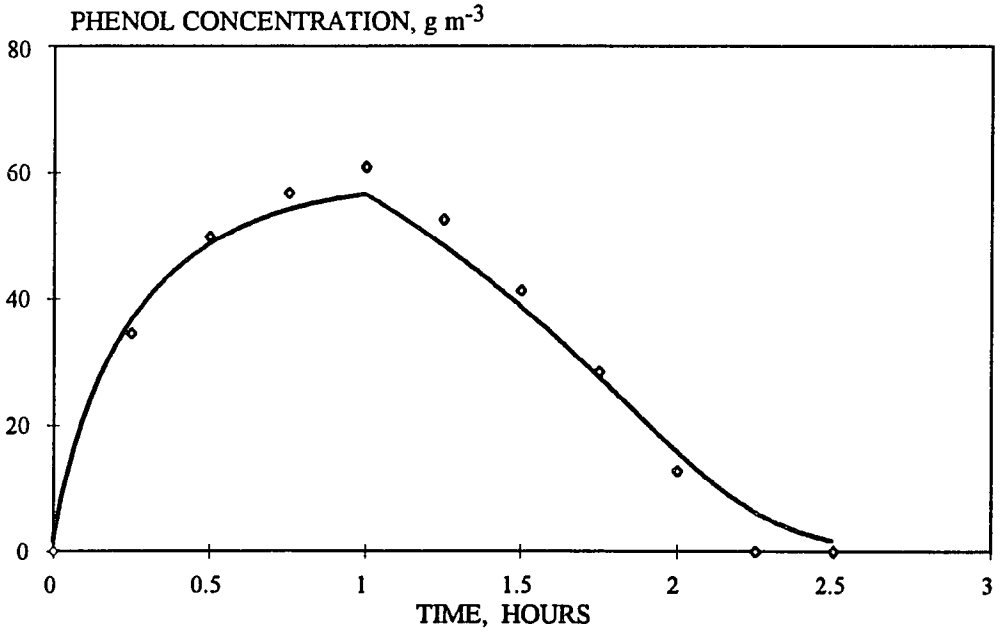

Figure C-2 Phenol concentration profile for the fourth cycle of the SFBR run with *P. resinovorans* - (SFBR-R). The curve indicates the model predictions.

Table C-2 Experimental Data for SFBR run (SFBR-P) with *Pseudomonas putida*

	Cycle 1			Cycle 6		
Time h	Optical density	Biomass concentration g m^{-3}	Phenol concentration g m^{-3}	Optical density	Biomass concentration g m^{-3}	Phenol concentration g m^{-3}
0	0.142	38.82	0	0.148	40.461	0
0.083	0.107	29.252	12.4	-	-	-
0.167	0.091	24.878	20.91	-	-	-
0.25	0.079	21.597	26.22	0.091	24.604	25.25
0.5	0.092	25.151	21.9	0.101	27.612	19.48
0.75	0.101	27.612	15.99	0.109	29.799	13.87
1	0.114	31.166	7.91	0.125	34.1332	5.26
1.167	0.13	35.54	1.42	-	-	-
1.333	0.138	37.727	0	0.148	40.461	0
1.5	0.138	37.727	0	0.148	40.461	0

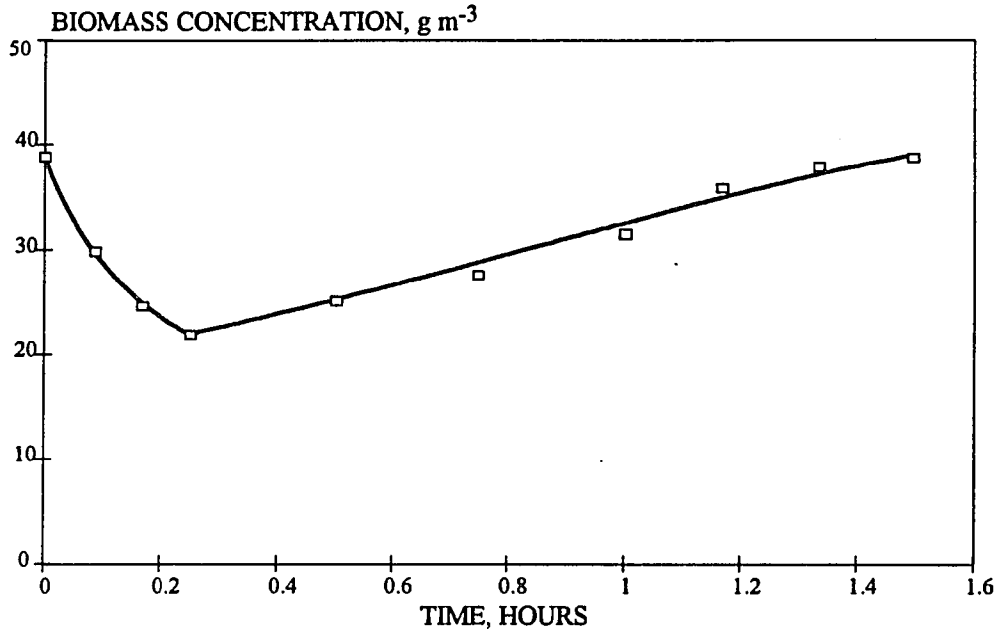

Figure C-3 Biomass concentration profile for the first cycle of the SFBR run with *P. putida* - (SFBR-P). The curve indicates model predictions.

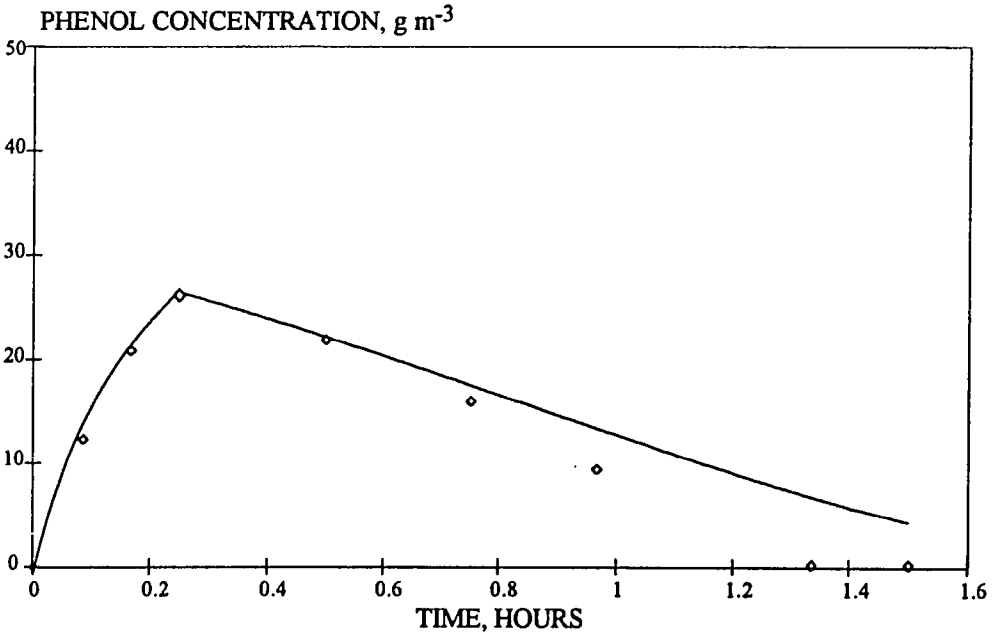

Figure C-4 Phenol concentration profile for the first cycle of the SFBR run with *P. putida* - (SFBR-P). The curve indicates model predictions.

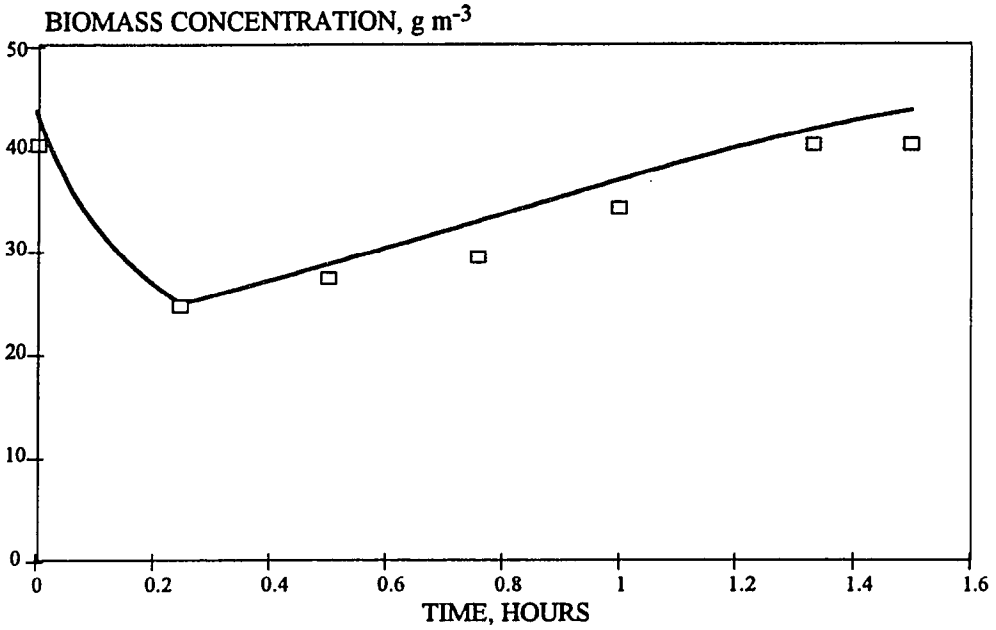

Figure C-5 Biomass concentration profile for the sixth cycle of the SFBR run with *P. putida* - (SFBR-P). The curve indicates model predictions.

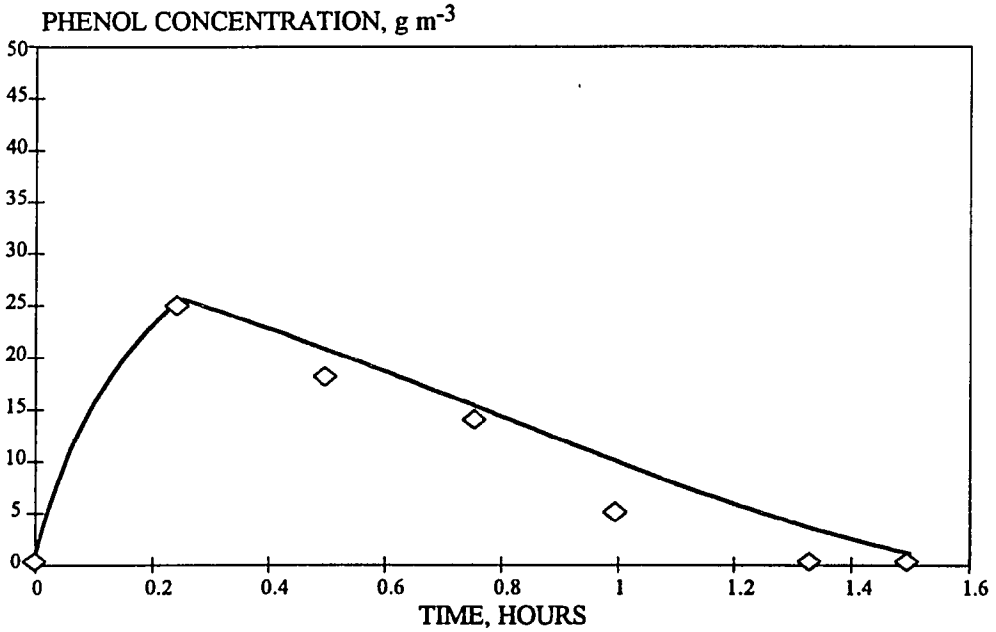

Figure C-6 Phenol concentration profile for the sixth cycle of the SFBR run with *P. putida* - (SFBR-P). The curve indicates model predictions.

Table C-3 Experimental data for SFBR run SFBR-M1

Cycle 1

Time h	Optical density	*P. putida* g m^{-3}	*P. resinovorans* g m^{-3}	Total Biomass g m^{-3}	Phenol g m^{-3}
0	0.253	12.8	56.35	69.16	5.03
0.25	0.178			48.66	25.25
0.5	0.142			38.82	34.4
0.75	0.124			33.89	37.72
1	0.117	4.41	27.56	31.98	38.55
1.5	0.142			38.82	27.33
1.75	0.163			44.56	17.67
2	0.205	9.09	46.94	56.04	7.08
2.25	0.225			61.51	0
2.5	0.225			61.51	0
3	0.225	7.82	59.71985	61.51	0

Table C-3 (contd)

Cycle 6

Time h	Optical density	*P. putida* g m^{-3}	*P. resinovorans* g m^{-3}	Total Biomass g m^{-3}	Phenol g m^{-3}
0	0.213	10.8	47.42	58.23	0
0.25	0.156			39.91	20.16
0.5	0.125			31.43	32.63
1	0.106	3.09	25.81	28.97	40.36
1.25	0.110			30.07	39.07
1.5	0.135			36.90	30.81
1.75	0.153			41.82	20.72
2	0.180	5.9	35.91	49.24	12.95
2.25	0.215			58.77	0.87
2.5	0.240				0
3	0.212	7.03	50.91	57.95	0

Table C-3 (contd)

Cycle 24

Time h	Optical density	*P. putida* g m^{-3}	*P. resinovorans* g m^{-3}	Total Biomass g m^{-3}	Phenol g m^{-3}
0	0.212	8.16	49.78	57.95	0
0.25	0.150			39.91	24.37
0.5	0.132	3.31	31.12	34.44	30.97
0.75	0.116			30.07	36.05
1	0.107			27.61	38
1.25	0.118			30.61	
1.5	0.136	5.09	29.9	35.26	32.92
1.75	0.163			41.92	26.66
2	0.189			46.66	15.75
2.25	0.234			63.97	2.13
2.5	0.206			56.31	0
3	0.204	2.57	53.31	55.77	0

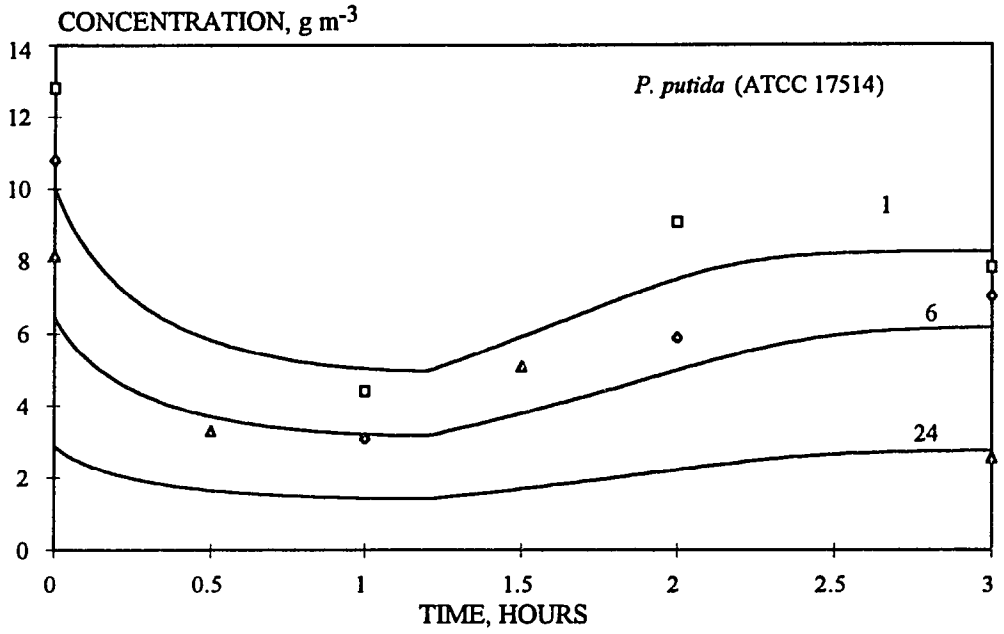

Figure C-7 *P. putida* concentration profiles for the 1st, 6th, and 24th cycle of SFBR-M1. Curves indicate model predictions. The data are correspondingly represented by □, ◇, and △.

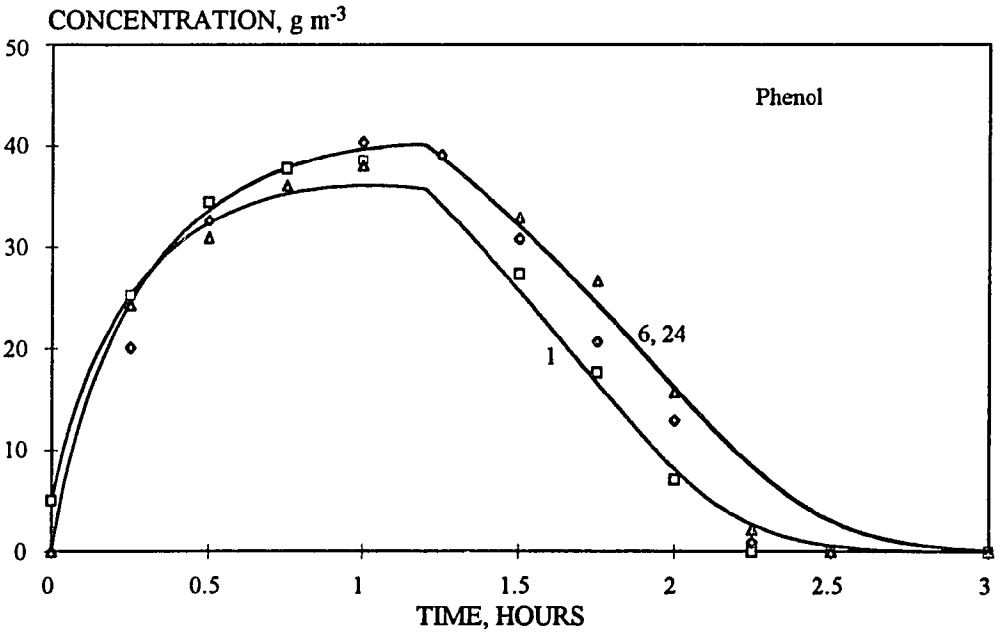

Figure C-8 Phenol concentration profiles for the 1st, 6th, and 24th cycle of run SFBR-M1. Curves represent model predictions. The data are correspondingly represented by □, ◇, and △.

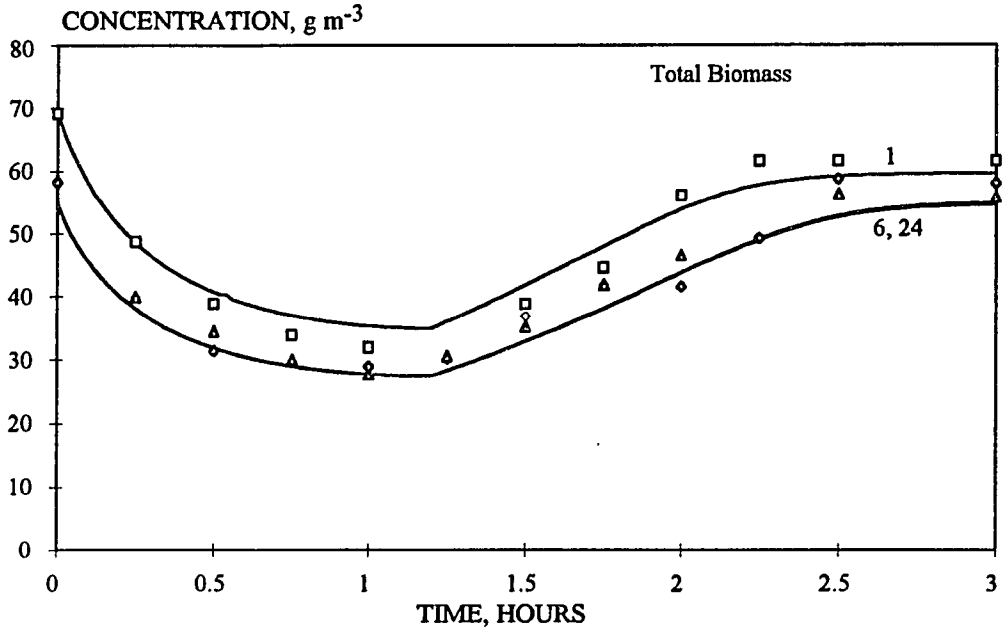

Figure C-9 Total Biomass concentration profiles for the 1st, 6th, and 24th cycle of SFBR-M1. Curves indicate model predictions. The data are correspondingly represented by □, ◇, and △.

Table C-4 Experimental data for SFBR run SFBR-M2

Cycle 1

Time h	Optical density	*P. putida* g m^{-3}	*P. resinovorans* g m^{-3}	Total Biomass g m^{-3}	Phenol g m^{-3}
0	0.279	22.48	53.79	76.724	0
0.25	0.194			53.036	63.65
0.5	0.155			42.374	95.19
0.75	0.132			36.087	112.26
1	0.126	8.426	26.02	34.446	124.39
1.25	0.131			35.813	127.34
1.5	0.144			39.367	122.37
2	0.185	12.796	37.78	50.576	107.72
2.25	0.210			57.41	97.38
2.5	0.262	19.45	52.176	71.626	81.77
2.75	0.281			76.821	67.14
3	0.337	23.775	68.355	92.13	49.02

Table C-4 (contd)

Cycle 16

Time h	Optical density	*P. putida* g m^{-3}	*P. resinovorans* g m^{-3}	Total Biomass g m^{-3}	Phenol g m^{-3}
0	0.532	69.935	75.305	145.44	0
0.25	0.386			105.79	61.23
0.5	0.323			88.303	82.92
0.75	0.285			77.914	92.11
1	0.270	39.7692	34.044	73.813	101.22
1.5	0.314			85.842	86.92
1.75	0.355			97.051	65.2
2	0.414	52.856	60.324	113.18	45.49
2.25	0.471			128.76	25.46
2.75	0.529			144.76	0
3	0.532	69.141	76.296	145.4	0

Table C-4 (contd)

Cycle 40

Time h	Optical density	*P. putida* g m^{-3}	*P. resinovorans* g m^{-3}	Total Biomass g m^{-3}	Phenol g m^{-3}
0	0.558	113.384	38.724	152.48	0
0.25	0.384			104.979	56.2
0.5	0.328			89.67	84.07
0.75	0.285			77.914	96.43
1	0.269	61.602	15.765	73.54	101.98
1.25	0.283			77.367	100.12
1.5	0.321			87.756	86.78
2	0.437			119.468	42.81
2.25	0.532	115.09	30.381	145.44	17.92
2.75	0.557			152.27	0
3	0.558	117.512	35.028	152.54	0

Table C-4 (contd)

Cycle 58

Time h	Optical density	*P. putida* g m^{-3}	*P. resinovorans* g m^{-3}	Total Biomass g m^{-3}	Phenol g m^{-3}
0	0.564	140.003	14.185	154.188	0
0.25	0.391			106.893	61.27
0.5	0.327			89.396	83.44
1	0.293	74.969	5.132	80.101	98.96
1.25	0.289			79.088	98.33
1.5	0.322			88.029	80.03
1.75	0.371			101.425	64.27
2		123.418	17.374		
2.25	0.515			140.792	21.32
2.5	0.549			150.087	0
2.75	0.567			155.008	0
3	0.567	142.737	12.271	155.008	0

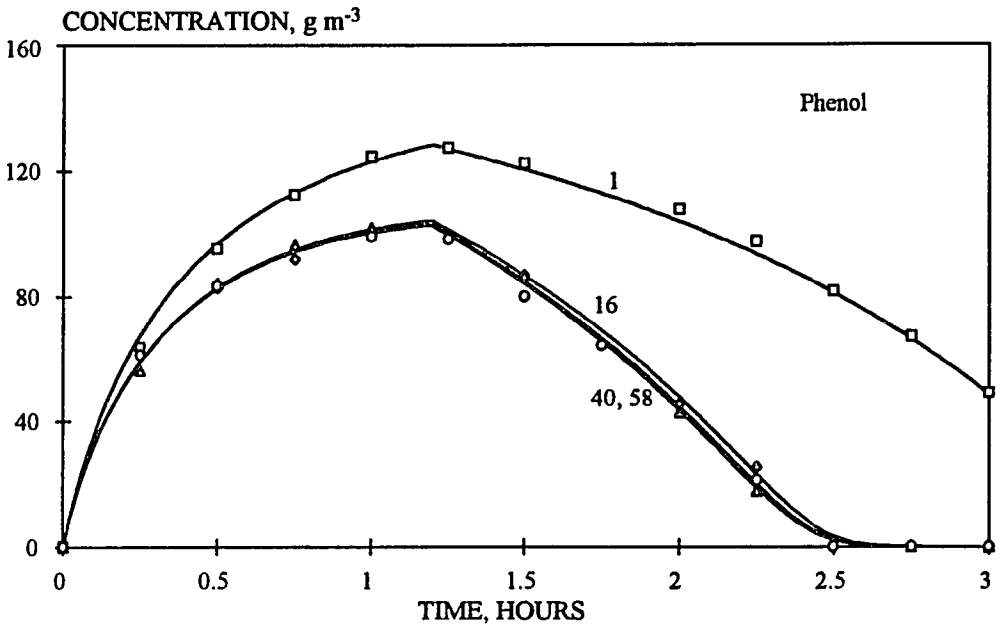

Figure C-10 Phenol concentration profiles for the 1st, 16th, 40th, and 58th cycle of SFBR-M2. Curves represent model predictions. The data are correspondingly represented by □, ◇, △, and ○.

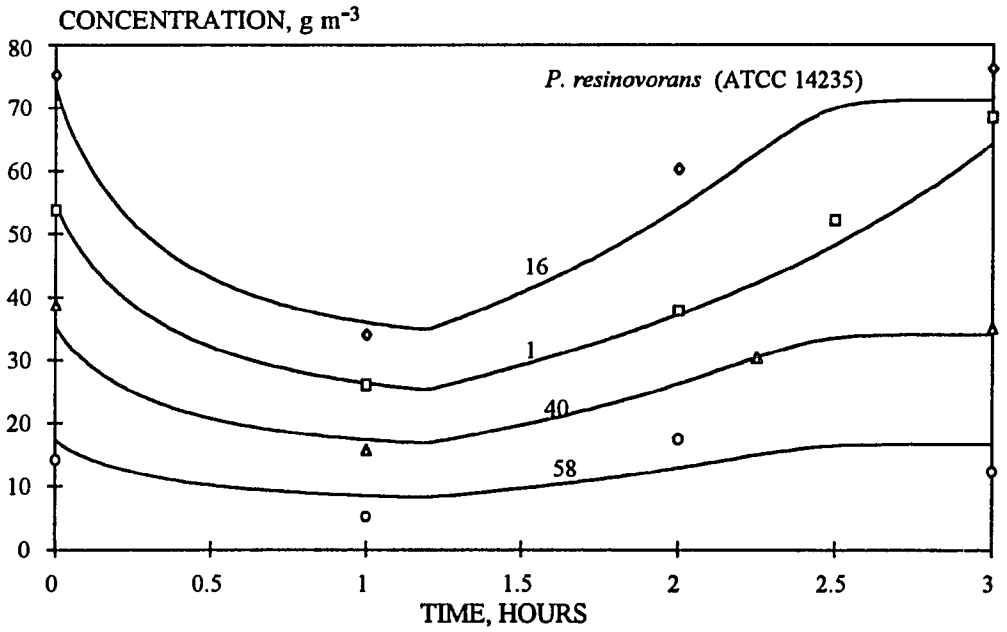

Figure C-11 *P. resinovorans* concentration profiles for the 1st, 16th, 40th, and 58th cycle of SFBR-M2. Curves represent model predictions. The data are correspondingly represented by □, ◇, △, and ○.

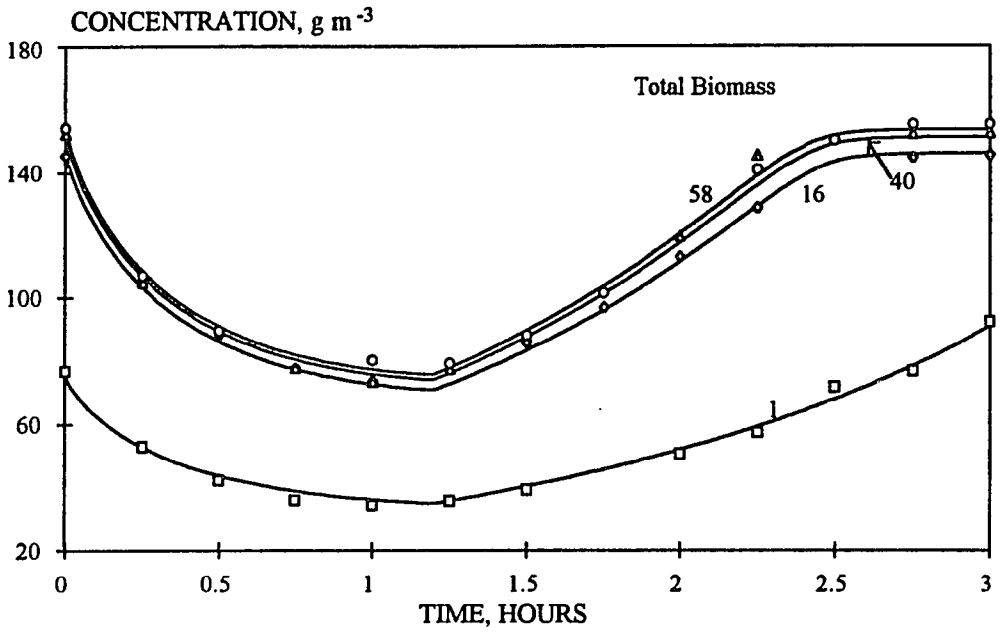

Figure C-12 Total biomass concentration profile for the 1st, 16th, 40th, and 58th cycle of SFBR-M2. Curves represent model predictions. The data are correspondingly represented by □, ◇, △, and ○.

Table C-5 Experimental data for SFBR run SFBR-M3

	Cycle 1			Cycle 24		
Time h	Optical density	Total Biomass g m^{-3}	Phenol g m^{-3}	Optical density	Total Biomass g m^{-3}	Phenol g m^{-3}
0	0.079	21.597	0	0.023	6.288	189.05
0.25				0.018	4.921	191.84
0.5	0.052	11.755	106.19	0.015	4.101	193.13
0.75	0.044	10.398	126.75			
1	0.042	9.568	137.92	0.011	3.007	197.21
1.25	0.041	9.842	142.72	0.013	3.554	194.96
1.5	0.052	11.482	140.58	0.015	4.101	193.92
2	0.055	15.036	139.63	0.016	4.374	192.7
2.25	0.062	16.95	136.89			
2.5	0.070	19.137	133.2	0.018	4.921	204.67
2.75	0.074	20.23	129.96			
3	0.084	22.964	126.85	0.020	5.468	187.5

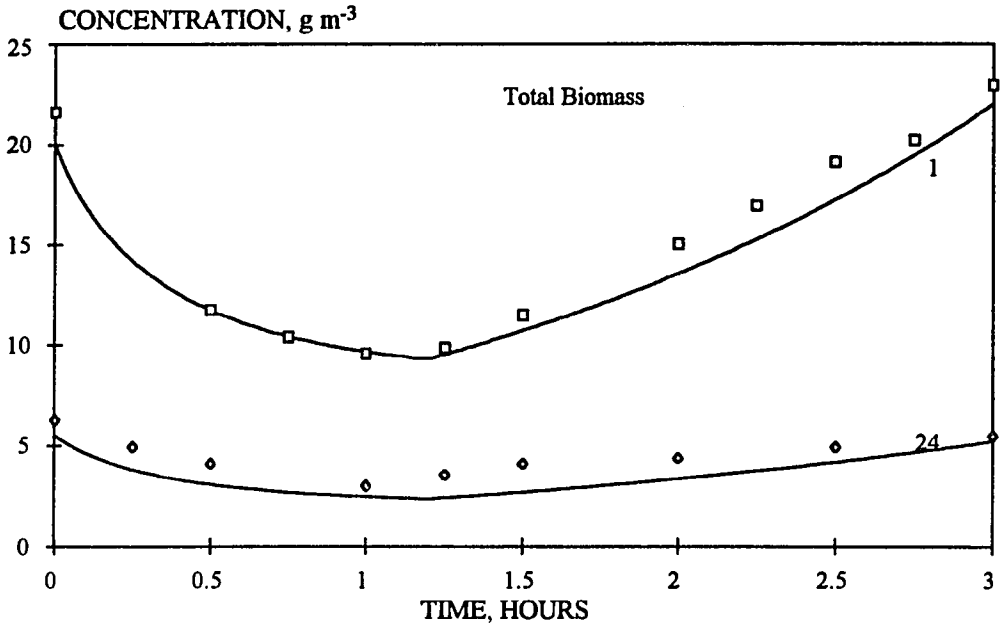

Figure C-13 Total biomass concentration profiles for the 1st, and 24th cycle of SFBR-M3. Curves represent model predictions.

Table C-6 Experimental data for SFBR run SFBR-M4

Cycle 1

Time h	Optical density	*P. putida* g m^{-3}	*P. resinovorans* g m^{-3}	Total Biomass g m^{-3}	Phenol g m^{-3}
0	0.157	23.05	19.86	42.92	0
0.5	0.126			34.45	163.84
1	0.097	17.89	11.35	29.25	235
1.5	0.097			26.52	279
2	0.092	13.83	11.31	25.15	301.6
2.5	0.091			24.87	336.26
3.66	0.121	21.29	11.78	33.08	335.88
4	0.152			41.56	330.06
4.5	0.174			47.56	317.18
5	0.218			59.59	292
5.5	0.278	39.54	20.043	76	297.24
6	0.307			83.92	265.46
6.5	0.349	58.83	25.08	95.41	244.06
6.875	0.409	76.65	35.34	111.81	233.12

Table C-6 (contd)

Cycle 21

Time h	Optical density	*P. putida* g m^{-3}	*P. resinovorans* g m^{-3}	Total Biomass g m^{-3}	Phenol g m^{-3}
0	0.325	238.75	116.64	355.39	0
0.5	0.279			305.09	74.26
1.0	0.272	207.69	89.74	297.44	78.32
1.5	0.296			323.68	45.32
2.0	0.337			368.52	0
2.5	0.340	262.44	121.37	371.8	0
3.0	0.351			383.82	0
3.5	0.357			390.39	0
4	0.357	254.74	123.36	387.11	0

Cycle 28

Time h	Optical density	*P. putida* g m^{-3}	*P. resinovorans* g m^{-3}	Total Biomass g m^{-3}	Phenol g m^{-3}
0.0	0.328	277.12	82.58	359.71	0
0.5	0.286			313.08	73.83
1.0	0.276	235.68	66.74	302.43	76.6
1.5	0.304			332	38.8
2.0	0.352	303.15	80.84	384	9.57
2.5	0.347			379	0
3.0	0.379				0
4.0	0.379				0

Table C-6 (contd)

Cycle 32 (Cycle 4 after perturbation as explained on p.54)

Time h	Optical density	*P. putida* g m^{-3}	*P. resinovorans* g m^{-3}	Total Biomass g m^{-3}	Phenol g m^{-3}
0.0	0.320	160.22	189.6	349.9	0
0.5	0.275			300.72	71.64
1.16	0.255	132.33	146.5	278.85	70.48
1.5	0.279			305.095	58.2
2.0	0.315	163.9	180.09	344.46	9.98
2.5	0.323			353.21	0
4.0	0.323			353.21	0

Cycle 39 (Cycle 11 after perturbation)

Time h	Optical density	*P. putida* g m^{-3}	*P. resinovorans* g m^{-3}	Total Biomass g m^{-3}	Phenol g m^{-3}
0.0	0.329	182.24	177.51	359.76	0
0.25	0.301			329.12	38.84
0.50	0.276	150.9	150.9	301.8	68.15
0.75	0.248			272.89	78.4
1.00	0.282	149.31	159.05	308.36	82.44
1.25	0.284			310.36	67.29
1.5	0.286	153.71	158.96	312.68	39.86
1.75	0.325			355.4	19.68
2.0	0.318	187.09	160.67	347.76	0
2.25	0.320			349.92	0
2.5	0.323			353.2	0
3.0	0.333			364.12	0
3.5	0.343			375.08	0
4.0	0.339	188.72	181.95	370.68	0

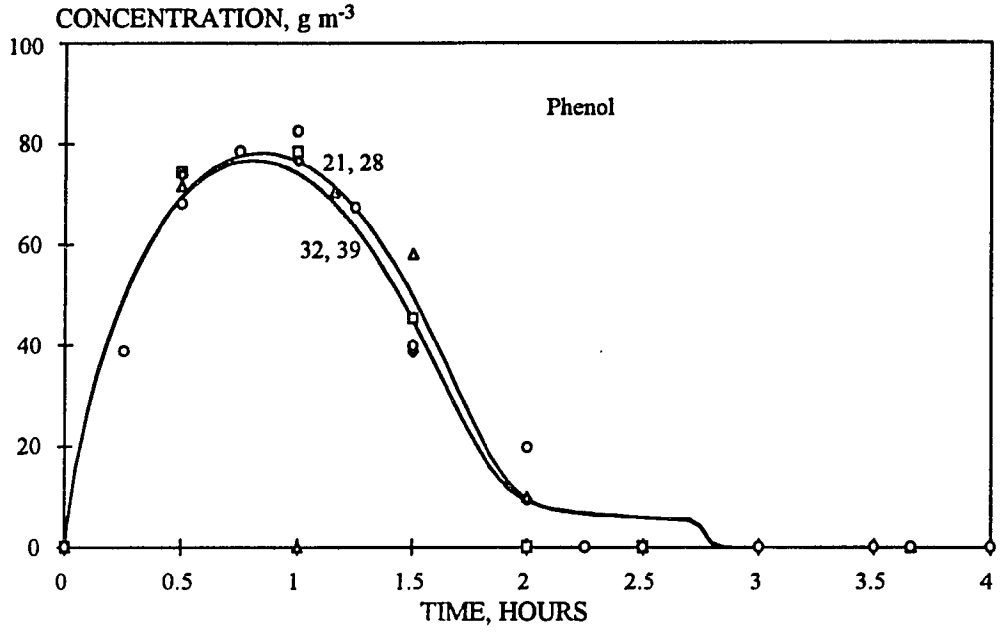

Figure C-14 Phenol concentration profiles for the 21st, 28th, 32nd, and 39th cycle of SFBR-M2. Curves represent model predictions. The data are correspondingly represented by □, ◇, △, and ○.

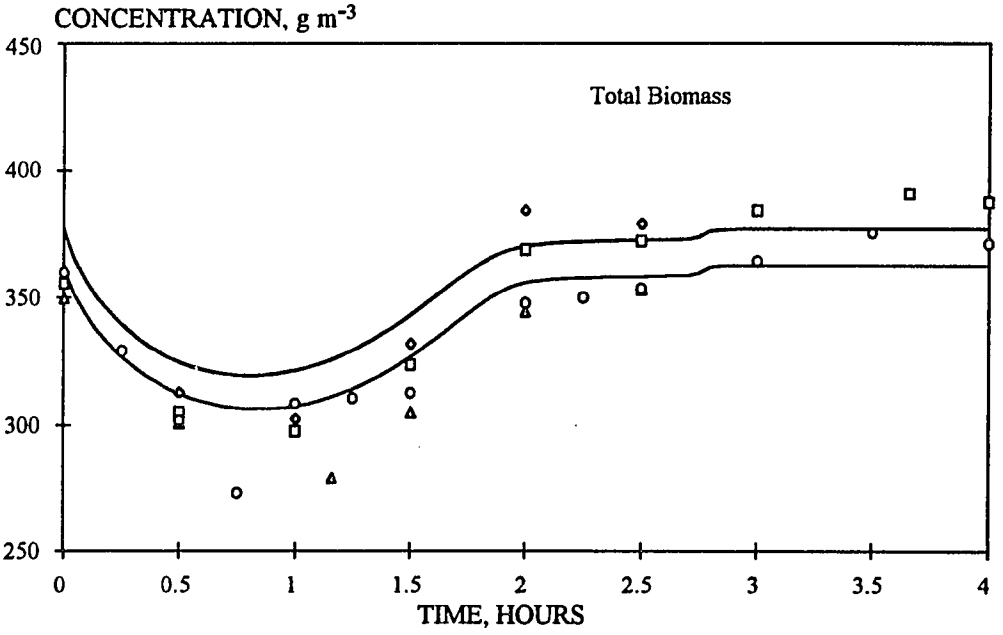

Figure C-15 Total Biomass concentration profile for the 21st, 28th, 32nd, and 39th cycle of SFBR-M2. Curves represent model predictions. The data are correspondingly represented by □, ◇, △, and ○.

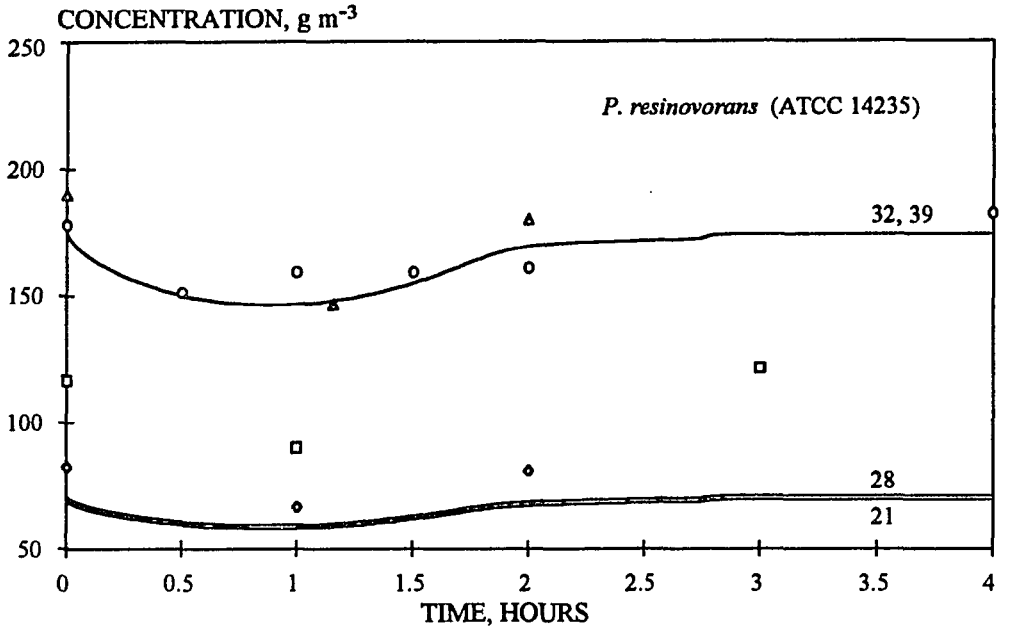

Figure C-16 *P. resinovorans* concentration profiles for the 21st, 28th, 32nd, and 39th cycle of SFBR-M4. Curves represent model predictions. The data are correspondingly represented by □, ◇, △, and ○.

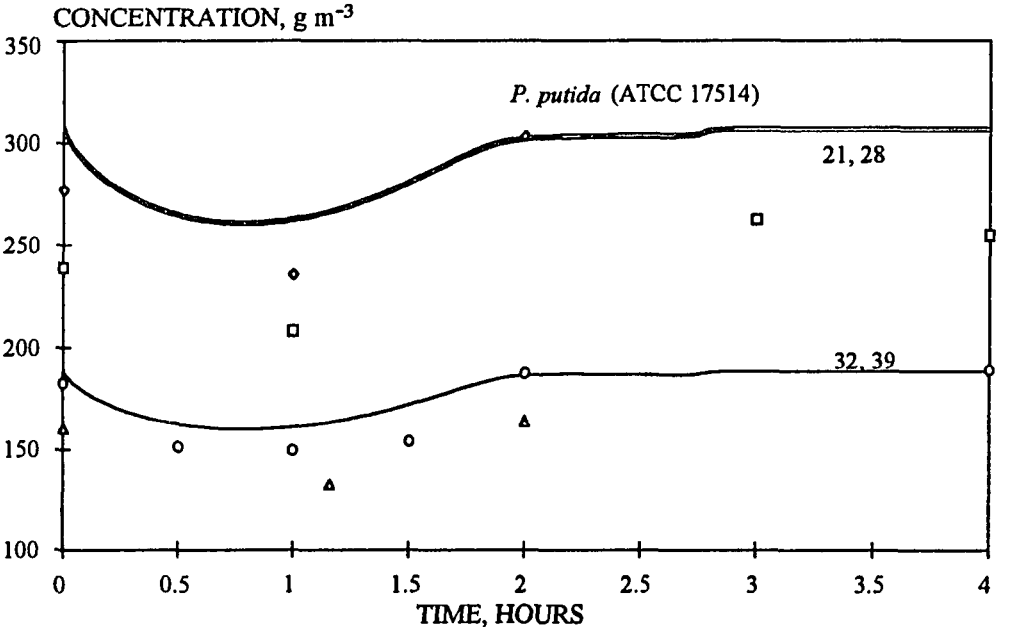

Figure C-17 *P. putida* concentration profiles for the 21st, 28th, 32nd, and 39th cycle of SFBR-M4. Curves represent model predictions. The data are correspondingly represented by □, ◇, △, and ○.

```
C       ********************************************************
C       PROGRAM FOR SOLVING MODEL EQUATIONS FOR A
C       SEQUENCING FED-BATCH REACTOR.
C       CASE CONSIDERED: TWO SPECIES FOLLOWING ANDREWS KINETICS
C       ********************************************************
        IMPLICIT DOUBLE PRECISION (A-H,O-Z)
        CHARACTER*10 FNAME
        WRITE(*,691)
691     FORMAT('$ enter the output file name CYCLE 1:')
        READ (*,695)fname
695     FORMAT(A10)
        OPEN (1,FILE=FNAME,STATUS='UNKNOWN')
        WRITE (*,692)
692     FORMAT('$ ENTER OUTPUT FILE NAME ALL CYCLES:')
        READ(*,695)FNAME
        OPEN (6,FILE=FNAME,STATUS='UNKNOWN')
        WRITE (*,693)
693     FORMAT('$ ENTER OUTPUT FILE NAME CYCLE 21 :')
        READ(*,695)FNAME
        OPEN (4,FILE=FNAME,STATUS='UNKNOWN')
        WRITE (*,694)
694     FORMAT('$ ENTER OUTPUT FILE NAME CYCLE 28:')
        READ (*,695)FNAME
        OPEN (10,FILE=FNAME,STATUS='UNKNOWN')
        WRITE (*,696)
696     FORMAT('$ ENTER DATA FILE NAME:')
        READ(*,695)FNAME
        OPEN (11,FILE=FNAME,STATUS='UNKNOWN')
C       ********************************************************
     .  READ (11,*)AMUA,AKSA,AKIA,YA,V0,VMAX,T1,T2,T3,S0,SF
     &  ,BA0,BB0,AMUB,AKSB,AKIB,YB
333     FORMAT(2X,'UA=',F10.5,2x,'KsA=',2x,f10.5,2X,'KiA=',2x,f10.5,2x,
     &  'YA=',f10.5)
        WRITE(6,433) AMUB,AKSB,AKIB,YB
433     FORMAT(2X,'UB=',F10.5,2x,'KsB=',2x,f10.5,2X,'KiB=',2x,f10.5,2x,
     &  'YB=',f10.5)
        WRITE(6,334)V0,VMAX
334     FORMAT(2X,'INITIAL VOL=',F5.2,2X,'Final Vol=',F5.2)
        WRITE (6,434)T1,T2,T3
434     FORMAT(2X,'T1=',F5.2,2X,'T2='F5.2,2X,'T3=',F5.2)
        WRITE (6,335)S0,SF
335     FORMAT(2X,'INITIAL SUBS.=',F8.4,2X,'SUBS. IN FEED=',F8.4)
        WRITE(6,435)BA0,BB0
435     FORMAT(2X,'INITIAL BIOMASS A =',F8.4,2X,'INITIAL BIOMASS B ='F8.4)
        DEL=V0/VMAX
        S1=T1/T3
        S3=(T3-T2)*(1/T3)
        GA=AKSA/AKIA
        GB=AKSA/AKIB
        W=AKSB/AKSA
        PHI=AMUB/AMUA
        ETA=YA/YB
        QR=((VMAX-V0)/T1)*S1
        U0=S0/AKSA
        XA0=BA0/(AKSA*YA)
        XB0=BB0/(AKSA*YA)
        UF=SF/AKSA
        BETA=AMUA*VMAX/QR
        WRITE(*,*)UF,BETA,QR,S1,DEL
c       ********************************************************
        DATA H,N/0.001,100/
c       ********************************************************
        U=U0
        XA=XA0
        XB=XB0
        WRITE(6,185)
```

```
185     FORMAT(7X,'TIME',8X,'BIO. CONC. A',2X,'BIO.CONC. B',3X,
     &  'PHENOL CONC.')
        ICOUNT=1
        BA=AKSA*YA*XA
        BB=AKSA*YA*XB
        SPH=AKSA*U
        TIME=0.0
        INDEX=(ICOUNT/5)*5-icount
        IF(INDEX.EQ.0) then
        WRITE(6,183)time,BA,BB,SPH
        WRITE(1,181)time,BA,BB,(BA+BB),SPH
        ENDIF
        DO 130 I=1,60
        AL=1.0
        T=0.001
        TIME=0.0
C
C       FILL PHASE
c
        ICOUNT=0
        WRITE(6,184)I
184     FORMAT(5X,'FILL PHASE',2X,'CYCLE No.=',I2)
        IF((I.EQ.1))then
        WRITE(1,181)TIME,BA,BB,(BA+BB),SPH
        ENDIF
        IF(I.eq.28)THEN
        WRITE(10,181)TIME,BA,BB,(BA+BB),SPH
        ENDIF
        IF(I.eq.21)THEN
        WRITE(4,181)TIME,bA,BB,(BA+BB),SPH
        ENDIF
50      ICOUNT=ICOUNT+1
        CALL RUNGE (H,T,U,XA,XB,S1,DEL,BETA,UF,AL,GA,GB,W,PHI,ETA)
        BA=aksA*YA*XA
        BB=AKSA*YA*XB
        SPH=aksA*U
        T1=T-0.001
        T2=T1*VMAX/QR
        INDEX=(ICOUNT/5)*5-icount
        IF ((I.EQ.21).and.((ICOUNT.EQ.1).or.(INDEX.EQ.0))) then
        WRITE(4,181)T2,bA,BB,(BA+BB),SPH
        endif
        IF ((I.EQ.1).and.((ICOUNT.EQ.1).or.(INDEX.EQ.0))) then
        WRITE(1,181)T2,bA,BB,(BA+BB),SPH
        ENDIF
        IF ((I.EQ.28).and.((ICOUNT.EQ.1).or.(INDEX.EQ.0))) then
        WRITE(10,181)T2,bA,BB,(BA+BB),SPH
        ENDIF
181     FORMAT(5(5X,F9.5))
        IF(T.LE.(1.0-DEL)*S1)THEN
        GO TO 50
        ENDIF
        WRITE(6,183)T2,BA,BB,SPH
C
C       REACT PHASE
C
        WRITE(6,186)I
186     FORMAT(5X,'REACT PHASE',2X,'CYCLE No.=',I2)
        AL=0
70      ICOUNT=ICOUNT+1
        CALL RUNGE (H,T,U,XA,XB,S1,DEL,BETA,UF,AL,GA,GB,W,PHI,ETA)
        BA=AKSA*YA*XA
        BB=AKSA*YA*XB
        SPH=aksA*U
        T1=T-0.001
        T2=T1*VMAX/QR
```

```
      BA=aksA*YA*XA
      BB=AKSA*YA*XB
      SPH=aksA*U
      T1=T-0.001
      T2=T1*VMAX/QR
      index=(ICOUNT/5)*5-icount
      if ((i.eq.21).and.(index.eq.0)) then
      WRITE(4,181)T2,bA,BB,(BA+BB),SPH
      endif
      if ((i.eq.1).and.((icount.eq.1).or.(index.eq.0))) then
      WRITE(1,181)T2,bA,BB,(BA+BB),SPH
      endif
      if ((i.eq.28).and.((icount.eq.1).or.(index.eq.0))) then
      WRITE(10,181)T2,bA,BB,(BA+BB),SPH
      endif
182   FORMAT(4(5X,F9.5))
      IF(T.LE.(1.0-DEL)*(1.0-S3))THEN
      GO TO 70
      ENDIF
      write(6,183)t2,bA,BB,SPH
C
C     DRAW PHASE
C
      WRITE(6,187)I
187   FORMAT(5X,'DRAW PHASE',2X,'CYCLE No.=',I2)
80    ICOUNT=ICOUNT+1
      CALL RUNGE (H,T,U,XA,XB,S1,DEL,BETA,UF,AL,GA,GB,W,PHI,ETA)
      BA=aksA*YA*XA
      BB=AKSA*YA*XB
      SPH=aksA*U
      T1=T-0.001
      T2=T1*VMAX/QR
      index=(ICOUNT/5)*5-icount
      if ((i.eq.21).and.(index.eq.0)) then
      WRITE(4,181)T2,bA,BB,(BA+BB),SPH
      endif
      if ((i.eq.1).and.((icount.eq.1).or.(index.eq.0))) then
      WRITE(1,181)T2,bA,BB,(BA+BB),SPH
      endif
      if ((i.eq.28).and.((icount.eq.1).or.(index.eq.0))) then
      WRITE(10,181)T2,bA,BB,(BA+BB),SPH
      endif
183   FORMAT(4(6X,F8.4))
      IF(T.LE.(1.00001-DEL)) THEN
      GO TO 80
      ENDIF
      write (6,183)t2,bA,BB,SPH
      write (6,105)I
105   format(2x,'*****************end of cycle*******',i2)
130   CONTINUE
C111   continue
      STOP
      END
C
C     INTEGRATION TO SOLVE THE MASS BALANCE ON SUBSTRATE &
C     BIOMASS OF TWO SPECIES
C     FOURTH ORDER RUNGE KUTTA METHOD
C
      SUBROUTINE RUNGE  (H,T,U,XA,XB,S1,DEL,BETA,UF,AL,GA,GB,W,PHI,ETA)
      IMPLICIT REAL*8 (A-H,O-Z)
      F1(T,U,XA,XB)=AL*(UF-U)/(S1*DEL+T)-
     &  (XA*U*BETA)/(1.0+U+(GA*U**2))-
     &  (XB*U*BETA*PHI*ETA)/(W+U+(GB*U**2))
      F2(T,U,XA,XB)=-(AL*XA)/(S1*DEL+T)+
     &  (XA*U*BETA)/(1.0+U+(GA*U**2))
      F3(T,U,XA,XB)=-(AL*XB)/(S1*DEL+T)+
```

```
&   (XB*U*BETA*PHI)/(W+U+(GB*U**2))
    AK1=H*F1(T,U,XA,XB)
    BK1=H*F2(T,U,XA,XB)
    CK1=H*F3(T,U,XA,XB)
    AK2=H*F1(T+H/2,U+AK1/2,XA+BK1/2,XB+CK1/2)
    BK2=H*F2(T+H/2,U+AK1/2,XA+BK1/2,XB+CK1/2)
    CK2=H*F3(T+H/2,U+AK1/2,XA+BK1/2,XB+CK1/2)
    AK3=H*F1(T+H/2,U+AK2/2,XA+BK2/2,XB+CK2/2)
    BK3=H*F2(T+H/2,U+AK2/2,XA+BK2/2,XB+CK2/2)
    CK3=H*F3(T+H/2,U+AK2/2,XA+BK2/2,XB+CK2/2)
    AK4=H*F1(T+H,U+AK3,XA+BK3,XB+CK3)
    BK4=H*F2(T+H,U+AK3,XA+BK3,XB+CK3)
    CK4=H*F3(T+H,U+AK3,XA+BK3,XB+CK3)
    U=U+(AK1+2*AK2+2*AK3+AK4)/6
    XA=XA+(BK1+2*BK2+2*BK3+BK4)/6
    XB=XB+(CK1+2*CK2+2*CK3+CK4)/6
    T=T+H
    RETURN
    END
```

APPENDIX D

Methodology for batch biodegradation kinetics and sensitivity analysis

Determination of Specific Growth Rates

In order to develop a method for measurement of specific growth rate for a species exhibiting inhibitory kinetics, the kinetic parameters were chosen as

$\mu^* = 0.9259\ h^{-1}$

$K_S = 11.248\ g\ m^{-3}$

$K_I = 141.142\ g\ m^{-3}$

$Y = 0.6045\ g\ g^{-1}$

The mass balance equations on the substrate and biomass (equation 3 and 5 of chapter 4 with $b_2 = Q_f = 0$) were numerically integrated. Eleven substrate concentrations were studied in the range of 20 - 200 g m^{-3} (Table 6.1). The initial biomass concentration in all cases was 5 g m^{-3}. The integrations were carried till the substrate concentration became zero. The biomass and substrate concentrations were recorded at 0.1 h intervals. These data were considered as equivalent to "perfect" experimental data. A plot of logarithm of biomass concentration versus time revealed that there was a linear regime, followed by a positive deviation from linearity. The data falling in the linear regime, as well as all growth data were regressed to a linear expression. Obviously, the correlation was better for the data falling in the linear regime. The slope which would be equal to the specific growth rate could be attributed to either the initial phenol concentration or the average substrate concentration. A non linear regression routine based on the Gauss-Marquardt method was used to regress the specific growth rate versus substrate data. The program listing is given at the end of this appendix. Comparison of the parameters obtained for each of the four cases showed that the best results were obtained when the slope of the linear regime was considered and attributed to the average phenol concentration in that regime. These slopes (specific growth rates) were then considered for sensitivity analysis by introducing an error (about 5%) in the data and/or by having fewer experimental points before or after the maximum. The values are given in Table D-1.

Table D-1 Specific growth rates for sensitivity analysis
The maximum occurs at $S^* = (K_s K_i)^{0.5} = 39.84$

Substrate concentration g m^{-3}	Linear regime h	Specific growth rate-actual h^{-1}	Specific growth rate Case Ia h^{-1}	Specific growth rate Case IIa h^{-1}	Specific growth rate Case IIIa h^{-1}	Specific growth rate Case IVa h^{-1}
20		0.5222	0.5483	0.5222	0.5483	0.5222
25	0-1	0.5558	0.5280	0.5558	0.5975	0.5558
30	0-1	0.5757	0.5469	0.5757	-	0.5757
35	0-1.4	0.5834	0.6125	0.5834	-	0.5834
40	0-1.4	0.5897	0.5897	0.5897	0.5897	0.5897
50	0-2	0.5827	0.5827	0.5535	0.5827	-
60	0-2	0.5531	0.5531	0.5807	0.5531	0.5531
80	0-2	0.5184	0.5184	0.5443	0.5184	-
100	0-2.5	0.4799	0.4799	0.5339	0.4799	-
150	0-2.5	0.4419	0.4419	0.4639	0.4419	0.4419
200	0-3.5	0.3834	0.3834	0.3642	0.3834	-

```
C       PROGRAM FOR SIMULATION OF LN B VS TIME
C       FOR ANDREWS MODEL
C       ****************************************
        DOUBLE PRECISION U,AKS,AKI,Y,S0,S,B0,B,H,T
        CHARACTER*10,FNAME
        WRITE(*,691)
691     FORMAT('$ ENTER OUTPUT FILENAME:')
        READ(*,695)FNAME
695     FORMAT(A10)
        OPEN(6,FILE=FNAME,STATUS='UNKNOWN')
        OPEN(4,FILE='SIMUL1.DAT',STATUS='OLD')
        READ(4,*)U,AKS,AKI,Y,S0,B0
        H=0.001
        WRITE(*,*)U,AKS,AKI,Y,S0,B0
        S=S0
        B=B0
        T=0.000
        ssum=s
        WRITE(6,182)T,S,B,DLOG(B),ssum
        T=0.001
        INDEX=1
        ind=1
10      CALL RUNGE(H,T,S,B,U,AKS,AKI,Y)
        ICOUNT=(INDEX/100)*100-INDEX
        IF(ICOUNT.EQ.0)THEN
        ind=ind+1
        SSum=SSum+s
        Savg=SSum/ind
        T1=T-H
        WRITE(6,182)T1,S,B,DLOG(B),Savg
182     FORMAT(5(3x,F10.6))
181     FORMAT(4(5X,F10.6))
        ENDIF
        IF(T.LE.10)THEN
        INDEX=INDEX+1
        GO TO 10
        ENDIF
        STOP
        END
C
C       SUBROUTINE FOR INTEGRATION OF THE MASS BALANCE
C       EQUATIONS USING FOURTH ORDER RUNGE-KUTTA
C       FOR MONOD MODEL
C
C
        SUBROUTINE RUNGE(H,T,S,B,U,AKS,AKI,Y)
        DOUBLE PRECISION U,AKS,AKI,Y,S0,S,B0,B,H,T
        F1(S,B)=-((U*S)/(AKS+S+((S**2)/AKI)))*(B/Y)
        F2(S,B)=((U*S)/(AKS+S+((S**2)/AKI)))*B
        AK1=H*F1(S,B)
        BK1=H*F2(S,B)
        AK2=H*F1(S+AK1/2,B+BK1/2)
        BK2=H*F2(S+AK1/2,B+BK1/2)
        AK3=H*F1(S+AK2/2,B+BK2/2)
        BK3=H*F2(S+AK2/2,B+BK2/2)
        AK4=H*F1(S+AK3,B+BK3)
        BK4=H*F2(S+AK3,B+BK3)
        S=S+(AK1+2*AK2+2*AK3+AK4)/6
        B=B+(BK1+2*BK2+2*BK3+BK4)/6
        T=T+H
        RETURN
        END
```

REFERENCES

1. Allsop, P. J., Y. Chisti, M. Moo-Young, and G. R. Sullivan. "Dynamics of Phenol Degradation by *Pseudomonas putida*. " *Biotechnol. Bioeng.* 41 (1993): 572-580.

2. Amundson, N. R. *Mathematical Methods in Chemical Engineering: Matrices and their Applications*. Prentice Hall. New York. 1966

3. Andrews, J. F. "A Mathematical Model for the Continuous Culture of Microorganisms Utilizing Inhibitory Substrates." *Biotechnol. Bioeng.* 10 (1968): 707-723.

4. Aris, R., and A. E. Humphrey. "Dynamics of a Chemostat in which Two Organisms Compete for a Common Substrate." *Biotechnol. Bioeng.* 19 (1977): 1375-1386.

5. Arora, M. L., E. F. Barth, and M. B. Umphres. "Technology Evaluation of Sequencing Batch Reactors." *J. Water Pollut. Contr. Fed.* 57 (1985): 867-875.

6. Bailey, J. E. "Periodic Operation of Chemical Reactors: A Review." *Chem. Eng. Comm.* 1 (1973): 111-124.

7. Bailey, J. E. "Periodic Phenomena." In: *Chemical Reactor Theory: A Review.* L. Lapidus and N. R. Amundson (eds.). Prentice Hall, Englewood Cliffs, NJ. 1977.

8. Baltzis, B. C., and A. G. Fredrickson. "Competition of Two Microbial Populations for a Single Resource in a Chemostat when one of them Exhibits Wall Attachment." *Biotechnol. Bioeng.* 25 (1983): 2419-2439.

9. Baltzis, B. C., and A. G. Fredrickson. "Coexistence of Two Microbial Populations Competing for a Renewable Resource in a Non-Predator-Prey System." *Bull. Math. Biol.* 46 (1984): 155-174.

10. Baltzis, B. C., G. A. Lewandowski, S-H. Chang, and Y-F. Ko. "Fill-and-Draw Reactor Dynamics in Biological Treatment of Hazardous Wastes." pp. 111-128. In: *Biotechnology Applications in Hazardous Waste Treatment.* eds. G. A. Lewandowski, P. M. Armenante, B. C. Baltzis (eds.), Engineering Foundation, New York· 1989

11. Baltzis, B. C., G. A. Lewandowski, and S. Sanyal. "Sequencing Batch Reactor Design in a Denitrifying Application." pp. 282-300. In: *Emerging Technologies in Hazardous Waste Management II. ACS Symp. Ser.* 468. eds. D. W. Tedder, F. G. Pohland. Am. Chemical Society, Washington, D.C. 1991.

12. Butler, G. J., and G. S. K. Wolkowicz. "A Mathematical Model of the Chemostat with a General Class of Functions describing Nutrient Uptake." *SIAM J. Appl. Math.* 45 (1985): 138-151.

13. Chi, C. T., and J. A. Howell. "Transient Behaviour of a Continuous Stirred Tank Reactor utilizing Phenol as an Inhibitory Substrate." *Biotechnol. Bioeng.* 18 (1976): 63-80

14. Chiesa, S. C., and R. L. Irvine. "Growth and Control of Filamentous Microbes in Activated Sludge: An Integrated Hypothesis." *Water Research* 19 (1985): 471-479.

15. Colvin, R. J., and A. R. Rozich. "Phenol Growth Kinetics of Heterogenous Populations in a Two Stage Continuous Culture System." *J. Water Pollut. Contr. Fed.* 58 (1986): 326-332

16. D'Adamo, P. C., A. F. Rozich, and A. F. Gaudy Jr. "Analysis of Growth Data with Inhibitory Carbon Sources." *Biotechnol. Bioeng.* 26 (1984): 397-402.

17. Davison, B. H., G. Stephanopoulos. "Effect of pH Oscillations on a Competing Mixed Culture." *Biotechnol. Bioeng.* 28 (1986): 1127-1137.

18. Davison, B. H., and G. Stephanopoulos. "Coexistence of *S. cerevesiae* and *E. coli* in a Chemostat Under Substrate Competition and Product Inhibition." *Biotechnol. Bioeng.* 28 (1986): 1742-1752.

19. Dennis Jr., J. E., and R. B. Schnabel. *Numerical Methods for Unconstrained Optimization and Nonlinear Equations.* Prentice Hall, Englewood Cliffs, NJ. 1983

20. Dennis, R. W., and R. L. Irvine. "Effect of Fill : React Ratios on Sequencing Batch Reactors." *J. Water Pollut. Contr. Fed.* 51 (1979): 255-263.

21. Doedel, E. J. 1986. *AUTO: Software for Continuation and Bifurcation Problems in Ordinary Differential Equations.* CIT Press, Pasadena, CA. 1986

22. Douglas, J. M. "Periodic Reactor Operation." *Ind. and Engg. Chem. Proc. Des. and Dev.* 6 (1967): 43-48.

23. Edwards, V. H., C. R. Ko, and A. Balaugh. "Dynamics and Control of Continuous Microbial Propagators to Subject Substrate Inhibition." *Biotechnol. Bioeng.* 14 (1972): 939-974.

24. Finn, R. K. "Use of Specialized Microbial Strains in the Treatment of Industrial Waste and in Soil Decontamination." *Experientia* 39 (1983): 1231-1236

25. Fredrickson, A. G., and H. M. Tsuchiya. "Microbial Kinetics and Dynamics." In: *Chemical Reactor Theory: A Review* eds. L. Lapidus and N. R. Amundson. Prentice-Hall, NJ·1977

26. Fredrickson, A. G., and G. N. Stephanopoulos. "Microbial Competition." *Science* 207 (1981): 972-979.

27.Guptapal, S. "Kinetics of Phenol Biodegradation using *Pseudomonas resinovorans.*" *M. S. Thesis.* New Jersey Institute of Technology, Newark. 1992

28. Hale, J. K., and A. S. Somolinos. "Competition for Fluctuating Nutrient." *J. Math. Biol.* 18 (1983): 255-280.

29. Haldane, J. B. S. *Enzymes.* Longmans, London. 1960

30. Hansen, S. R., and S. P.Hubbell. "Single-Nutrient Microbial Competition: Qualitative Agreement Between Experimental and Theoretically Forecast Outcomes." *Science.* 207 (1980): 1491-1493.

31. Harder, W., and H. Veldkamp. "Competition of marine psychrophilic bacteria at low temperatures." *Antonie van Leeuwenhoek J. Microbiol. Serol.* 37 (1971): 51-63.

32. Hill, G. A., and C. W. Robinson. "Substrate Inhibition Kinetics: Phenol degradation by *Pseudomonas putida.*" *Biotechnol. Bioeng.* 17 (1975): 1599-1615.

33. Hoepker, E. C., and E. D. Schroeder. "The Effect of Loading Rate on Batch Activated Sludge Effluent Quality." *J. Water Pollut. Contr. Fed.* 51 (1979): 264-273.

34. Horn, F. J., and R. C. Lin. "Periodic Processes: A Variational Approach." *Ind. and Engg. Chem. Proc. Des. and Dev.* 6 (1967): 21-30.

35. Hsu, E. H. "Treatment of a Petrochemical Wastewater in Sequencing Batch Reactors." *Environ. Prog.* 5 (1986): 71-81.

36. Hsu, S. B. "Limiting Behavior for Competing Species." *SIAM J. Appl. Math.* 34 (1978): 760-763.

37. Hsu, S. B. "A Competition Model for a Seasonally Fluctuating Nutrient." *J. Math. Biol.* 9(1980): 115-132.

38. Hsu, S. B., S. P. Hubbell, and P. Waltman. "A Mathematical Theory for Single-Nutrient Competition in Continuous Cultures of Microorganisms." *SIAM J. Appl. Math.* 32 (1977): 366-383.

39. Hutchinson, D. H., and C. A. Robinson. "Kinetics of Simultaneous Batch Degradation of p-Cresol and Phenol By *Pseudomonas putida*." *Appl. Microbiol. Biotechnol.* 29 (1988): 599-604.

40. Hutchinson, G. E. "The Paradox of the Plankton." *Am. Natur.* 95(1961.): 137-144.

41. Irvine, R. L., and A. W. Busch. "Sequencing Batch Biological Reactors-An Overview." *J. Water Pollut. Contr. Fed.* 51 (1979): 235-243.

42. Irvine, R. L., and R. O. Richter. "Comparative Evaluation of Sequencing Batch Reactor." *J. Environ. Eng. Div., ASCE.* 104 (1978): 503-514.

43. Irvine, R.L., and L. H. Ketchum. "Sequential Batch Reactors for Biological Wastewater Treatment." *CRC Crit. Rev. Envr. Contr.* 18(1989): 255-294.

44. Irvine, R. L., L. H. Ketchum, R. E. Breyfogle, and E. F. Barth. "Municipal Application of Sequencing Batch Treatment at Culver, Indiana." *J. Water Pollut. Contr. Fed.* 55(1983): 484-488.

45. Janke, D., R. Pohl, and W. Fritsche. "Regulation of Phenol Degradation in *Pseudomonas putida*." *Z. Aug. Mikrobiol.* 21(1981): 295-303

46. Jannasch, H. W. "Enrichment of Aquatic Bacteria in Continuous Culture." *Arch. Mikrobiol.* 59 (1967): 165-173.

47. Jones, G. L, F. Jansen, and A. J. McKay. "Substrate Inhibition of the Growth of Bacterium NCIB 8250 by Phenol." *J. Gen. Microbiol.* 74 (1973): 139-148.

48. Keller, H. B. "Numerical Solution of Bifurcation and Non linear Eigenvalue Problems." In: *Applications of Bifurcation Theory.* ed. P. H. Rabinowitz. Academic Press. NewYork. 1977

49. Keverikides I. G., L. D. Schmidt and R. Aris. "Some Common Features of Periodically Forced Reacting Systems." *Chem. Eng. Sci.* 41 (1986): 1263-1276.

50. Kotturi, G., C. A. Robinson, and W. E. Inniss. "Phenol Degradation by a Psychrotrophic Strain of *Pseudomonas putida.*" *Appl. Microbiol. Biotechnol.* 34 (1991): 539-543.

51. Lee, J., H-C. Chang, S. J. Parulekar, and J. Hong. "An Alternate Method for Estimation of Cell Growth Kinetics from Batch Cultures."*Biotechnol. Bioeng.* 37 (1991): 26-34.

52. Lenas, P., and S. Pavlou. "Chaotic Response of a Periodically Forced System in Two Microbial Species." In: *Chaotic Dynamics: Theory and Practice.* ed. T. C. Bountis. Plenum, NY. 1992

53. Lester, J. N, Perry, R., and A. H. Dadd. "Cultivation of a Mixed Bacterial Population of Sewage Origin in the Chemostat." *Water Res.* 13 (1979): 545-551

54. Lewandowski, G. A., and B. C. Baltzis. "Analysis of Sequencing Batch Bioreactors in Large-Scale Denitrifying Applications." *Chem. Eng. Sci.* 47 (1992): 2389-2394.

55. Lewis, P. H. "A note on the Continuous Flow Culture of Mixed Populations of *lactobaccili* and *streptococci.*" *J. Appl. Bacteriol.* 30 (1967) 406-409

56. Livingston, A. G., and H. A. Chase. "Modeling Phenol Degradation in a Fluidized-Bed Bioreactor." *AIChE J.* 35 (1989): 1980-1992.

57. Matsubara, M., N. Watanabe, and S. Hasegawa. "Bifurcations in a Bang-Bang Controlled Mixed Culture System." *Chem. Eng. Sci.* 41 (1986): 523-531.

58. Meers, J. L. "Effect of Dilution Rate on the Outcome of Chemostat Mixed Culture Experiments." *J. Gen. Microbiol.* 67 (1971): 359-361.

59. Molin, G., and I. Nilsson. "Degradation of Phenol by *Pseudomonas putida* ATCC 11172 in Continuous Culture at Different Ratios of Biofilm Surface to Culture Volume." *Appl. and Environ. Microbiol.* 50 (1985): 946-950.

60. Pavlou, S., and I. G. Kevrekidis. "Microbial Predation in a Periodically Operated Chemostat: A Global Study on the Interaction between Natural and Externally Imposed Frequencies." *Math. Biosci.* 108 (1992): 1-55.

61. Pavlou, S., I. G. Kevrekidis, and G. Lyberatos. "On the Coexistence of Competing Microbial Species in a Chemostat under Cycling." *Biotechnol. Bioeng.* 35 (1990): 224-232.

62. Pawlowsky, U., and J. A. Howell. "Mixed Culture Biooxidation of Phenol. I. Determination of Kinetic Parameters." *Biotechnol. Bioeng.* 15 (1973):889-896.

63. Powell, E. O. "Criteria for Growth of Contaminants and Mutants in Continuous Culture." *J. Gen. Microbiol.* 18 (1958): 259-268.

64. Powell, G. E. "Structural Instability of the Theory of Simple Competition." *J. Theor. Biol.* 132 (1988): 421-435.

65. Silverstein, J. A., and E. D. Schroeder. "Performance of SBR Activated Sludge Processes with Nitrification/Denitrification." *J. Water Pollut. Contr. Fed.* 55 (1983): 377-384.

66. Slater, J. H. *Mixed Culture Fermentation.* Academic. New York. 1981.

67. Smith, H. L. "Competitive Coexistence in an Oscillating Chemostat." *SIAM. J. Appl. Math.* 40 (1981): 498-522.

68. Sokol, W. "Oxidation of an Inhibitory Substrate by Washed Cells." *Biotechnol and Bioeng.* 30 (1987): 921-927.

69. Sokol, W. "Dynamics of a Continuous Stirred Tank Biochemical Reactor Utilizing Inhibitory Substrate." *Biotechnol Bioeng.* 30 (1987): 921-927.

70. Sokol, W., and J. A. Howell. "Kinetics of Phenol Oxidation by Washed Cells." *Biotechnol. Bioeng.* 23 (1981): 2039-2949.

71. Stephanopoulos, G., A. G. Fredrickson, and R. Aris. "The Growth of Competing Microbial Populations in a CSTR with Periodically Varying Inputs." *AIChE J.* 25 (1979): 863-872.

72. Stephanopoulos, G., R. Aris, and A. G Fredrickson. "A Stochastic Analysis of the Growth of Competing Microbial Populations in a Continuous Biochemical Reactor." *Math. Biosci.* 45 (1979): 99-135.

73. Stewart, F. M., and B. R. Levin. "Partitioning of Resources and the Outcome of Interspecific Competition: A model and Some General Considerations." *Am. Natur.* 107 (1973): 171-198.

74. Summary Report-Sequencing Batch Reactors United States Environmental Protection Agency--EPA/625/8-86/011. 1986

75. Szetela, R. W., and T. Z. Winnicki. "A Novel Method for Determining the Parameters of Microbial Kinetics." *Biotechnol. Bioeng.* 23 (1981): 1485-1490.

76. Tang, W. T., and L. S. Fan. "Steady State Phenol Degradation in a Draft-Tube, Gas-Liquid-Solid Fluidized Bed Reactor." *AIChE J.* 33 (1987):239-249.

77. Wang, K-W. "Biodegradation of Phenol and 4-Chlorophenol Using a Single Species in a Sequencing Batch Reactor." *M. S. Thesis.* New Jersey Institute of Technology, Newark, NJ. 1991

78. Wedding, R.T., C. Hansch, and T. R. Fukuto. "Inhibition of Maleate Dehydrogenase by Phenols and the Influence of Ring Substituents on their Inhibitory Effectiveness." *Arch. Biochem. Biophys.* 121 (1967): 9-21.

79. Yang, R. D., and A. E. Humphrey. "Dynamic and Steady State Studies of Phenol Biodegradation in Pure and Mixed Cultures." *Biotechnol. Bioeng.* 17 (1975): 1211-1235.

80. Ying, W-C., R. R. Bonk, V. H. Lloyd, and S. A. Sojka. "Biological Treatment of a Landfill Leachate in Sequencing Batch Reactors." *Environ. Prog.* 5 (1986): 41-49.

81. Yoon, H, G. Klinzing, and H. W. Blanch. "Competition for Mixed Substrates by Microbial Populations." *Biotechnol. Bioeng.* 19 (1977): 1193-1210.